

University of Alberta
Department of Civil Engineering



Structural Engineering Report No. 32

**CAS-S16-1969 Steel Structures
for Buildings - Seminar Notes**

by
P.F. Adams
G.L. Kulak
and
J. Longworth

November, 1970

STRUCTURAL ENGINEERING

Report No. 32

CSA—S16-1969 STEEL STRUCTURES FOR BUILDINGS

Seminar Notes

BY

P. F. Adams, G. L. Kulak and J. Longworth

**DEPARTMENT OF CIVIL ENGINEERING
THE UNIVERSITY OF ALBERTA
EDMONTON, CANADA**

NOVEMBER, 1970

Steel Structures for Buildings

LECTURE I

Wind Loadings For Buildings

J. Longworth

Wind Loadings for Buildings

Introduction

The 1970 Edition of the National Building Code of Canada introduces major changes in the treatment of the effects of wind on buildings. These changes reflect an improved understanding of the nature of wind gusts and the dynamic response of structures obtained from extensive research, in scale model testing in wind tunnels and, to a much more limited extent, from observations of behavior of actual buildings.

It is necessary to define as accurately as possible all loadings on a structure in order to justify the use of modern analysis and construction techniques. Traditional static wind loads are unrealistic, often leading to either over-conservative design or inadequate design. Modern structures respond to wind in a manner different from their predecessors. These new buildings have different aerodynamic characteristics, their density has been drastically reduced (from about 25 lb. per cu.ft. to less than 10 lbs. per cu.ft.), the strength and stiffness characteristics of the structural materials have changed and damping (the capacity to dissipate sway energy) has decreased significantly. Through new methods of analysis and the computer, opportunities exist for structural optimization.

Nature of Wind

Wind velocity increases with height. The relationship between velocity and height depends on the degree of roughness of the terrain over which the wind passes. Figure 1 shows velocity profiles for three different terrain roughness conditions.

Wind tunnel tests indicate that for steady state wind the velocity profile on the windward face of a building is directly related to the velocity profile of the wind. However on the leeward face, pressures do not vary nearly as much with height. Typical results for two terrain roughnesses are shown in Figure 2.

Gusts appear on a record of velocity measurements as fluctuations superimposed on the mean velocity. Measurements taken at three locations on a tall mast are shown in Figure 3. From this figure it is apparent that the mean velocity increases with height and remains comparatively steady throughout the record. The amplitude of the fluctuations about the mean is approximately the same at all heights. Rapid fluctuations at the different heights do not give any indications of being associated with one another but slow variations, over a minute or so, do appear to be related.

Quasi-Static Approach to Wind Loading

The quasi-static approach to the effects of wind is over-simplified in that it ignores the dynamic nature of wind. The provisions of the 1965 Edition of the National Building Code of Canada are based on this traditional approach to wind loading. Design wind loads are computed on the basis of stagnation or velocity pressure, modified for height and adjusted on the basis of building shape and location on the surface. The basic equation is expressed in the following form:

$$p = q C_h C_p$$

p = design wind pressure normal to surface

q = reference velocity pressure

$$= 1/2 \rho V^2$$

$$= 0.0027V^2 \text{ (in psf. for } V \text{ in mph.)}$$

C_h = height factor

$$= \left(\frac{h}{30}\right)^{1/5}$$

C_p = pressure coefficient

The reference velocity pressure is based on a gust velocity likely to be exceeded once in thirty years. This value is determined on the basis of data obtained from a Dines pressure tube anemometer which has a response time of about 2 to 3 seconds. There is an established relationship between gust velocity and the mean hourly velocity, or the number of miles of wind passing an anemometer in one hour.

$$V_g = 5.8 + 1.29\bar{V}$$

where V_g = gust velocity

\bar{V} = mean hourly velocity

This relationship has been used to derive gust velocity from hourly velocity for locations where only hourly velocity was available.

The use of gust velocity implies that the effect of gustiness is simply to magnify the static effect of a steady state mean velocity. This is an over-simplification of the true nature of the gust effect.

The value of $\left(\frac{h}{30}\right)^{1/5}$ for the height factor is based on velocity profile in which velocity varies as the 1/10 power of the height. Although it is well established that terrain roughness affects the velocity profile, no allowance was made for this variation.

Pressure coefficients are the non-dimensional ratios of wind-induced pressures on a building to the dynamic pressure (velocity pressure) due to wind velocity measured in the undisturbed air stream. Pressure coefficient values are empirical constants usually obtained from wind tunnel tests of scale models. Supplement No.3 of the 1965 Edition contains data for a variety of building shapes which is based on Standards of the Swiss Association of Engineers and Architects. These coefficients include external coefficients for windward and leeward surfaces and internal coefficients which will affect the design of individual walls of the structure.

Dynamic Action of Wind on Structures

The 1965 provisions do not contain any reference to the dynamic nature of wind or the dynamic response of the structure.

The dynamic action of wind on structures can be attributed to the following causes:

1. buffeting by gusts
2. buffeting by vortices and turbulence shed in the wake of the structure
3. buffeting by vortices shed by other structures

The nature of wind on structures may be considered as the summation of a steady force associated with the mean wind velocity and fluctuating forces associated with gusts. During the past ten years there has been considerable research on the formulation of factors which properly recognize the dynamic effects of wind. Appropriate design values of wind pressures can now be established reflecting the above factors, together with wind velocity estimates derived from statistical studies of extreme velocities and aerodynamic pressure coefficients derived from wind tunnel tests.

The response of a tall, slender building to a randomly fluctuating force can be evaluated by treating it as a rigid, spring-mounted cantilever whose dynamical properties are specified by a single natural frequency and an appropriate damping value. Various empirical formulae have been proposed for determining the natural frequency of a building, based on the results of tests that have been made on actual structures. These formulae will not give the frequency of a particular building with absolute certainty, however they do provide sufficient accuracy for the purpose of analysis. Building height appears to be the most significant factor governing natural frequency with frequency decreasing decreasing with height. Two relationships are frequently used:

$$n_0 = \frac{\sqrt{b}}{0.05H}$$

where n_0 = natural frequency in c.p.s.

H = height in feet

b = breadth or depth in feet

$$\text{or } n_0 = \frac{1}{0.1N}$$

where N = number of storeys

From information available it appears that a fairly wide range of natural frequencies is possible for buildings; ranging from about 10 c.p.s. for low-buildings to about 0.1 c.p.s. for extremely tall buildings. The frequency of the Empire State Building, which is over 1500 feet tall, is about 1/8 c.p.s. The above empirical formulae give good agreement with this observed value.

Damping affects the degree of dynamic magnification attainable in a structure. For structures vibrating in a high wind damping arises from two sources; first, the inherent mechanical damping of the structure and second, from aerodynamic forces as the structure moves through the strong current of air. It therefore depends on the type of construction, the natural frequency, the massiveness of the structure and on its aerodynamic properties. Results of tests involving forced vibration of structures indicate that for modern steel structures the critical damping ratio varies from about 0.005 to 0.01, and for concrete structures from about 0.01 to 0.02.

Structural response to the action of wind is approached from the point of view of spectrum analysis. (see Figure 4). The basic concepts of this approach may be explained as follows. From available meteorological data a spectrum of wind velocities is prepared. The area under this spectrum is equal to the variance, or mean square fluctuation energy. The translation of the velocity fluctuations into aerodynamic forces depends on a transfer function known as aerodynamic admittance. This function in effect describes how the turbulence of the wind is modified by its encounter with the building, and in its ability to produce a loading effect on the structure.

The wind velocity spectrum can be represented by an algebraic

expression based on observations of real wind. The aerodynamic admittance function can also be expressed algebraically on the basis of somewhat simplified assumptions which, however, are in reasonable agreement with limited experimental evidence.

Aerodynamic forces are translated into structural response through another transfer function known as mechanical admittance which is simply the square of the familiar resonance curve. The resulting response spectrum is peaked at the natural frequency.

Wind Loading Provisions - 1970 NBC

The 1970 Edition of the National Building Code includes three different approaches to the determination of wind loads on buildings:

1. Simple procedure similar to that included in the 1965 Edition.
This procedure is intended for the majority of buildings for which wind loading does not have a major effect on the structural design. It yields wind pressures and suctions very similar to those determined by the 1965 provisions.
2. Detailed procedure based on a dynamic approach to the action of wind gusts. This procedure gives a more accurate evaluation of wind loads. For low buildings it tends to yield lower values of wind load than the simple procedure, while for higher buildings it may yield higher values.
3. Special wind tunnel tests. These are recommended whenever the cost, importance, unusual nature of the building and/or site, or other such considerations justify the expense involved.

SIMPLIFIED METHOD

The equation for design wind pressure is given as

$$p = q C_g C_e C_p$$

where p = design wind pressure

q = reference velocity pressure

$$= 1/2 \rho \bar{V}^2$$

\bar{V} = mean hourly velocity

C_g = gust effect factor

C_e = exposure factor

C_p = pressure coefficient

The approach to the effect of gusts has been changed. Instead of gust velocity, the 1970 code is based on the mean hourly velocity. The effect of gusts is introduced as a gust effect factor. The implied gust effect factor in the 1965 Edition varied from 2.04 at 60 mph. design gust velocity to 1.84 at 120 mph. and was the same for the structure as a whole or for a part of it such as a window or wall panel. In the 1970 Edition the gust factor in the simple procedure is considered as 2.0 for the structure as a whole, and 2.5 for cladding or windows. This reflects the localized nature of gusts. In the 1965 Edition the gust velocity value was selected on the basis of a probability of being exceeded of 1 in 30. Since the consequences of wind damage are less serious for cladding than for structural members, the risk may be considered acceptably small if the reference velocity is based on a probability of being exceeded of 1 in 10 for cladding in comparison with 1 in 30 for structural members. In other words, for cladding more severe gust effects can be expected than for the total structure due

to the smaller areas involved. However, because of the less severe consequences of cladding damage, reference velocities with a shorter return period may be employed.

The concept of relating wind load to the consequence of damage is a new approach. The requirements related to this concept may be summarized as follows:

Table 1

<u>Design Criterion</u>	<u>Probability of being exceeded in any one year</u>
Deflection and vibration	1 in 10
Strength of structural members	1 in 30
Design of structural members for strength for buildings essential for post-disaster services	1 in 100
Design of cladding	1 in 10

As an example of the effect of probability on reference velocity pressures, the following values pertain to Edmonton:

Table 2

<u>Probability of being exceeded in any one year</u>	<u>Hourly Wind Pressure (psf)</u>
1 in 10	6.6
1 in 30	8.5
1 in 100	10.7

The relationship between velocities with different probabilities of occurrence varies with location.

The exposure factor for the simplified procedure in the 1970 requirements is identical to the height factor of the 1965 Edition. In other words,

$$C_e = \left(\frac{h}{30}\right)^{1/5}$$

The pressure coefficient C_p in the 1970 code is identical to C_p in the 1965 code. However, on the basis of recent research, new values of C_p for flat roof buildings of height greater than twice the width are now available.

In summary, the simplified procedure yields similar results to the 1965 wind loading provisions but two significant differences have been introduced. The form of the equation for wind pressure has been adjusted to include a gust effect factor and the concept of using loads based on different probability of exceedance related to the importance of the element being designed, has been introduced.

DETAILED METHOD

The equation for design wind pressure in the detailed procedure is identical to that used in the simplified method:

$$p = q C_g C_e C_p$$

wherein all the terms are as previously defined. The reference velocity pressure, q is determined on the basis of mean hourly velocity whose probability of exceedance is chosen on the basis of seriousness of damage. (see Table 1).

The exposure factor C_e is based on the mean velocity profile which is dependent on the general roughness of the terrain over which the wind travels before it reaches the building. Three categories of exposure have been defined to represent degrees of surface roughness:

Exposure A (open or standard exposure) - open level terrain with only scattered buildings, trees or other obstructions, open water or shorelines thereof. This is the exposure on which reference wind speeds are based.

$$C_e = (h)^{0.28}, \quad C_e > 1.0$$

Exposure B suburban and urban areas, wooded terrain, centres of large towns.

$$C_e = 0.6 \left(\frac{h}{60}\right)^{0.50}, \quad C_e > 0.5$$

Exposure C centres of large cities with heavy concentrations of tall buildings. At least 50% of the buildings should exceed four storeys.

$$C_e = 0.4 \left(\frac{h}{100}\right)^{0.72}, \quad C_e > 0.4$$

In the above equations, h is the height in feet above the ground.

Figure 5 is a plot exposure factors for the three terrain roughnesses.

Exposure B or C should not be used unless the appropriate terrain roughness persists in the upwind direction for at least one mile, and the exposure factor should be varied according to the terrain if the roughness differs from one direction to another. Abrupt changes in ground slope near the building site may result in significantly higher wind speeds than over level ground, and thus exposure A may have to be applied in such situations even though the surface roughness may seem appropriate for B or C.

Exposure factors are applied to wind pressure rather than velocity. Where it is necessary to determine the hourly mean velocity at a specific

height, the reference velocity is multiplied by $\sqrt{C_e}$. The exposure factor is required for three different purposes in the detailed analytical approach. $\sqrt{C_e}$ is required for the determination of the hourly mean velocity at the top of the structure

$$\bar{V}_H = \bar{V} \sqrt{C_e}$$

where \bar{V} = reference velocity

V_H is required in the determination of the gust factor C_g .

C_e is required directly in determining the gust factor C_g since it is involved in the coefficient of variation for the total loading effect. C_e is also used in the basic equation for design pressure. In this latter use, C_e varies continuously with height for the windward face, but for the leeward face it is considered as constant with a value determined at half the height of the building. This latter value is a simplification of wind tunnel test results.

The gust factor C_g is the ratio of the expected peak response, or loading effect, to the mean loading effect. It includes allowance for the variable effectiveness of different sizes of small gusts and for the magnification effect caused by gusts in resonance with the structure vibrating as a single degree of freedom cantilever. It may be expressed in the form

$$C_g = 1 + g \left(\frac{\sigma}{\mu} \right)$$

where $\frac{\sigma}{\mu}$ = the coefficient of variation, or the standard deviation divided by the mean, for the total loading effect

and g = the number of standard deviations by which the peak load effect is expected to exceed the mean load effect.

The coefficient of variation $\frac{\sigma}{\mu}$ is equal to the square root of the area under the loading effect spectrum. (See Figure 6). This area may be defined as the sum of two components; one, the area under the broad hump is represented by the so-called background turbulence factor B , the other, the area under the resonant peak is represented by the value $\frac{sF}{\beta}$. $\frac{\sigma}{\mu}$ also depends on $\frac{K}{C_e}$ which relates to scaling the effect to an appropriate input turbulence level. Both K and C_e are related to surface roughness.

$$\frac{\sigma}{\mu} = \frac{K}{C_e} B + \frac{sF}{\beta}$$

where s = size reduction factor depending on H and D , the dimensions of the windward face. See Figure 7.

F = gust energy ratio at the natural frequency of the structure; a function of the natural frequency and the mean wind velocity. See Figure 8.

β = critical damping ratio

K = a factor related to the surface roughness coefficient of the terrain

= 0.08 for Zone A

= 0.10 for Zone B

= 0.14 for Zone C

C_e = exposure factor

B = background turbulence factor; a function of the dimensions H and D of the windward face of the structure. See Figure 9.

The peak factor g is a function of the average fluctuation rate v . This fluctuation rate depends on the natural frequency n_0 , the gust energy ratio F , the background turbulence factor B , the size reduction factor s and the critical damping ratio β and is expressed as

$$v = n_0 \frac{sF}{sF + \beta B}$$

Figure 10 is a plot of this relationship.

Finally, in the equation for the design wind pressure p , there is the pressure coefficient C_p . This is defined in exactly the same way as in the simplified approach and values for it are obtained from wind tunnel tests. Figure 11 indicates values of C_p for flat roof buildings of height greater than twice the width.

Therefore it is seen that the exposure factor C_e and the gust factor C_g are determined differently in the detailed procedure. The result of the detailed procedure is a design pressure distribution which is applied to the structure as a static load but which has been determined in such a manner as to produce the same deformations and stresses, i.e. the same response, in the structure as the actual dynamic wind load.

Comparison of Simplified and Detailed Procedures

A comparison of values obtained from the two methods indicate that for lower, stiffer structures the simplified method yields higher values than the detailed method, indicating that the simplified method is conservative. A designer may be prepared to accept the conservative values if wind is not a significant factor in the design. On the other hand, for taller, more flexible structures, the simplified approach may yield lower values than the detailed method. This implies that it is not adequate to use the simplified method and the detailed procedure must be used to determine the effects of wind.

Load Combinations

The combination of wind load with other loadings is considered on the basis of probability of maximum values of the various loads occurring simultaneously. This concept is defined in the 1970 Edition as indicated in Table 3.

Table 3

<u>Combination</u>	<u>Probability Factor</u>
D+W	1.0
D+L+W	0.75
D+T+W	0.75
D+L+T+W	0.66

wherein D = dead loads

W = wind

L = live load due to occupancy; snow, ice and rain; earth and hydrostatic pressure; horizontal components of static or inertia forces

T = contraction or expansion due to temperature changes, shrinkage, moisture changes, creep in component materials, movement due to differential settlement, or combination thereof

Wind and earthquake is not considered to be a combination of loads of sufficient probability to be a concern in structural design.

Lateral Deflection Due to Wind

Lateral deflection of tall buildings under wind loading may require consideration from the standpoints of serviceability and/or comfort criteria. There is a general trend towards more flexible structures, partly because adequate strength can now be achieved by using higher strength materials which may not provide a corresponding increase in stiffness. Lateral deflection may result in cracking of masonry and interior finishes. Unless precautions are taken to permit movement of interior partitions without damage, a maximum lateral deflection limitation should be specified. Accordingly, the 1970 Edition of NBC requires that the lateral deflection due to wind of a slender building, whose height is greater than four times its minimum effective width, shall not exceed the following ratios:

Storey deflection to storey height	1/500
Total deflection to total height	1/500

These limits may be waived if the design is based on a detailed dynamic analysis of the deflection and their effects.

Building movement maybe perceptible to humans when the amplitude of acceleration reaches about 1% of the acceleration due to gravity, or about 1/3 ft. per sec². Lateral deflection of a tall building in response to turbulent wind action consists of a fluctuation about a mean deflected position with maximum lateral accelerations usually occurring at the fundamental resonant frequency of the building. The peak acceleration in the direction of the wind can be related to the maximum lateral deflection by the following approximation:

$$A = \left[\frac{4\pi^2 n_0^2}{C_g} \sqrt{\frac{K_s F}{C_e \beta}} \right] \Delta$$

where A = peak acceleration in direction of wind (ft./sec²)

Δ = maximum lateral deflection (ft.)

C_g , C_e , n_0 , β , K , s , F are as previously defined.

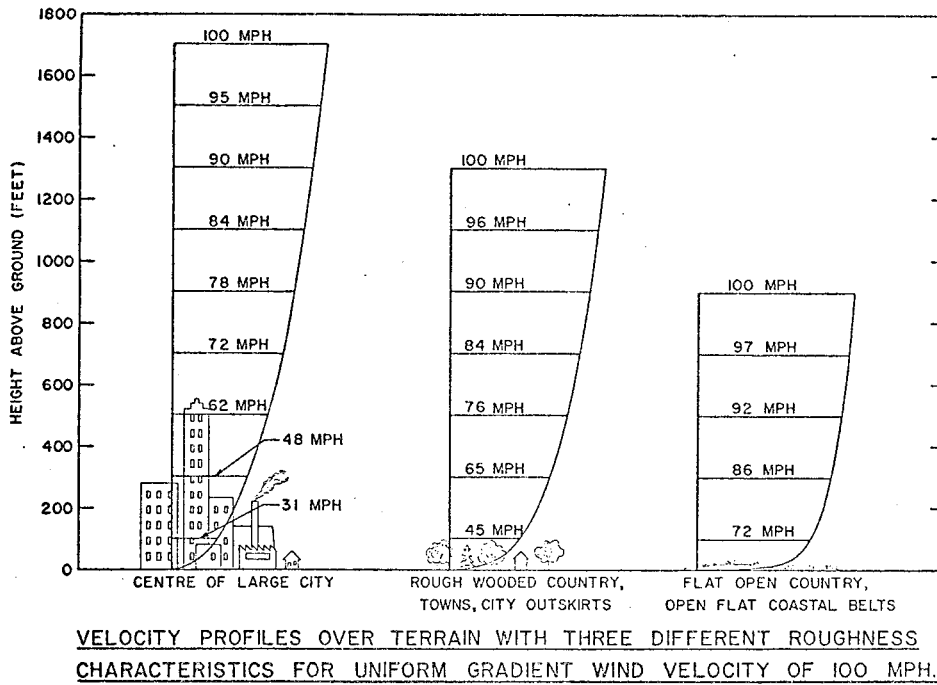
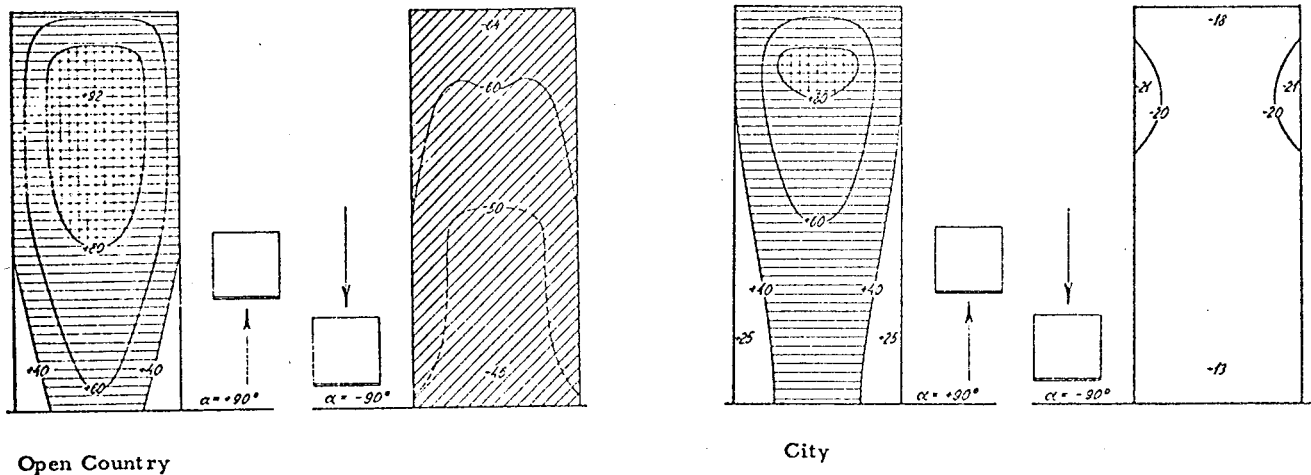
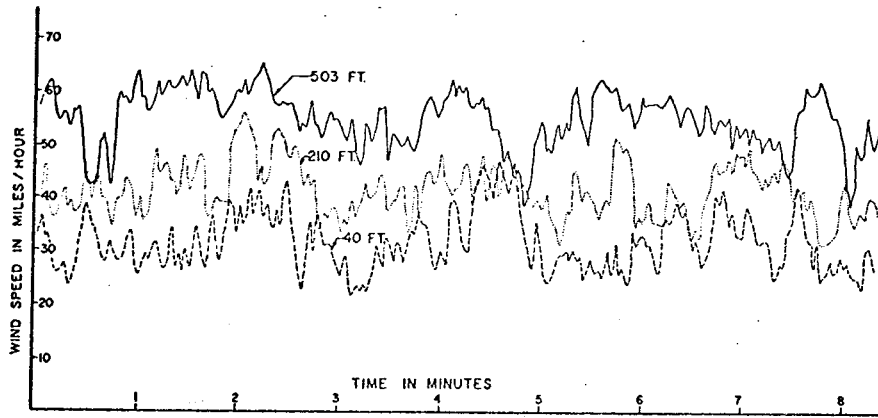


FIGURE 1



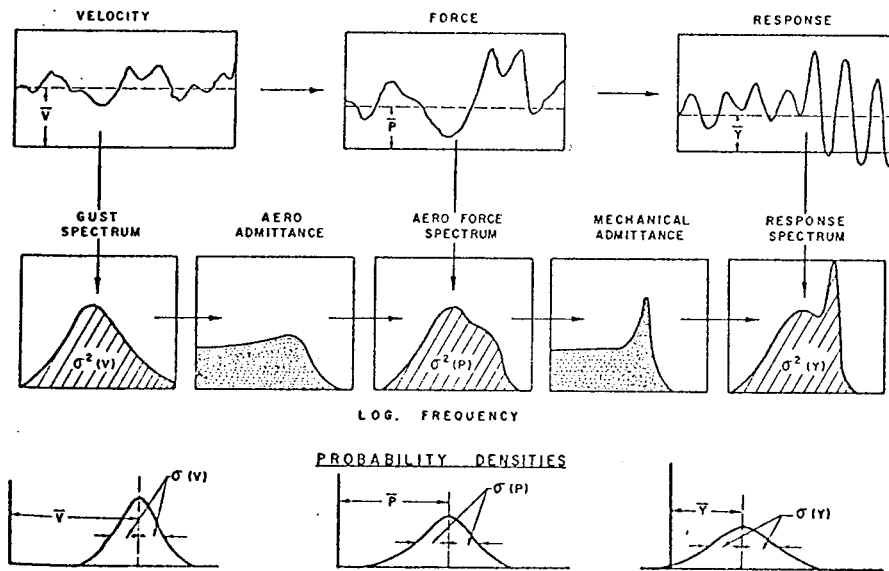
DISTRIBUTION OF MEAN PRESSURE COEFFICIENTS ON TALL BUILDING IN TWO BOUNDARY LAYER VELOCITY PROFILES

FIGURE 2



WINDSPEED AT THREE HEIGHTS ON A 500 FT MAST

FIGURE 3



ELEMENTS OF THE STATISTICAL APPROACH TO GUST LOADING

FIGURE 4

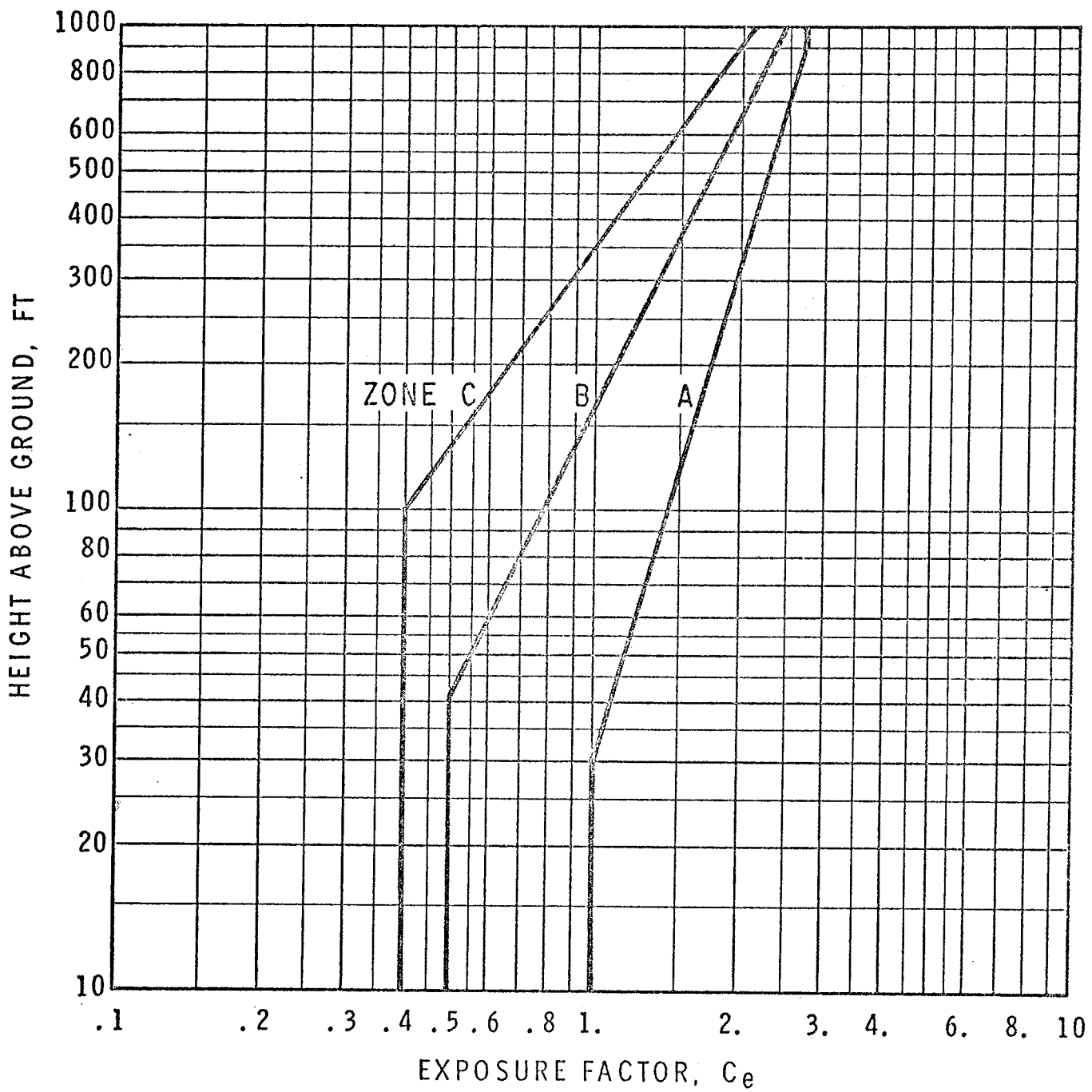
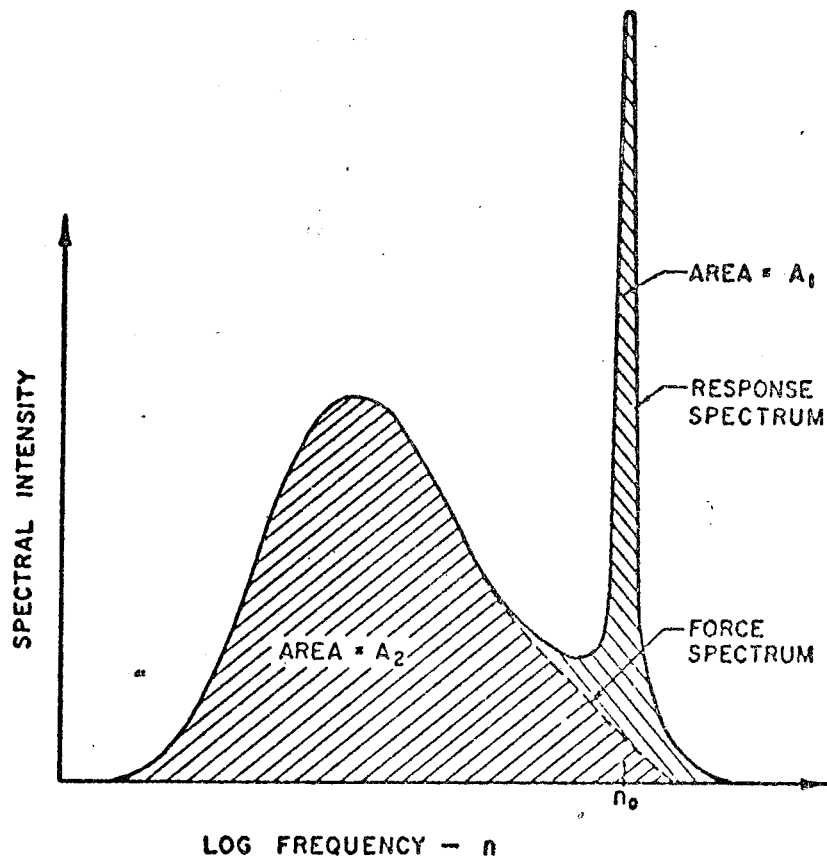


FIGURE 5



RELATIONSHIP BETWEEN RESPONSE AND FORCE SPECTRA FOR LIGHTLY DAMPED SYSTEM

FIGURE 6

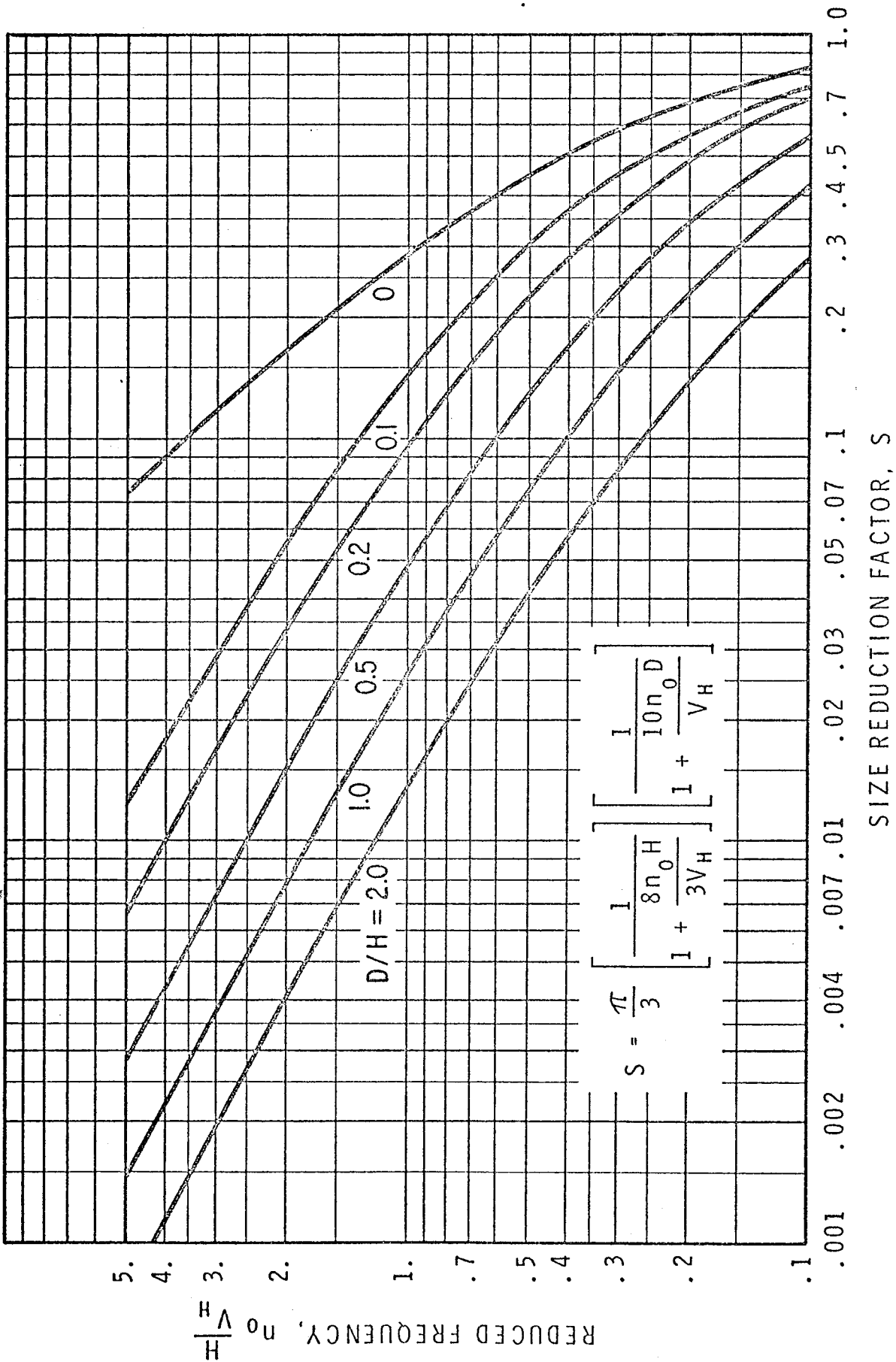
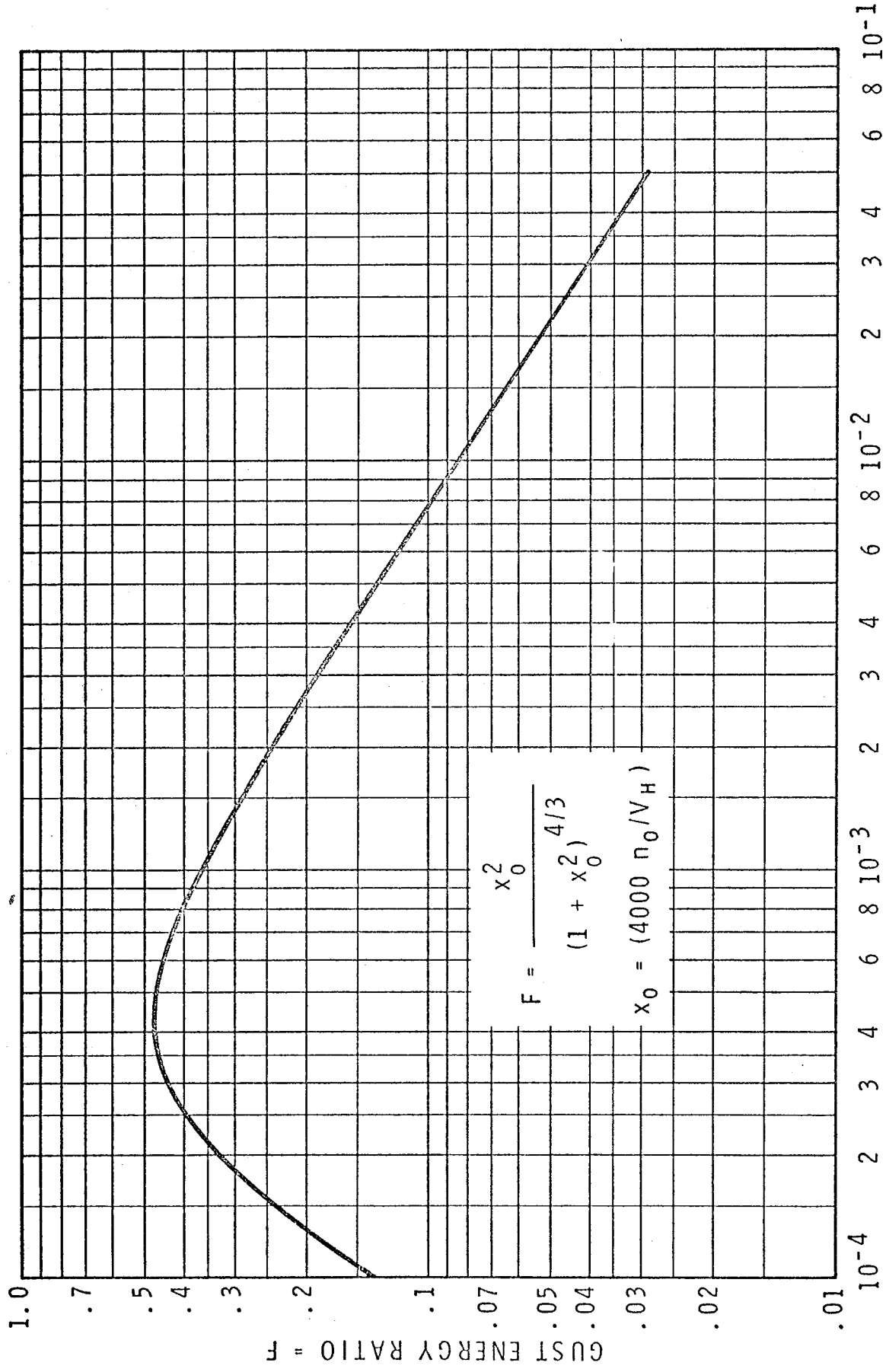


FIGURE 7



INVERSE WAVELENGTH, WAVES/FT, n_0/V_H

FIGURE 8

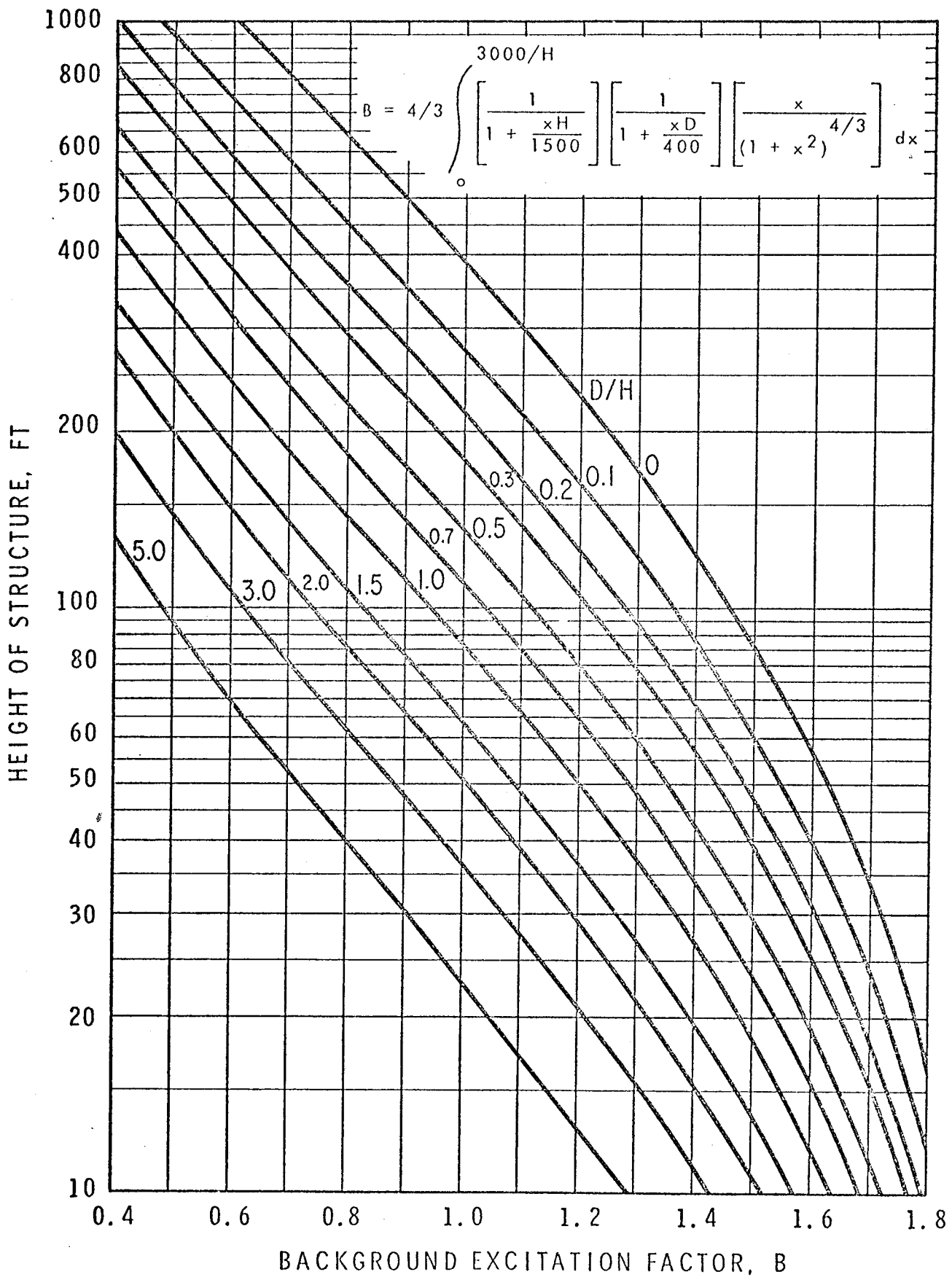


FIGURE 9

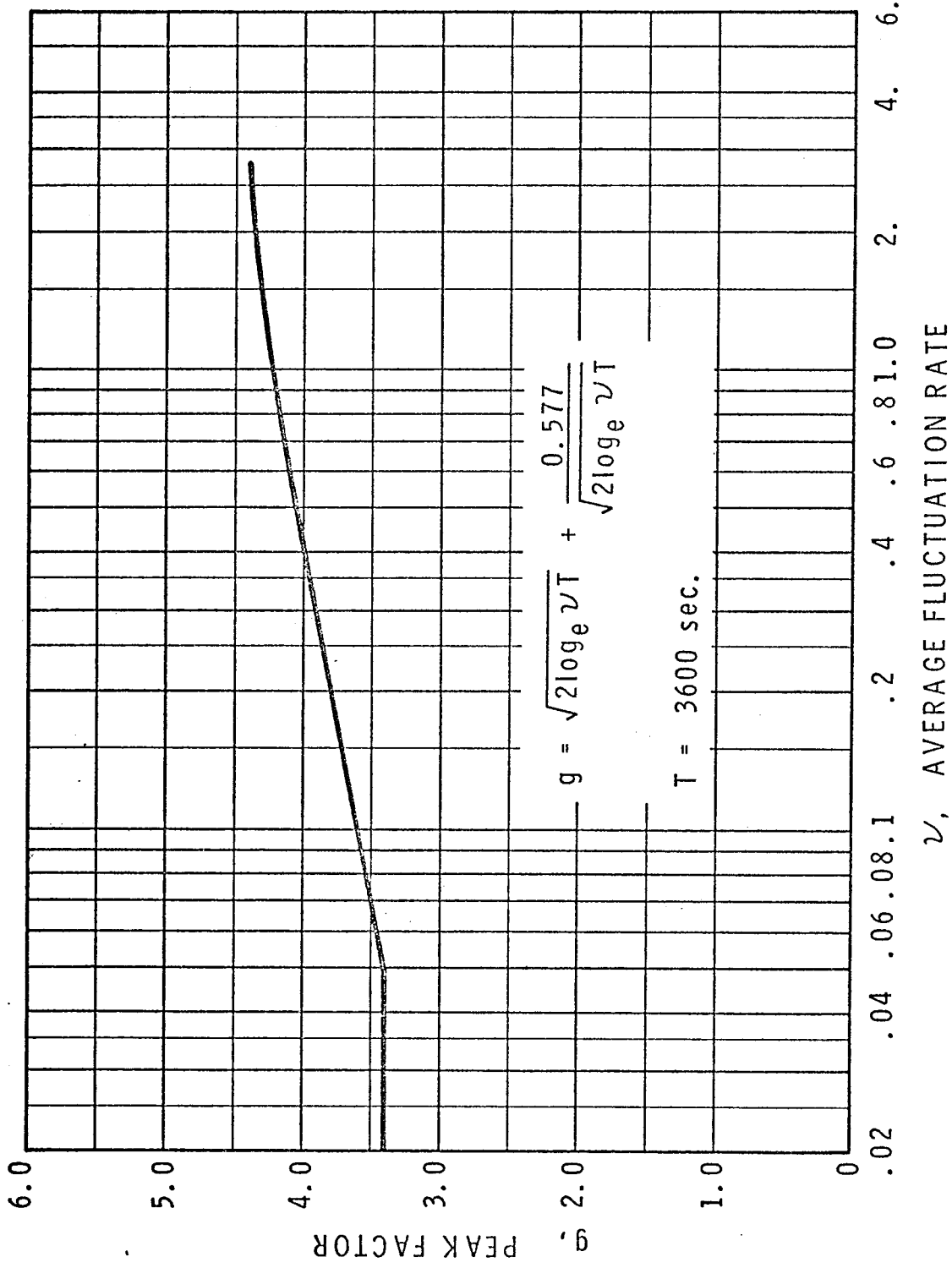
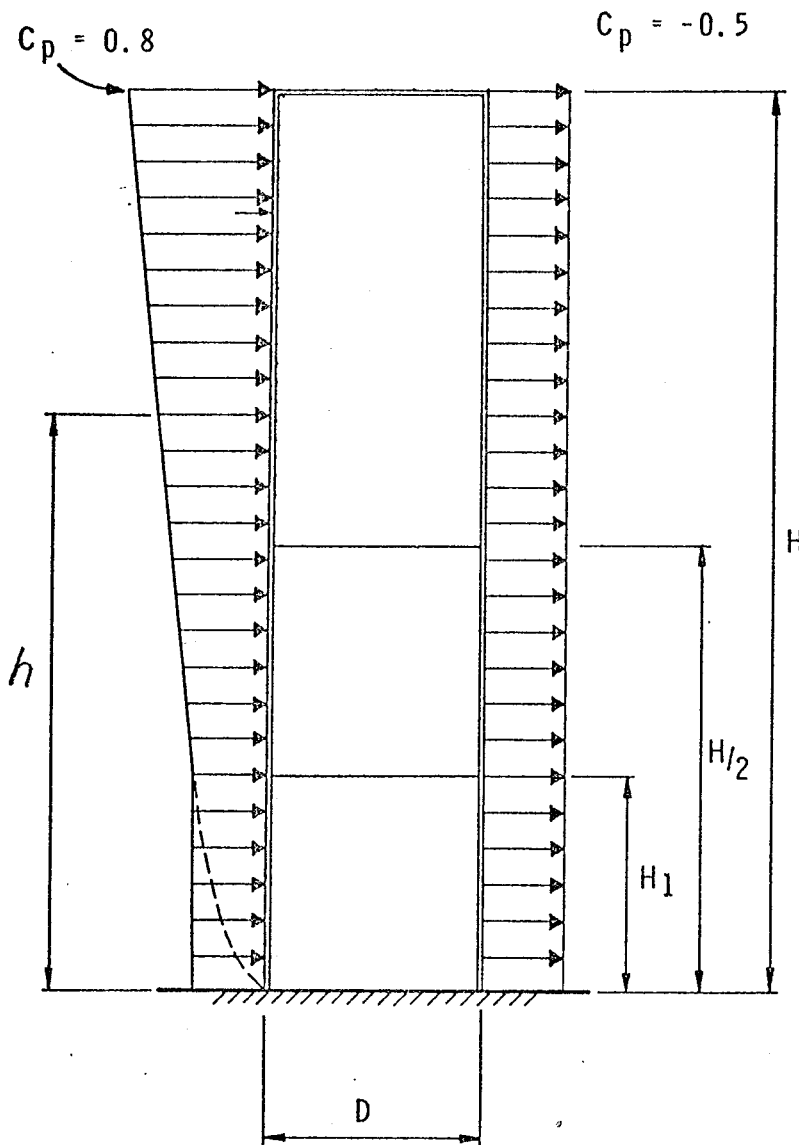


FIGURE 10



ELEVATION OF BUILDING

EXPOSURE FACTOR: For the calculation of exposure factor C_e , use $1/2$ the height H for the leeward wall, the height H for the roof, and the actual height h to the level under consideration for the windward wall .

HEIGHT H_1 : The height to which C_e is always constant is 30 ft for both the simplified method and zone A, 40 ft for zone B and 100 ft for zone C.

FIGURE 11

Steel Structures for Buildings

LECTURE II

Tension Members

Basic Fastener Behavior

G.L. Kulak

Design of Tension Members

There have been some significant changes in S16 with regard to the design of tension members, particularly affecting situations in which very high strength steels are used. I would like to start by discussing the basic design philosophy of steel tension members, then to point out the particular problem that can arise with these newer steels, and finally to examine how the Code has dealt with the situation.

The basis that has been established for the design of steel tension members considers that the limit of usefulness of the member is given by the load at which contained plastic flow commences. In other words, the yield load is used as the limit against which a factor of safety is applied (Fig. 1). Beyond this point, significant and relatively uncontrolled elongation occurs.

As well as looking at individual member behavior, however, we must look at the overall behavior of the structure of which this member is a part. Here, it is considered desirable that the system or assemblage have a capacity for distortion or geometrical adjustment before failure by fracture. In an axially loaded structure, this means that the connections should be proportioned so that yielding takes place in the gross cross-section of the member before the joint fails. This joint failure can be by fastener failure (either bolts or welds) or by tearing of the member through the net section. Thus, although the individual member is beyond its limit of usefulness, the criterion for satisfactory behavior

of the structure or assemblage of which the member is a part demands this further deformation capacity.

In steels like A36 and G40.12, the spread between yield and ultimate strengths is so large that the deformation capacity has been automatically ensured in the past. The ratio of tensile strength to yield level is 1.61 for A36 steel and 1.41 (for 44 ksi yield level) for G40.12 steel. In other words, we can expect a large reserve in both load and ductility beyond the yield level for such steels. On the other hand, the newer, high-strength steels have a very low spread between yield and ultimate, and special precautions must be taken to ensure member ductility. For example, the ratio of tensile strength to yield strength is as low as 1.15 for the highest strength structural steel now available, A514. Figure 2 shows a hypothetical but entirely realistic set of circumstances for this steel. In fact, as delivered properties of A514 steel show an even lower ratio of ultimate to yield than I have used here.

Figure 3 illustrates quite dramatically the effect of changing the ratio of net area to gross area upon the ductility of a member. These were A514 steel members with a line of holes drilled to simulate a joint. Based upon the measured properties of the material, the minimum ratio of A_n/A_g should be 0.93 if yielding is to occur through the main section of the member before fracture through the net section. These members have A_n/A_g ratios ranging from 0.80 (Specimen A) to 0.95 (Specimen D). The increase in ductility of member D as compared to the others is appreciable,

its elongation being 3.44 times that of the next most ductile member.

If certain critical A_n/A_g ratios must be equalled or exceeded when specifying tension members of high strength steels, it obviously is essential to know whether these efficiencies can, in fact, be obtained. The joint efficiency in carbon steel structural joints is commonly limited to 85%, for example. Based on the test results in Fig. 3 and on tests of full-size A514 steel joints, it was considered that efficiencies as high as 95% were attainable. These would probably not be very practical connections. Nevertheless, the possibility of their use must be included. The Code sets forth the efficiencies as a function of the ratio F_y to T.S. as follows:

$$F_y/T.S. \leq 0.70 \dots 85\% \text{ (Includes A36, A440, G40.12)}$$

$$0.70 < F_y/T.S. \leq 0.85 \dots 90\% \text{ (Includes A572 steels)}$$

$$0.85 < F_y/T.S. \dots 95\% \text{ (A514 steel)}$$

The Committee then took the point of view that if the designer is not able to provide a member meeting the criterion of gross cross-sectional yielding before fracture at the net section, such a member should have a higher factor of safety than that normally provided. Accordingly, the allowable tensile stresses are (Fig. 4)

$$F_t = 0.60 F_y$$

or,

$$F_t = 0.50 \text{ T.S.}$$

except that when $(A_n/A_g) < (F_y/T.S.)$,

$$F_t = 0.60 \text{ T.S. } (A_n/A_g)$$

or

$$F_t = 0.50 \text{ T.S.}$$

The factor of safety, on net area, is a minimum of 1.67 on yield and 2.0 on tensile strength. When member ductility is not assured a higher factor of safety is demanded.

The foregoing discussion regarding ductility has implied that failure of these high-strength steel members would always be by tearing of the plate rather than shear failure of the fasteners. It will be shown later that for present allowable stress levels in fasteners, this will always be the case.

Introduction to Connections: Fastening Elements

As a preliminary to discussing the behavior of certain types of commonly used connection details, I would like now to look at the load - deformation characteristics of both welds and high-strength bolts.

The load - deformation response of a 3/4 inch diameter A325 bolt is shown in Fig. 5. The mean ultimate bolt load (double shear) was 74 kips and the mean deformation at failure was 0.34 inches. The allowable load for such a bolt is currently 19.44 kips and so the factor of safety of a single bolt is about 3.8. This value is reduced for more than two bolts in line but even for very long joints, it is still about 2.2. It should also be noted that the load - deformation response shows little, if any, elastic portion. Much of our conventional design of connections assumes that the response is completely elastic.

A similar curve for a fillet weld acting in shear is shown in Fig. 6. Here the angle of loading with respect to the axis of the weld must be taken into account. It has long been recognized that a transverse weld is appreciably stronger than a longitudinal one. As the figure shows, the increase in strength comes at the expense of a considerable decrease in deformation capacity, however. Again, we note that the weld response is generally not elastic.

The allowable stresses for fillet welds have been increased in the 1969 Code from 22 1/2% to 30% of the ultimate tensile strength of the

weld material. In the test results shown, the tensile strength of the weld in the basic case (longitudinal weld) was 61.6 ksi. The corresponding factor of safety is 3.42. We shall be examining the factor of safety in typical welded connections later on. Before leaving this discussion of basic fastener behavior, it is also worthwhile to note the relative deformation of welds and high-strength bolts. The most ductile of these 1/4 inch fillet welds deformed 0.10 inches while the 3/4 inch diameter A325 bolt discussed earlier had a maximum deformation almost 3 1/2 times that value.

The S16 Code has traditionally confined its remarks on fasteners and connections to setting allowable stresses for the fastening elements along with some aspects of installation and inspection. The basic change then has been the increase in allowable stresses for welds. In addition, however, some new details for bolted connections have been included which should be useful to designers. In particular, certain types of corrosion treatments such as galvanizing can now be used on the faying surfaces in friction-type connections. Of interest to those involved with the field erection of steel structures is the allowance by the Code of oversize or slotted holes in bolted parts. Tests have shown that neither oversize holes (up to 1/4 inch greater than fastener diameter) nor slotted holes significantly reduce the expected preload in the installed bolt. Washers should be used in most cases, however, to prevent galling of the material under the bolt head or nut.

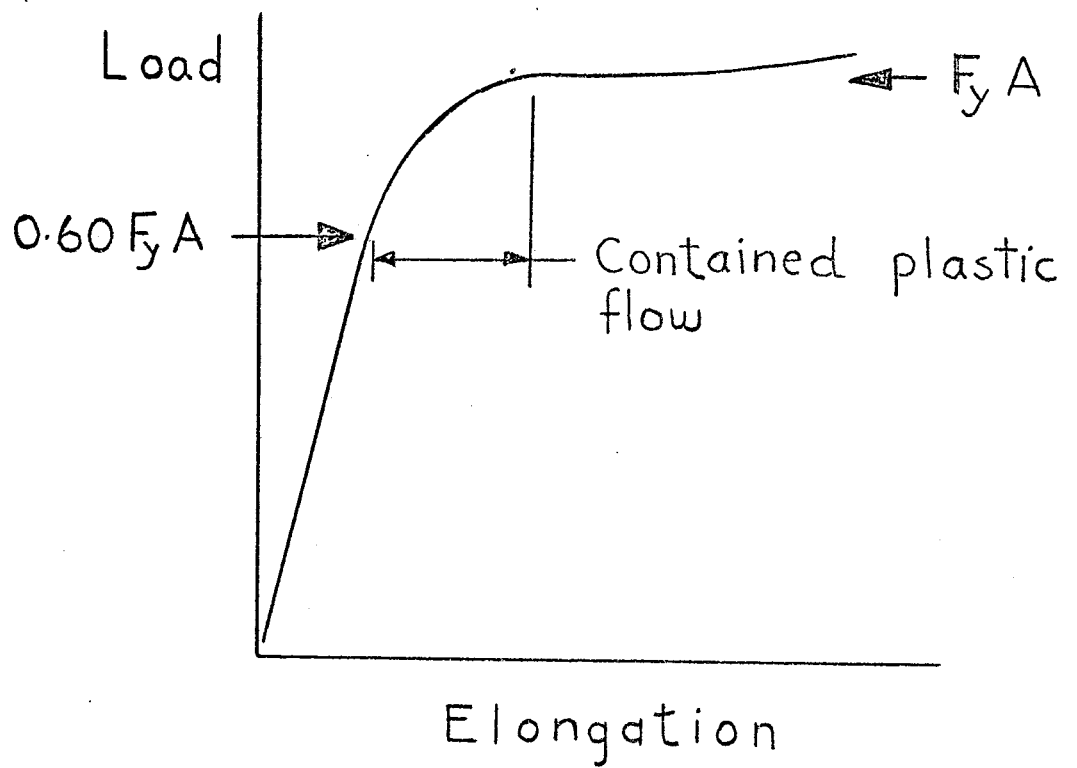
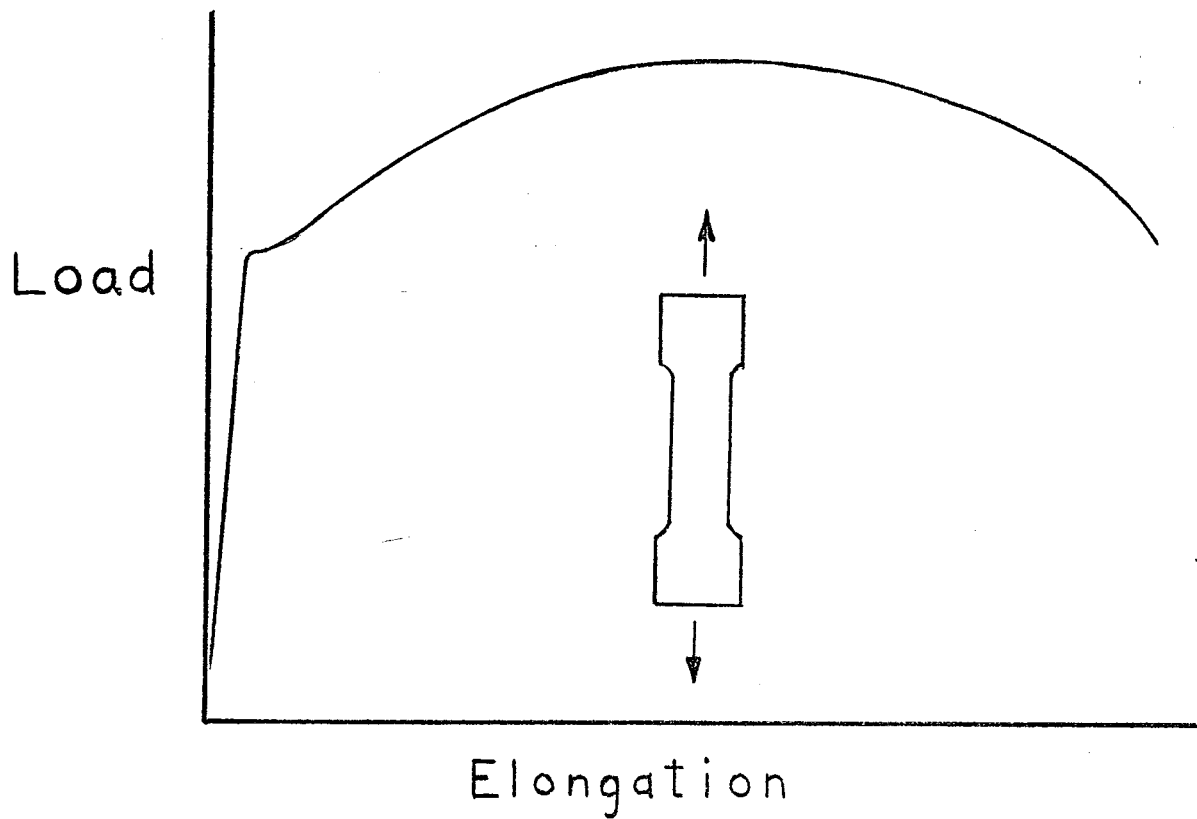


Fig. 1

A514 Steel Structural Shapes —

$$F_y = 100 \text{ ksi}$$

$$\text{T.S.} = 115 - 140 \text{ ksi}$$

say, 120

Assume member = 10^{\square} gross

$$\text{and } A_n = 80\% A_g = 8^{\square}$$

Then, yield load of main member

$$= A_g \cdot F_y = 1000 \text{ kips}$$

But ultimate load of connection
(net section)

$$= A_n \cdot \text{TS} = 960 \text{ kips}$$

Fig. 2

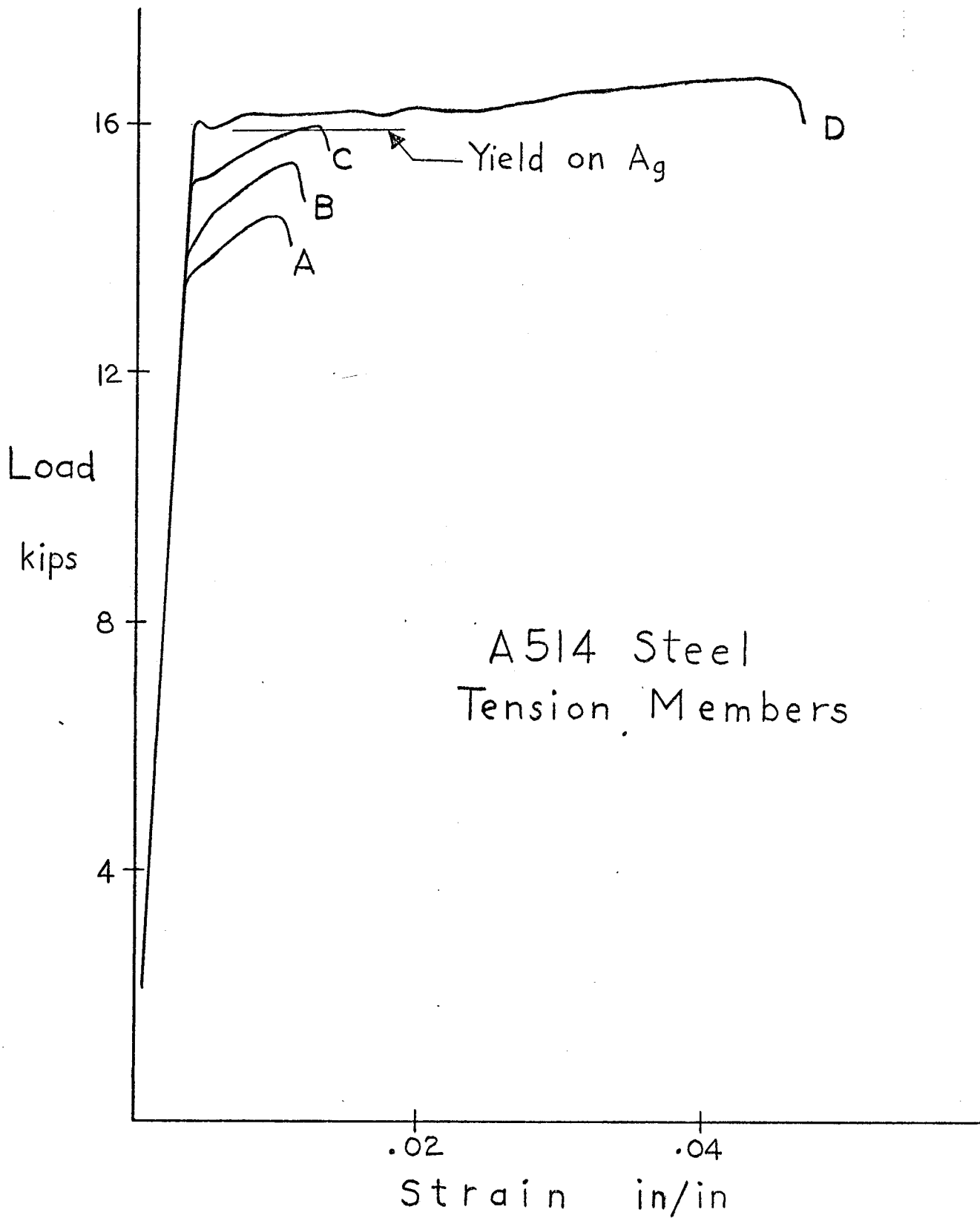


Fig. 3

$$F_t = 0.60 F_y$$

or,

$$F_t = 0.50 \text{ T.S.}$$

except that when

$$\frac{A_n}{A_g} < \frac{F_y}{\text{T.S.}} \text{ ,}$$

$$F_t = 0.60 \text{ T.S.} \left[\frac{A_n}{A_g} \right]$$

or,

$$F_t = 0.50 \text{ T.S.}$$

Fig. 4

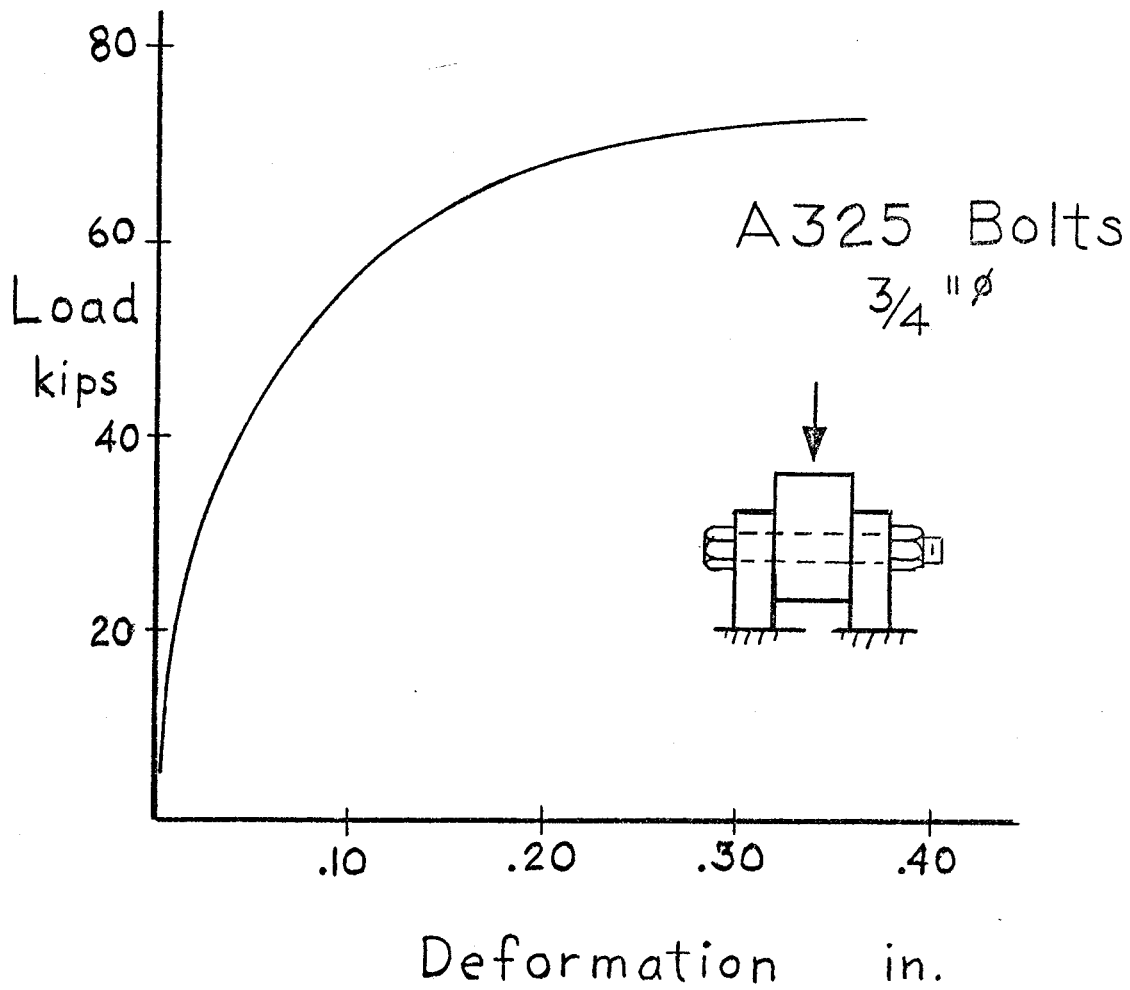


Fig. 5

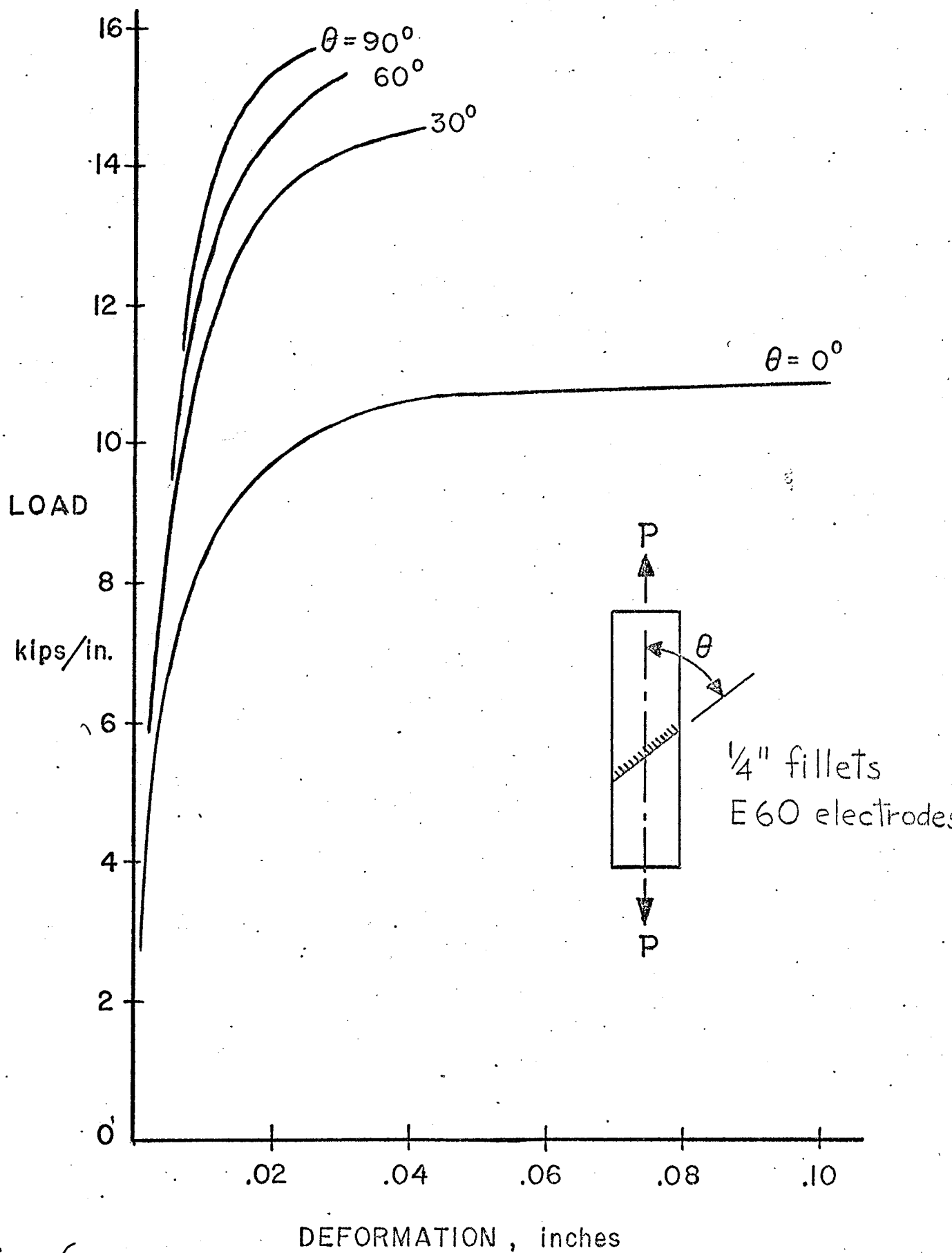


Fig. 6

Steel Structures for Buildings

LECTURE III

MEMBER STABILITY PROVISIONS IN CSA-S16-1969

STEEL STRUCTURES FOR BUILDINGS

P.F. Adams

MEMBER STABILITY PROVISIONS IN CSA-S16-1969

STEEL STRUCTURES FOR BUILDING

INTRODUCTION

In the design of a steel structure to resist static loads, the ultimate strength of the member is taken as the basis for allowable stress design, while the ultimate strength of the complete structure forms the basis for plastic design. With a few major exceptions, the load capacity of a steel member is generally terminated by some form of instability, either local instability of the plate elements making up the cross-section, or overall instability of the entire member. This paper reviews briefly the development of the member stability provisions of CSA Standard S16-1969, Steel Structures for Buildings, primarily as they apply to the allowable stress design technique.

Material and Cross-Sectional Properties

A schematic stress-strain (σ - ϵ) curve obtained from a tension test of a coupon cut from the cross-section of a steel member is shown in Fig. 1. For CSA-G40.12 steel the specified minimum yield stress is 44 ksi and the tensile strength is 62 ksi. The elongation at fracture is approximately 20%.

Typically, the strain at fracture is 200 times that at the initiation of yielding and 20 times that at the initiation of strain hardening. For this reason the ultimate strength (except in tension members) is seldom associated with fracture and instead is accompanied by instability after portions of the member have yielded.

Even under a uniform load, however, all portions of the cross-section do not yield at the same instant. This is because of the "locked in" residual stresses induced by the rolling and cooling (or welding) process. A typical residual stress distribution is shown in Fig. 2. A number of such measurements, on specimens of low carbon and low alloy steel, have indicated that the maximum residual stresses, at the flange tips, are approximately 13 ksi, in compression.

These residual stresses are normal longitudinal stresses and effectively lower the yield point of the member. This is illustrated by the results of a compression test on a short column as shown in Fig. 3. The figure plots the stress, $\sigma=P/A$ against the longitudinal strain ϵ . Unlike the behavior of the tension coupon shown as the dashed lines, the response of the complete cross section deviates from that predicted by elastic theory at a stress of approximately 70% of the yield stress, σ_y . This corresponds to a stress level in the material of approximately 25 ksi which is 11 ksi less than the yield stress and illustrates clearly the influence of the residual stress. On additional loading, the stress strain curve bends gradually until the yield stress is attained. Further deformation proceeds at a relatively constant load.

Unloading of the member (approximately at the onset of strain hardening) is accompanied by local buckling of the flanges. The flanges twist about the flange-to-web junction and the web deforms to maintain the right angle at the junction. This local twisting motion decreases the capacity of the section and prevents an increase in load due to the presence of strain hardening.

Since the flange acts much like a column, the occurrence of local buckling can be delayed by decreasing the plate slenderness ratio (the ratio of flange half width-to-thickness, b/t).

Fig. 4 shows the relationship between the applied end moment, M , and the resulting end rotation, θ , for a beam subjected to a uniform bending moment. The beam is assumed to be braced laterally so that unloading is triggered by local buckling of the compression flange. In the worst case plotted the beam is able to achieve the yield moment, M_y , before unloading occurs. This corresponds to the attainment of the yield stress at the extreme fibres of the member and this type of behavior forms the basis for the design of "non-compact" members in bending. In this case the flange buckling situation is not severe and for I type shapes the width of the projecting flange plate, b , is limited to

$$b/t \leq \frac{100}{\sqrt{F_y}} \quad * (14.1.1)$$

where t represents the plate thickness.

Next in order of severity is the "compact" section. It is assumed that this section will reach the plastic moment capacity, M_p , before buckling occurs, thus the flange is fully yielded. In this case

$$b/t \leq 64/\sqrt{F_y} \quad (14.4)$$

Finally in order to use a shape in a plastically designed structure,

* Numbers in brackets refer to the appropriate section in CSA-S16-1969. The nomenclature used also coincides with that of CSA-S/16.

local buckling must not occur until after the section has achieved M_p and endured a significant amount of inelastic deformation. In this, most severe, case

$$b/t \leq 54/\sqrt{F_y} \quad (30.11)$$

Although the major share of the bending moment is carried by the flanges, the slenderness of the web must also be limited to ensure that premature web buckling does not limit the moment capacity of the section. For the web, the limits will depend on the proportion of axial load carried by the member. A large axial load will cause the neutral axis to migrate from mid-depth of the member toward the tension flange. Thus a larger amount of the web plate will be subjected to compression. The limits are correspondingly more severe. For example, for compact sections (and sections used in plastically designed structures)

$$\frac{h}{w} \leq \frac{420}{\sqrt{F_y}} \left[1 - 1.4 \frac{f_a}{F_a} \right]$$

$$\text{if } \frac{f_a}{F_a} \leq 0.28$$

and for larger values of $\frac{f_a}{F_a}$

$$\frac{h}{w} \leq 255 / \sqrt{F_y} \quad (14.4)$$

Since the compact section is able to achieve a higher ultimate moment capacity than the non-compact section (M_p as opposed to M_y) the allowable stresses are correspondingly higher, for example:

$$F_b = 0.66 F_y \quad (16.2.4.1)$$

for compact sections and

$$F_6 = 0.60 F_y \quad (16.2.4.1)$$

for non compact sections.

The above limitations (b/t) also apply to elements such as stiffeners and in these situations the width of the stiffener is often fixed by practical considerations and the plate thickness required above may be excessive. In this case two choices are open; the designer may take the load (stress) by accounting for only a portion of the stiffener, provided that this portion does meet the b/t limit; or he may compute the actual stress in the stiffener and use 1.67 times this stress in place of F_y , to compute the b/t limit. (14.1.3)

Assuming that the appropriate plate slenderness limits are maintained, local buckling will be postponed until after the member has unloaded due to overall instability and the various design provisions may be based on this mode of failure.

Design of Beams

As the length, L , of the beam shown in Fig. 4 is increased, the mode of failure (or unloading) will change from local buckling of the compression flange to lateral buckling of the complete member. Lateral buckling may occur at any stage of the loading history; at moment values less than M_y , between M_y and M_p , and after the beam has attained the plastic moment capacity, M_p .

The resistance to lateral buckling depends upon the lateral bending stiffness of the cross-section as well as the resistance developed by the St. Venant and the warping torsional contributions. The St. Venant torsional resistance is that resistance developed by the shear stresses in the individual plates making up the cross-section. The St. Venant stiffness is the product GK_T , where G represents the torsional rigidity of the material and K_T is a cross-sectional property, $K_T = \frac{1}{3} \sum bt^3$ for each plate. The shear stress distribution is shown in Fig. 5.

The warping resistance is generated by cross-bending of the flanges. As the beam twists the cross-section rotates about its centroidal axis and this motion induces lateral bending strains in

the flanges. These strains result in the development of flange bending moments and accompanying shear forces, as shown in Fig. 6. The couple produced by the shear forces makes up the warping torsional resistance and is a function of $EI_y (d-t)^2 / 4$.

For a beam subjected to a constant bending moment distribution and having simply supported boundary conditions the moment at which lateral buckling will occur is given by:

$$M_o = \frac{\pi}{L} \sqrt{EI_y GK_T \left[1 + \frac{\pi^2}{4L^2} \frac{EI_y (d-t)^2}{GK_T} \right]}$$

After approximating the various cross-sectional properties (neglecting the bending contribution of the web) and substituting the material constants, this expression can be arranged in terms of an allowable bending stress, F_{bc} , as:

$$F_{bc} = F_1$$

$$\text{where } F_1 = \sqrt{F_2^2 + F_3^2} \quad (16.2.4)$$

$$\text{and } F_2 = \frac{12000}{Ld/A_f}$$

$$F_3 = \frac{149000}{(L/r_t)^2}$$

In the above expressions L and d represent the length of the beam and its depth, respectively, A_f represents the area of the compression flange and r_t the radius of gyration (about the y axis) of a tee composed of the compression flange and one-sixth of the web.

The expression for F_2 contains a factor of safety of 1.67 and that for F_3 contains a factor of safety of 1.92. F_1 thus provides a factor of safety of at least 1.67 against elastic buckling and is valid up to the stage where the stress at the instant before buckling will cause partial yielding of the cross section. Due to the presence

of relatively large residual stresses at the flange tips, this will occur when the stress is approximately $2/3 F_y$; or in terms of allowable stresses, when F_1 is approximately $2/3 F_{bt}$ where F_{bt} is the allowable stress for a completely braced beam; $0.60 F_y$ or $0.66 F_y$ for non-compact and compact sections respectively.

For stresses above this level, the assumptions made in deriving the elastic buckling expressions are no longer valid as the compression flange has been considerably weakened by yielding at the flange tips. Empirically, therefore, the allowable bending stress is reduced to:

$$F_{bc} = 1.15 F_{bt} \left[1 - \frac{0.28 F_{bt}}{F_1} \right] \quad (16.2.4)$$

However, in no case may the allowable bending stress, based on lateral buckling, F_{bc} be greater than F_{bt} since this provides the required factor of safety against local buckling.

The factors of safety obtained by the above procedure are illustrated in Figs. 7, 8, 9 and 10 for both torsionally weak and torsionally strong members. The critical moments are shown by the full lines while the allowable values are given by the dashed lines. In most cases the factors of safety would be considered adequate, in the case of stocky members the computed factors may be less than 1.67, however, this neglects the 10-20% increase that would be due to the influence of strain hardening.

Figures 11, 12 and 13 compare the allowable stresses from these new provisions with those of the 1965 code. In most cases the new requirements are more liberal. For slender beams this will always be the case since the 1965 requirements used only the larger of F_2 and F_3 .

The requirements of this clause are still very conservative due to the assumptions regarding boundary and loading conditions. Although the requirements specify that L is the length of the beam between supports, it would be logical to take L as the distance between points of contraflexure on the laterally buckled shape of the compression flange. The implication herein is that points of zero bending moment, therefore, also act as braced points.

The procedure is illustrated in Fig. 14, by the simply supported beam braced laterally at the load and reaction points and at two intermediate points. The bending moment diagram is shown in the second portion of the figure. The two central unbraced lengths, $L/4$, are critical for lateral buckling and are restrained by the end lengths. The buckled shape of the compression flange is shown in the third part of the figure with the two central lengths buckling simultaneously. To obtain the effective length of the critical span, one half of the span is represented by the frame shown at the bottom of the figure; the column represents the critical central length and the beam represents the end restraining length. The effective length factor is then obtained from the nomograph used for axially loaded columns.

The second element of conservatism is the assumption of a uniform bending moment over the complete member length. This very severe condition is seldom met in practice and any moment gradient substantially reduces the severity of the lateral buckling problem. The Column Research Council recommends the use of an equivalent moment factor; in terms of the present specifications, the allowable stress, F_1 , should be multiplied by C_1 where

$$C_1 = 1.75 - 1.05 M_1/M_2 + 0.3 (M_1/M_2)^2$$

$$C_1 \leq 2.3$$

Where M_1 is the lesser end moment and M_2 the greater end moment on the segment, as shown in Fig. 14. This ratio varies from 1.0 to -1.0. Values of C_1 are tabulated for various loading and end conditions in the CRC Guide.

Design of Beam Columns

Present design procedures for members subjected to axial force and applied moments (beam-columns) are based on the ultimate strength of the member. The computation of the ultimate strength is a complex procedure which must account for the inelastic action of the material as well as the "secondary" moments produced by the axial force acting on the deflected member.

To facilitate the design of beam-columns, the ultimate strength results have been approximated by using "interaction equations". These equations relate the bending moment and axial force on the member to limiting values of these same quantities. The equations account for slenderness effects, boundary conditions and variations in the bending moment along the member length. Although the interaction equations are empirical they predict the ultimate strength of a beam-column with a reasonable degree of reliability and have become a valuable design tool.

The Analysis of Beam-Columns Subjected to Equal End Moments

The beam-column shown in the inset to Fig. 15 is of length L , and is subjected to a constant axial load, P , and equal end moments, M , which increase monotonically to deform the column in a symmetrical single curvature mode. The deformation is characterized by the end slope, θ . The member is assumed to be pinned at both ends and translation is prevented.

Because the bending moment distribution on the column depends on the deflected shape, the ultimate strength cannot be obtained directly. Instead a series of points defining the moment-rotation ($M - \theta$) curve

for the member must be established. The peak of this curve then represents the ultimate value of M that can be maintained under the prescribed axial force, P .

Interaction Equations

Maximum values of M for various P/P_y and L/r_x ratios and for several boundary conditions and loading cases have been established by the procedure described above. The forces and moments which can be resisted by a given member are related through the interaction equations. These equations, written below in terms of allowable stresses, have been adjusted to provide consistent factors of safety against local failure (Eqn. 1) and against overall failure through inelastic instability (Eqn. 2).

$$\frac{f_a}{0.60 F_y} + \frac{f_b}{F_b} \leq 1.0 \quad (1)$$

(17.1.1)

$$\frac{f_a}{F_a} + \frac{C_m f_b \alpha}{F_b} \leq 1.0 \quad (2)$$

In Equations (1) and (2):

f_a = computed axial stress

F_a = axial stress permitted if axial force alone existed

f_b = computed bending stress

F_b = compressive bending stress permitted if bending moment alone existed

C_m = coefficient used to determine the uniform equivalent bending stress assumed to act over the member length

α = amplification factor equal to $\frac{1}{(1-f_a/F'_e)}$

$F'_e = \frac{149,000}{\left(\frac{KL}{r_x}\right)^2}$ where KL/r_x is the effective

slenderness ratio in the plane of bending.

F_y = specified minimum yield point of the steel.

Equivalent Uniform Moment

If the primary bending moment is not uniform over the member length, the strength of the column will be greater than that indicated by Equation (2) since the curvature will be reduced in the regions of low moment. To account for this strength increase, an equivalent bending stress factor is computed as

$$C_m = 0.6 + 0.4 M_1/M_2 \text{ for members in single curvature and}$$

$$= 0.6 - 0.4 M_1/M_2 \text{ for members in double curvature, but not less than 0.4.}$$

The above factors are for members prevented from translation, if sway is permitted,

$$C_m = 0.85.$$

The above procedures are routine for columns subjected to moments applied at the member ends, however, the application of these same procedures to transversely loaded members is not well known.

Design Procedures for Laterally Loaded Beam-Columns

A simply supported beam-column subjected to a concentrated transverse load, R , may be divided into segments as shown in Fig. 16. Each segment can then be treated as a beam-column of length $L/2$, subjected to an axial force, P , and an end moment M . The end of each segment translates through a distance, δ , and its rotation is θ measured from the chord.

Compatibility requires that the end rotation and the sway displacement be related by:

$$\theta = \frac{2\delta}{L}$$

and for equilibrium:

$$M = \frac{RL}{4} + P\delta$$

The beam-column subjected to lateral loads may be analysed as two segments subjected to end moments, therefore the design of such a member could be performed on the same basis. In the design procedure, each segment of the member would be checked against Eqns. 1 and 2. The moment used in computing f_b would be that at the segment end (RL/4 for a simply supported beam) and $C_m = 0.85$ since the segments in question are free to translate. The values of F_a and F'_e would be computed by using the effective length of the complete member.

Design Example

The member to be designed is shown schematically in Fig. 17. The design will be illustrated using the allowable stress technique.

Member Length 12'-0"
 Axial Force 90 kips
 Transverse Force 22 kips
 G40.12 steel $F_y = 44$ ksi

The resulting bending moment distribution is shown in Fig. 17.

Try 10WF33

$$\frac{KL}{r_x} = \frac{0.8 \times 144}{4.20} = 27.4$$

$$F_a = 25.4 \text{ ksi} \quad (16.2)$$

$$F'_e = \frac{149,000}{\left(\frac{KL}{r_x}\right)^2} = 198$$

$$\frac{64}{\sqrt{F_y}} = 9.7 \quad (14.4)$$

$$\frac{b}{2t} = \frac{7.96}{2 \times 0.433} = 9.2 < 9.7$$

Section Compact

$$F_b = 0.66 F_y = 29.0 \text{ ksi}$$

Check Lower Segment

$$f_a = \frac{P}{A} = \frac{90.0}{9.71} = 9.27 \text{ ksi}$$

$$f_b = \frac{M}{S} = \frac{45.6 \times 12}{35.0} = 15.6 \text{ ksi}$$

$$C_m = 0.85$$

Equation (1)

$$\frac{f_a}{0.60 F_y} + \frac{f_b}{F_b} \leq 1.0$$

$$\frac{9.27}{26.4} + \frac{15.6}{29.0} \leq 1.0$$

$$0.35 + 0.54 \leq 1.0$$

$$0.89 \leq 1.0 \text{ Satisfactory}$$

Equation (2)

$$\frac{f_a}{F_a} + \frac{C_{mf} f_b}{F_b \left[1 - \frac{f_a}{F_e} \right]} \leq 1.0$$

$$\frac{9.27}{25.4} + \frac{0.85 \times 15.6}{29.0 \left(1 - \frac{9.27}{198} \right)} \leq 1.0$$

$$0.37 = 0.49 \leq 1.0$$

$$0.86 \leq 1.0 \text{ Satisfactory}$$

Since the maximum bending moment on the upper segment is also 45.6' kips, the upper segment will be satisfactory by inspection and the 10WF33 is adequate to resist the applied forces.

Crane Columns

A crane column, free to translate at the crane rail bracket, may be treated in a manner similar to that discussed above for laterally loaded columns. An unbraced crane column is shown schematically in Fig. 18.

As the loads are increased, the column deforms as shown in Fig. 19. (depending on the relative values of the rotation and the translation at the crane rail bracket). In this figure, γ , represents the rotation of the member at the bracket, measured from the vertical; while Δ represents the translation of the rail bracket. As the load P_2 is increased, the column deforms causing an end moment, M_1 , to develop in the upper portion of the crane column, while the lower portion develops an end moment, M_2 . For the deformation pattern shown in Fig. 19 equilibrium requires that $P_{2e} = M_1 + M_2$ as indicated in Fig. 20.

The upper segment of the crane column shown in Fig. 18 is subjected to an axial load, P_1 and an end moment M_1 . Compatibility conditions at the bracket require that the end rotation of this portion of the column, θ_1 be equal to $\gamma - \Delta/L_1$, measured from the chord. This segment is shown in Fig. 21.

The lower segment of the crane column is subjected to an axial load equal to $P_1 + P_2$ and an end moment, M_2 . In this case the end rotation is given by $\theta_2 = \gamma + \Delta/L_2$ as shown in Fig. 22. For equilibrium of each segment (in the deformed position) the end shears on the upper and lower segments, H_1 and H_2 , can be computed; the algebraic sum of the shears must be equal to the horizontal load H ; as shown in Fig. 21.

Design Procedure for Crane Columns

The design procedure for a member used as a crane column consists of assuming a member size; dividing the member into segments at the crane rail bracket; then checking each segment of the member against

the interaction equations. Since each segment is free to sway $C_m = 0.85$. The values of F_a and F'_e are based on the total length of the column since it is over this length that the secondary moments will be developed.

Design Example

The column to be designed is shown in Fig. 23. The design will be performed using the allowable stress technique.

$$P_1 = 190 \text{ kips}$$

$$P_2 = 50 \text{ kips}$$

$$H = 5.0 \text{ kips}$$

$$L_1 = 132 \text{ inches}$$

$$L_2 = 210 \text{ inches}$$

$$e = 20 \text{ inches}$$

Try 12 WF 58

$$G 40.12 \text{ Steel } F_y = 44 \text{ ksi}$$

The bending moment distribution on the crane column is obtained from an elastic analysis and is shown in Fig. 23. The upper and lower portions of the column will be checked separately, however, the amplification factor, effective length and axial load capacity will be computed on the total column length as for the laterally loaded column.

$$\frac{KL}{r_x} = 0.8 \left(\frac{132 + 210}{5.28} \right) = 52$$

$$F_a = 22.1 \text{ ksi}$$

$$\left(\text{Based on } \frac{KL}{r} = 52 \right)$$

(16.3.2)

$$F'_e = \frac{149,000}{\left(\frac{KL}{r_x}\right)^2} = 55$$

$$F_y = 44 \text{ ksi}$$

$$b/2t = 10.01/(2 \times 0.64) = 7.8$$

$$64/\sqrt{F_y} = 64/\sqrt{44} = 9.7 > 7.8.$$

Section is Compact

$$F_b = 0.66 F_y = 29.0 \text{ ksi}$$

Check Upper Portion

$$f_a = \frac{P}{A} = \frac{190}{17.06} = 11.14 \text{ ksi}$$

$$f_b = \frac{M}{S} = \frac{197}{78.1} = 2.53 \text{ ksi}$$

Equation (1)

$$\frac{f_a}{0.60 F_y} + \frac{f_b}{F_b} \leq 1.0$$

$$\frac{11.14}{0.60 \times 44} + \frac{2.53}{29.0} \leq 1.0$$

$$0.51 \leq 1.0 \text{ satisfactory}$$

$$C_m f_b = 0.85 f_b = 0.85 \times 2.53 = 2.15 \text{ ksi}$$

Equation (2)

$$\frac{f_a}{F_a} + \frac{C_m f_b}{F_b \left[\frac{1 - f_a}{F'_e} \right]} \leq 1.0$$

$$\frac{11.14}{22.1} + \frac{2.15}{29.0 \left[1 - \frac{11.14}{55} \right]} \leq 1.0$$

$$0.60 \leq 1.0 \text{ O.K.}$$

The upper portion of the column is satisfactory.

Check Lower Portion

$$f_a = \frac{P}{A} = \left(\frac{190 + 50}{17.06} \right) = 14.10 \text{ ksi}$$

$$f_b = \frac{M}{S} = \frac{803}{78.1} = 10.26 \text{ ksi}$$

Equation (1)

$$\frac{f_a}{0.60F_y} + \frac{f_b}{F_b} \leq 1.0$$

$$\frac{14.10}{0.60 \times 44} + \frac{10.26}{29.00} \leq 1.0$$

$$0.89 \leq 1.0 \text{ O.K.}$$

$$f'_b = 0.85 f_b = 0.85 \times 10.26 = 8.71 \text{ ksi}$$

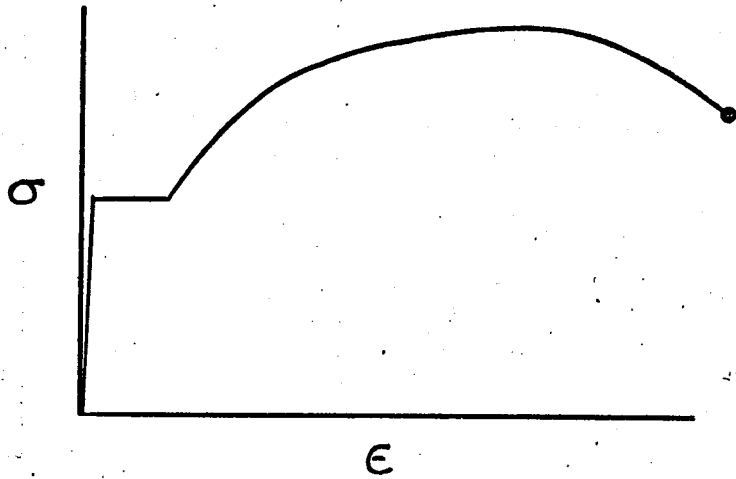
Equation (2)

$$\frac{f_a}{F_a} + \frac{C_m f_b}{F_b \left(1 - \frac{f_a}{F'_e} \right)} \leq 1.0$$

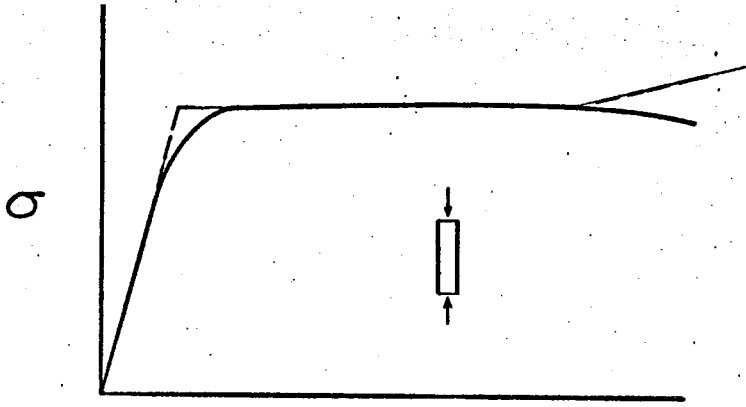
$$\frac{14.10}{22.10} + \frac{8.71}{29.00 (1 - 0.26)} \leq 1.0$$

$$1.05 > 1.0 \text{ NG.}$$

The top portion of the column is not satisfactory. Thus under the allowable stress rules the 12 WF 58 is not adequate to resist the applied loads and a stronger section should be checked.



ϵ
FIG. 1



ϵ
FIG. 3

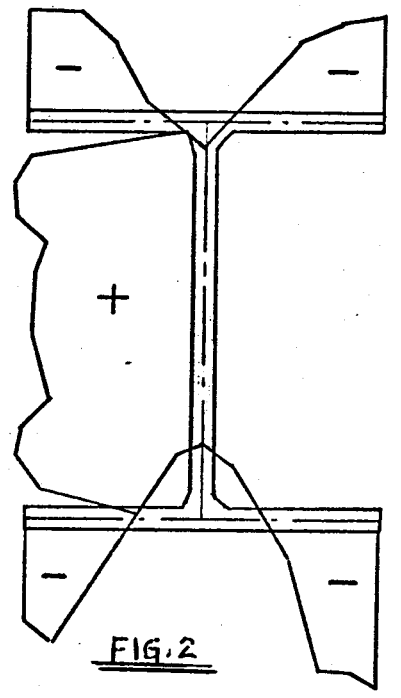
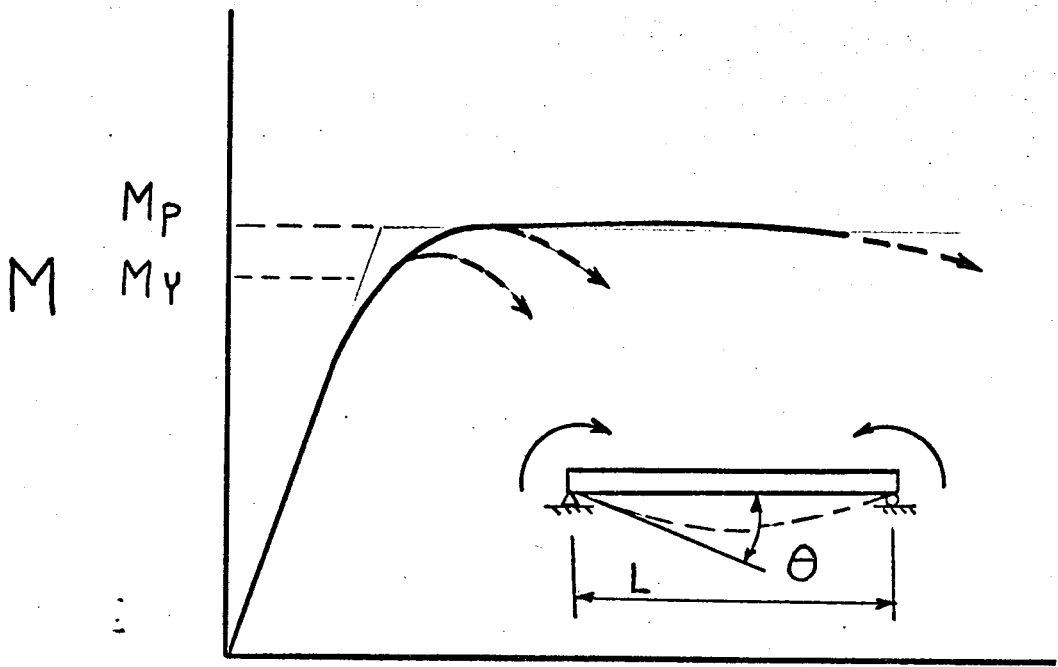


FIG. 2



θ
FIG. 4.

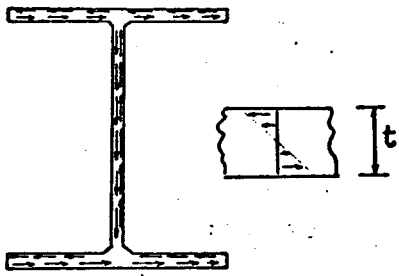


FIG 5

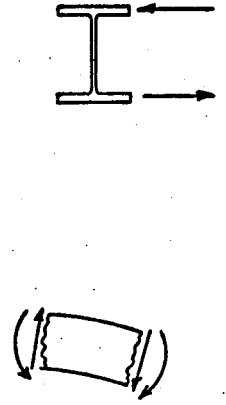
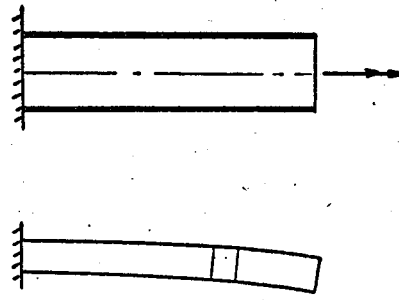


FIG. 6

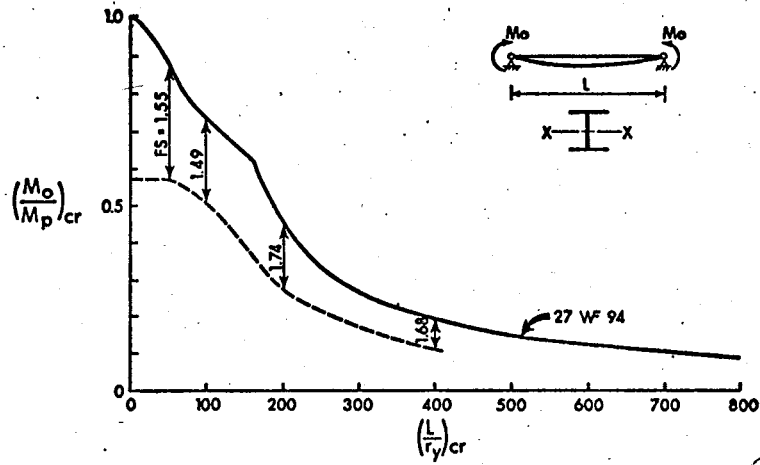


FIG 7

(NM) 7

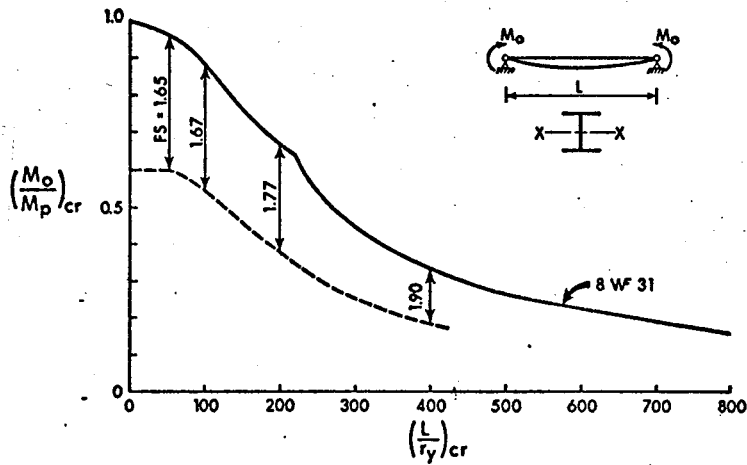


Fig. 8

(NM) 8

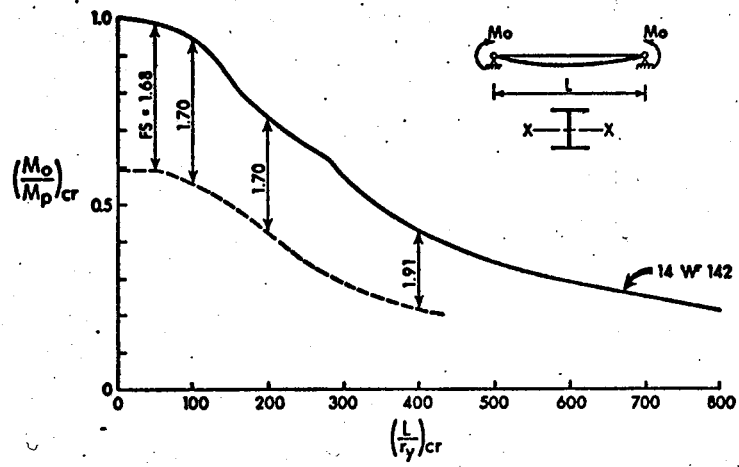


FIG. 9.

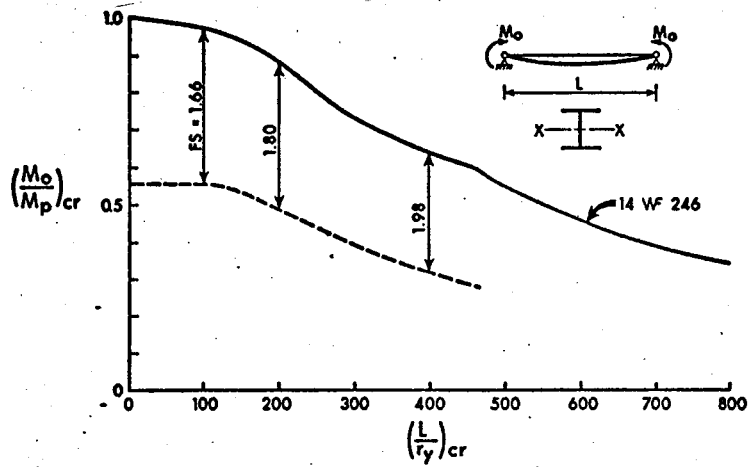


FIG. 10

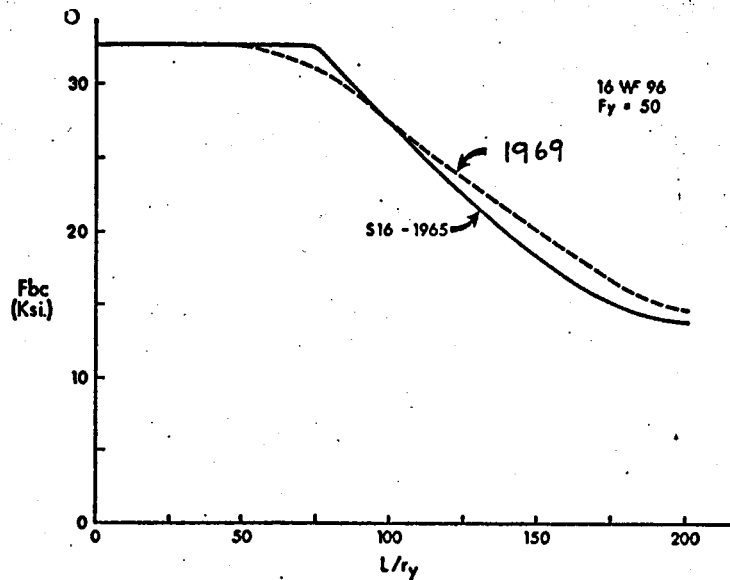


FIG. 11

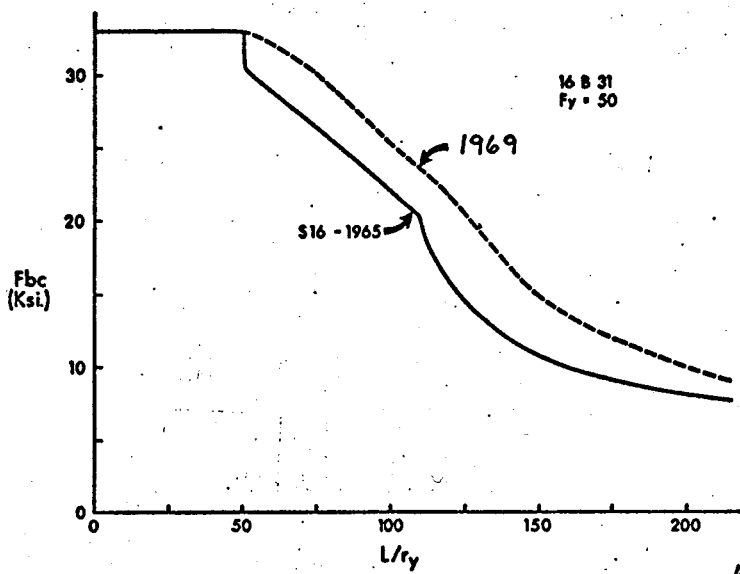


FIG. 12

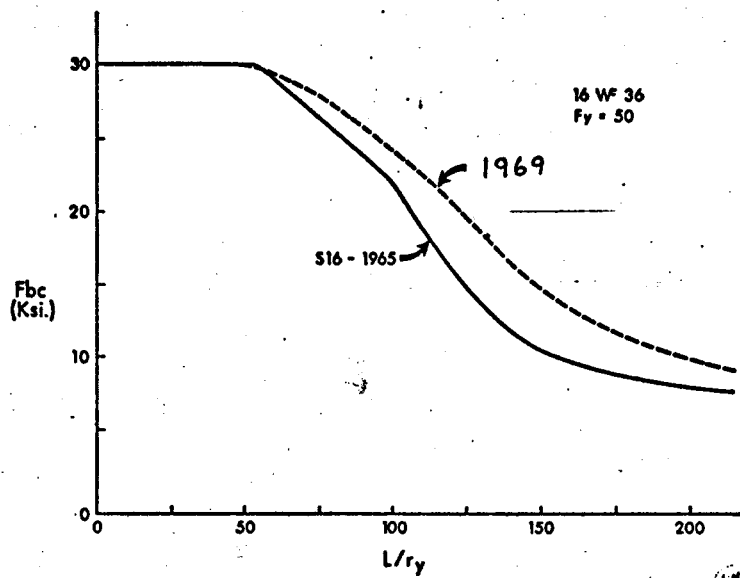


FIG. 13

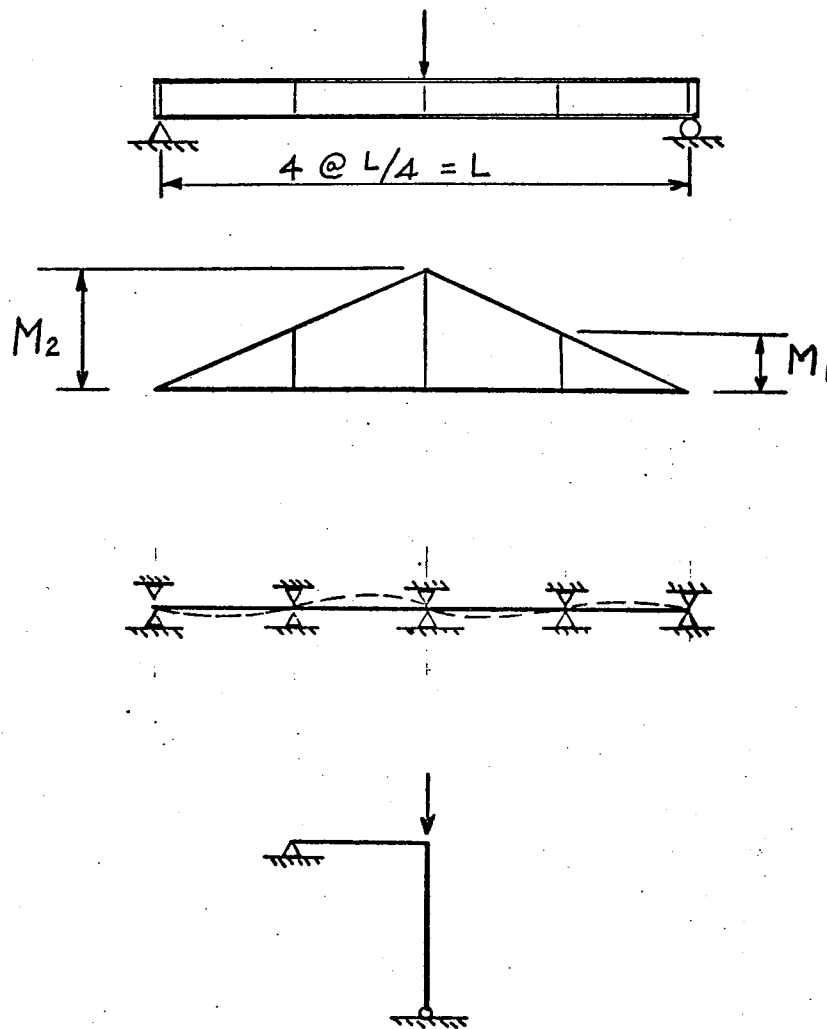


FIG. 14

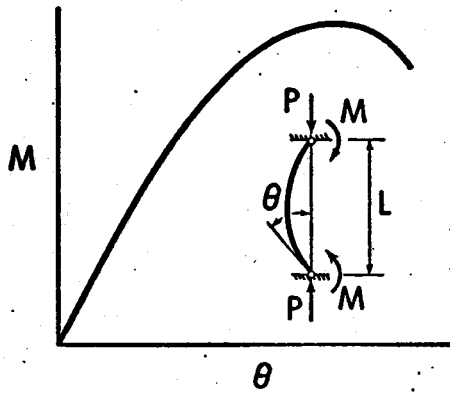


FIG. 15

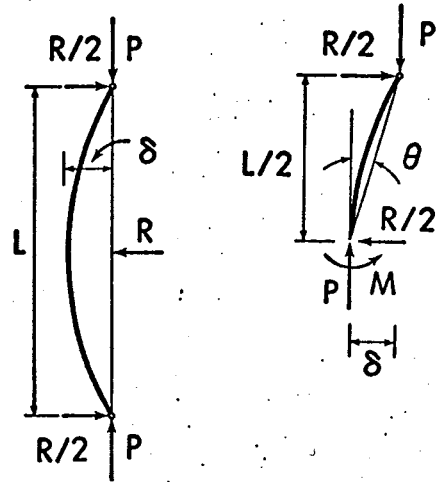


FIG. 16

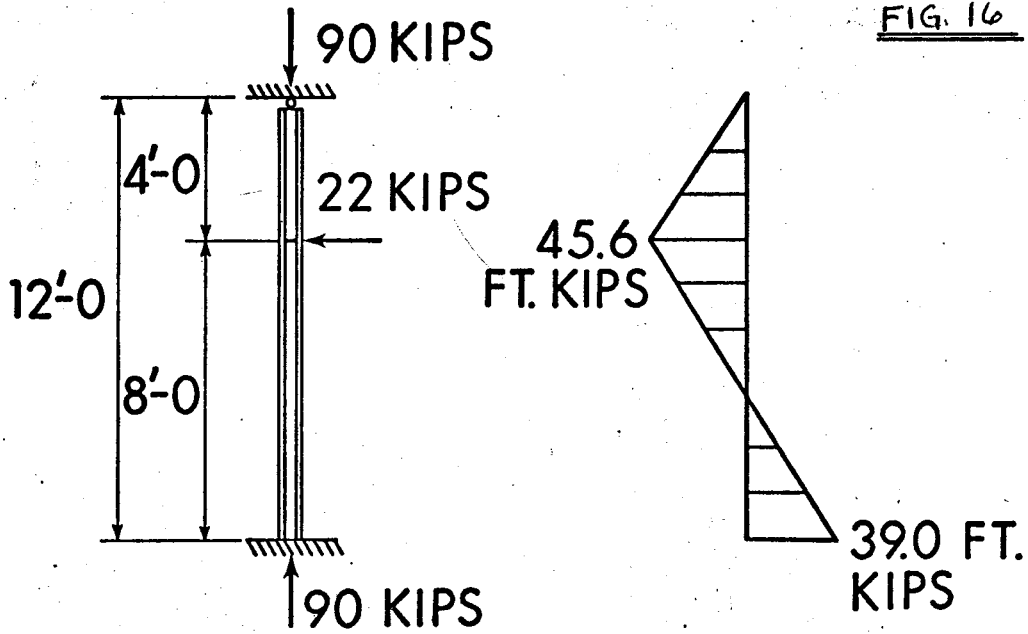


FIG. 17

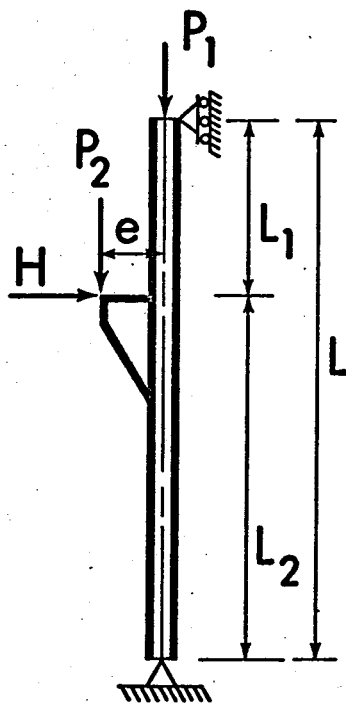


FIG. 18.

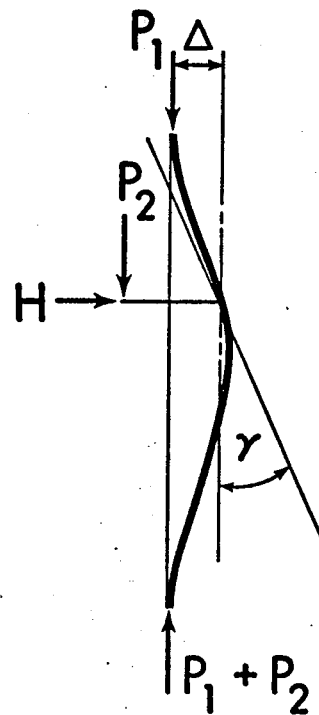


FIG. 19

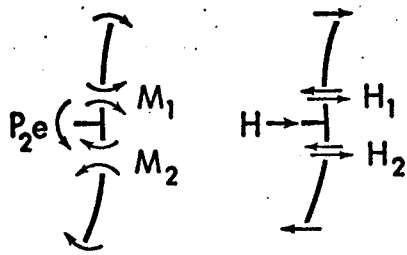


FIG. 20

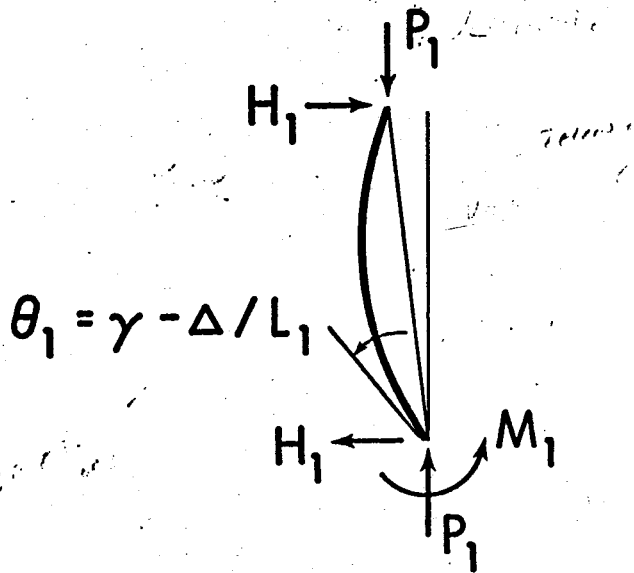


FIG 21

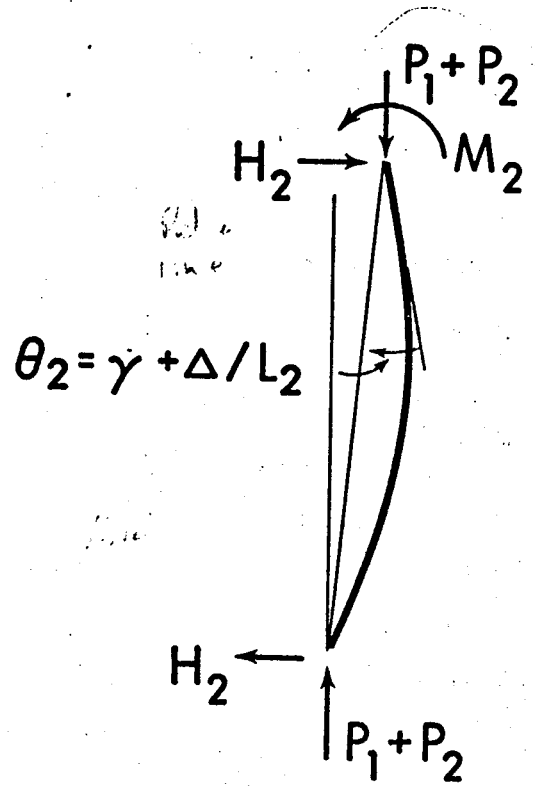


FIG 22.

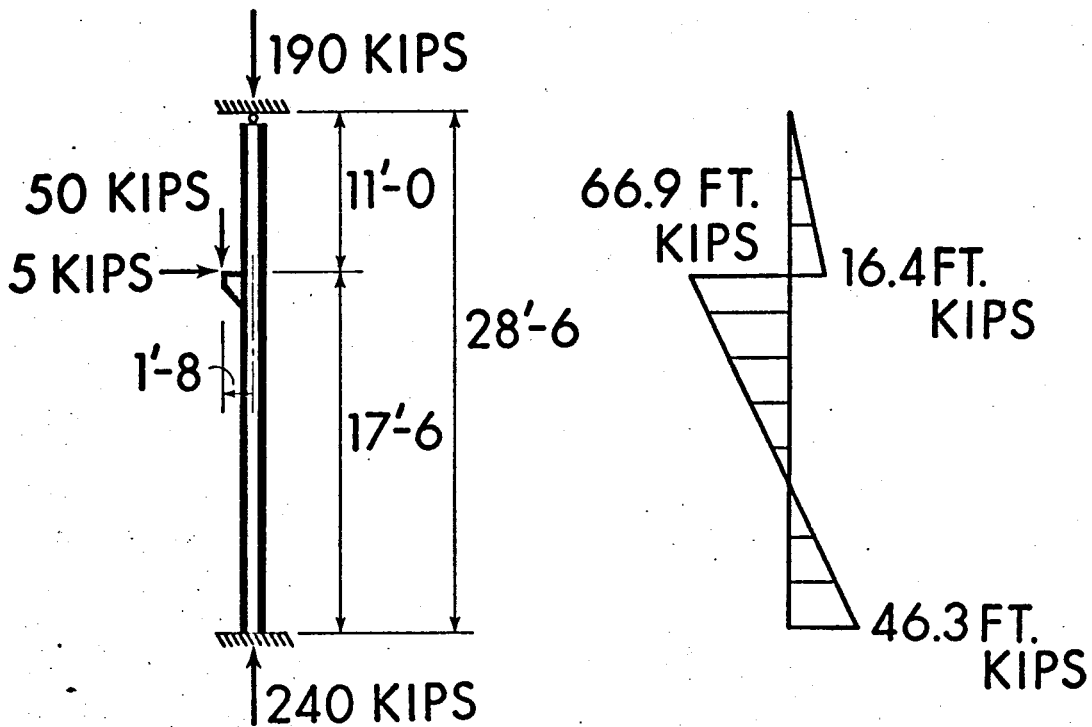


FIG. 23

Steel Structures for Buildings

LECTURE IV

Composite Members

J. Longworth

Composite Members

Introduction

As early as the 1920's investigations were conducted into the composite action of members in which the only shear connection was the bond between concrete and steel in cases where steel beams were either partially or completely encased in concrete. In the 1930's various types of mechanical shear connectors were developed in Europe to supplement bond in transferring shear. The 1944 Edition of the American Association of State Highway Officials Specifications included somewhat limited provisions for the use of certain mechanical connectors and composite construction rapidly became accepted for highway bridges.

The development of specifications for composite building member design followed somewhat later. In 1956 a Joint Committee of the American Society of Civil Engineers and the American Concrete Institute was organized to prepare recommendations for the design and construction of structures composed of prefabricated beams combined with cast-in-place slabs. The Committee reviewed existing information and practices and prepared a report entitled Tentative Recommendations for the Design and Construction of Composite Beams and Girders for Buildings. This report was published in 1960.

The Joint Committee report formed the basis for the section on Composite Beams in the 1965 edition of CSA Standard S16 which represented the first Canadian specification related to composite interaction achieved by mechanical shear connectors. The introduction of this design specification

has resulted in increasing use of composite beams in building structures. Experience has proven these designs to be economical even when only considering the composite action in positive moment regions. Increased stiffness of composite beams appreciably reduces deflections.

The 1965 Specification provided for composite action in positive moment regions. It included information on such items as effective width of concrete slab, differences between shored and unshored construction and design considerations for mechanical shear connectors. CSA Specification S16-1970 includes a number of revisions and additions to the section on composite design. Provision is now made for the design of steel - concrete composite beams in which the concrete slab is cast on cellular steel floor units. Requirements are provided for continuous beams. Certain changes have been introduced in the design of shear connectors.

Positive Moment Behavior

a) Elastic Behavior

After a steel beam has been erected, its lower flange is subjected to tension which can be calculated by general flexural theories. Immediately after casting, the slab which is still plastic adds no strength but merely dead load, increasing the lower flange stresses. After the slab has hardened, it becomes the top flange of the composite section; additional loads, causing further tension in the lower flange, are resisted by the entire composite section. However, this tension is less per unit load because the composite section is stronger. If the steel beam is

shored until the concrete has attained some desired level of strength, dead load of beam as well as superimposed load will be carried by composite action. Stresses due to loads carried in composite action may be computed on the basis of a transformed section in which the concrete slab is transformed into a hypothetical equivalent area of steel by multiplying the contributing slab width by the modular ratio E_s/E_c .

b) Effect of Creep

Under the action of continuous loads resisted by composite action, the concrete will creep. This results, in effect, in an increase of the modular ratio, producing a relaxation of the stresses in the concrete and an increase in the steel stresses.

c) Ultimate Moment

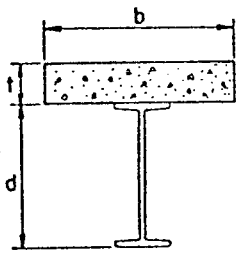
The behavior of composite beams loaded beyond the elastic range is significantly affected by the non-linear character of the load-slip curve for the connectors. Any analysis in the plastic range that also considers the nonlinearity of the load-slip curves is necessarily complicated and becomes too involved to be used in design. However, the computation of the ultimate moment on the basis of the plastic stress distribution is simple.

Ultimate strength is not affected by the method of construction i.e. shored or unshored construction. Assuming that sufficient number of shear connectors can be provided such that the flexural strength is not reduced by failure or deformation of shear connectors, the static ultimate strength of a composite beam may be determined from a simplified stress

distribution.

Case I corresponds to the stress distribution distinguished by the location of the neutral axis at ultimate load in the concrete slab. Case II is characterized by the location of the neutral axis at ultimate load within the steel beam.

Case I



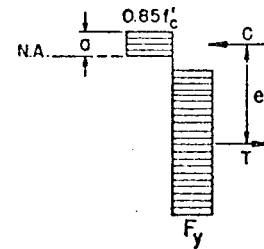
$$C = 0.85f'_c ba$$

$$T = A_s F_y$$

$$a = \frac{A_s f_y}{0.85f'_c b}$$

$$e = \frac{d}{2} + t - \frac{a}{2}$$

$$M_u = T e = A_s F_y \left(\frac{d}{2} + t - \frac{a}{2} \right)$$



Case II

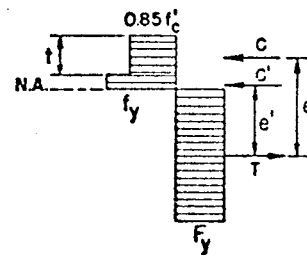
$$C = 0.85f'_c bt$$

$$T = C + C'$$

$$T + C' = A_s F_y$$

$$C' = \frac{A_s F_y - 0.85f'_c bt}{2}$$

$$M_u = C e + C' e'$$



With the normal proportions which occur in composite beams, failure under positive moment is initiated by yielding of the steel

section, progressing to the point where strains are of such a magnitude that the ultimate value of concrete strain ($e_{cu} = 0.03$) is reached and the concrete crushes. Figure 1 indicates typical behavior of a composite section in positive moment expressed in terms of the moment-curvature relationship.

Negative Moment Behavior

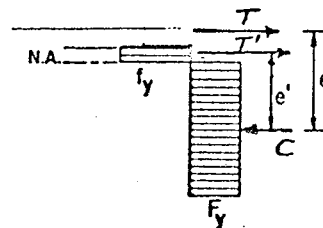
At relatively low values of load, the tension capacity of the concrete is reached and transverse cracks occur. Indeed shrinkage cracks may be present at the outset. Therefore moment capacity beyond that of the steel beam alone arises from the presence of longitudinal slab steel which is brought into interaction by means of the shear connectors.

If sufficient shear connectors are provided, behavior of the section will be essentially elastic in the lower range of load. The non-linearity of the load-slip curve will affect the behavior of the section and any analysis involving this feature is complicated. However conditions at ultimate moment may be expressed in simple plastic terms by considering the entire section (steel beam and longitudinal reinforcement) at the yield condition. This is identical to considering the simple plastic moment for a steel section. There are two possible conditions depending on the position of the neutral axis. However, only rarely will the neutral axis be located in the slab. For the case of the neutral axis below the slab the following relationships arise.

$$T = A_{sr} F_{yr}$$

$$C = T + T'$$

$$C + T' = A_s F_y$$



$$T' = \frac{A_s F_y - A_{sr} F_{yr}}{2}$$

$$M_u = T e + T' e'$$

In the above equations the values of e and e' are dependent on the geometry of the steel cross section. Figure 2 indicates typical moment-curvature relationships for composite beams in negative bending. Figure 3 indicates that longitudinal bars in the test beams reach yield before ultimate moment occurs.

Buckling Behavior

The flexural behavior of a composite section may be expressed in terms of the moment-curvature relationship or the load-deflection relationship. Typical results of tests on composite beams indicate moment-curvature relationships similar to those for plain steel beams. Ultimate load for positive moment test specimens is reached when the concrete crushes. However negative moment test specimens reach values of ultimate load related to buckling effects. If lateral buckling is prevented, local buckling will govern the magnitude of the ultimate moment. Because of the fact that a greater portion of the steel beam in a composite section in negative bending is subjected to compression than a plain steel beam, the buckling tendency for the composite section is increased. This may result in decreased curvature capacity. Tests performed at the University of Alberta indicate that ultimate moments greater than simple plastic moment values are attained in negative moment specimens in which sufficient shear connectors are employed to create yielding of the slab reinforcement at ultimate conditions. However light beam sections which still qualify as compact sections when considered as plain beams

tend to have reduced rotation capacity when employed in composite sections. See Figure 4. This reduced rotation capacity results in decreasing values of the ratio M_u/M_p with increasing area of longitudinal slab steel.

Shear Connectors

In order to attain the ultimate moment capacity defined previously in the discussion of behavior, there are certain minimum shear connector requirements which must be maintained. For example, consider the case of positive moment. From the section of zero moment to the section of ultimate moment the following values of total shear act on the shear connectors between the two sections.

Case I (Neutral axis in slab)

$$V_u = T = A_s F_y$$

Case II (Neutral axis below slab)

$$V_u = C = 0.85F'_c A_c$$

In the case of negative moment, from a section of zero moment to a section of maximum moment, at ultimate conditions the shear to be resisted by shear connectors between the two sections is $V_u = A_{sr} F_{yr}$ in order that the full capacity of the longitudinal slab reinforcement be developed.

In both positive and negative cases, for equilibrium

$$V_u = \Sigma q_u$$

for the minimum number of shear connectors required. Σq_u represents

the sum of the ultimate strengths of the shear connectors in the length being considered.

Headed stud shear connectors have been evaluated in both push out and beam tests. Results indicate that for ratios of height to diameter of stud greater than 4, the ultimate capacity may be expressed by the relationship

$$q_u = 930 d_s^2 \sqrt{f_c}$$

For smaller H/d ratios q_u decreases. Concrete strengths of 3,000 psi and higher will develop the full strength of the studs.

Effect of Slip

Early studies from the point of view of elastic design based the useful capacity of connectors on a maximum allowable slip of 0.004 inches maximum. The useful capacity of connectors was then determined from tests to be the load which would cause this amount of slip. From beam tests to ultimate load it is apparent that slips much larger than 0.004 inches can be tolerated. It appears that the only limitation on the amount of slip allowed at ultimate load is the amount which connectors can deform without failure. Values for this can be obtained from push-out tests. Slip is not a matter of serious concern in the design of composite structures for static loads.

Slabs on Cellular Steel Floor Units

The characteristics of composite beams incorporating cellular floor units with ribs transverse to the span differ from those of composite beams with full concrete slab. One of the major differences is the stiffness of the shear connectors. The presence of open cells in the slab reduces the stiffness. This reduced stiffness results in a loss of interaction and reduced efficiency of the composite beam. In addition to reduced stiffness, the presence of hollow cells in the slab results in a lower ultimate shear connector strength when compared to a solid slab.

Tests indicate that the degree of interaction achieved and the mode of cracking is influenced by the geometry of the ribs. Results of tests at McMaster University (see Figures 5 and 6) indicate that with a rib height-to-width ratio greater than one, cracking of the ribs occurred in the elastic range. With a ratio equal to one, cracking closely followed the onset of local yielding of the beam. With a ratio less than one, a load in excess of first yield load can be achieved.

Provisions of CSA S16 - 1969

a) Flexural Provisions

CSA S16 - 1969 provides for the design of continuous composite beams. The effective slab which may be considered in both positive and negative regions for slabs extending on both sides shall not exceed one-

fourth the beam span, the flange width of the steel beam plus 16 times the slab thickness or the average distance from the centre of the steel beam to the centres of adjacent steel beams.

The code requires that slab reinforcement be provided not only to support loads but also to control cracking both parallel and transverse to the span. Reinforcement parallel to the beam and within the effective slab width may be included in computing the properties of the composite section resisting negative moment. Such reinforcement must be adequately anchored by embedment in concrete which is in compression.

The flexural stress provisions are essentially based on working stress conditions. The section properties of the composite section are computed according to elastic theory, neglecting any concrete area in tension. The transformed area of concrete in compression in terms of equivalent area of steel is determined by dividing by the modular ratio E_s/E_c . Loads are considered in terms of the strength of concrete at the time of their application - those applied prior to and those applied subsequent to the time when the concrete has reached 75% of its required (28 day) strength.

The steel beam alone must adequately support loads applied prior to hardening of the concrete at stresses normally assigned to plain beams. Unshored as well as shored construction may be considered to carry superimposed loads in composite action and stresses are computed

on the basis of total load being carried by composite action. This provision is based on the fact that there is no significant difference in ultimate moment capacity for shored and unshored construction. In order to ensure that an unshored beam designed on the basis of total load carried by composite action, will not be deficient in strength of the steel section alone for loads before the concrete attains adequate strength, the code requires a limit on the value of S_{tr} in unshored construction as follows

$$S_{tr} = S_s \left(1.35 + 0.35 \frac{M_L}{M_D} \right)$$

where M_L = moment caused by loads applied subsequent to the time when the concrete has reached 75% of its required strength

M_D = moment caused by loads applied prior to the time when the concrete has reached 75% of its required strength

S_s = section modulus (referred to tension flange) of the steel beam

S_{tr} = section modulus (referred to tension flange) of the transformed composite section

This provision ensures that the unshored steel beam will not be stressed above approximately $0.82F_y$.

b) Shear Connection

Connectors required to produce full composite action in positive moment are designed on the basis that at ultimate load they must resist a total horizontal shear between the zero moment and maximum moment sections equal to

$$V_h = A_s F_y$$

$$\text{or } V_h = 0.85f'_c bt$$

whichever is the lesser value.

In a negative moment region where suitably anchored longitudinal reinforcement is considered to act compositely with the steel beam, the total horizontal shear to be resisted at ultimate load between zero moment and maximum moment sections is

$$V_h = A_{sr} F_{yr}$$

The number of connectors N_u is determined on the basis of

$$N_u = V_h / q_u$$

c) Incomplete Composite Action

If the number of connectors used is less than the number required for full composite action, the resulting section will have a moment capacity between that for the steel beam alone and the fully developed composite section. The code considers this effect by relating

the section modulus of the tension flange as a function of the resistance of the shear connectors. The increase in section modulus is considered as directly related to increase shear resistance. This results in the relationship

$$S_{\text{eff}} = S_s + \frac{V'_h}{V_h} (S_{\text{tr}} - S_s) \quad (\text{see figure on p. 14})$$

where S_{eff} = section modulus of the tension flange for a section in which the horizontal shear resistance is V'_h

The horizontal shear resistance is directly related to the number of shear connectors provided.

$$\frac{V'_h}{V_h} = \frac{N'}{N_u}$$

The above relationships are useful in two regards. If fewer than the number of shear connectors required for full composite action are provided, partial composite action is produced. The code permits this condition and requires that the transformed section used in computation of stresses be modified by considering the effective width of concrete reduced by the ratio N/N_u where

N = number of shear connectors provided

and N_u = number of connectors required for full composite action

Further, the code requires the determination of the number of

shear connectors between any concentrated load in that region and the nearest point of zero moment.

For full composite action

$$S_{\text{eff}} = S_s + \frac{V'_h}{V_h} (S_{\text{tr}} - S_s)$$

$$= S_s + \frac{N'}{N_u} (S_{\text{tr}} - S_s)$$

$$\frac{S_{\text{eff}}}{S_{\text{tr}}} = \frac{S_s}{S_{\text{tr}}} + \frac{N'}{N_u} \left(1 - \frac{S_s}{S_{\text{tr}}}\right)$$

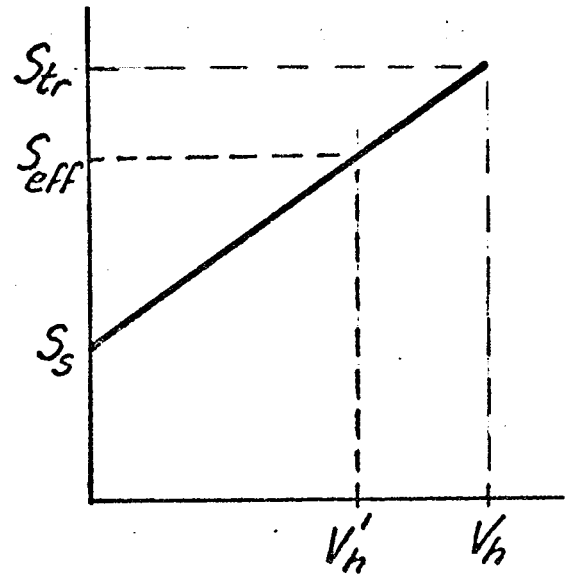
but $\frac{S_{\text{eff}}}{S_{\text{tr}}} = \frac{M}{M_{\text{max}}}$

$$\frac{N'}{N_u} = \left(\frac{M}{M_{\text{max}}} - \frac{S_s}{S_{\text{tr}}} \right) \left(\frac{1}{1 - \frac{S_s}{S_{\text{tr}}}} \right)$$

$$N' = N_u \left[\frac{\frac{M}{M_{\text{max}}} - \frac{S_s}{S_{\text{tr}}}}{1 - \frac{S_s}{S_{\text{tr}}}} \right]$$

Let $\beta = \frac{S_{\text{tr}}}{S_s}$

$$N' = N_u = \left[\frac{\beta \frac{M}{M_{\text{max}}} - 1}{\beta - 1} \right]$$



For incomplete composite action, if the number of connectors provided between zero and maximum moment sections is N , then

$$N' = N \left[\frac{\beta M - 1}{M_{max} \beta - 1} \right]$$

The Code sets limits on the use of incomplete composite action. In determining load-carrying capacity, no composite action is to be assumed if $N < 0.5 N_u$. In deflection computations, no composite action is to be assumed if $N < 0.25 N_u$.

For incomplete composite action, stresses are based on a reduced effective slab width

$$b' = \frac{N}{N_u} b$$

where b' = effective slab width for incomplete composite action based on N connectors
 b'' = effective slab width for complete composite action

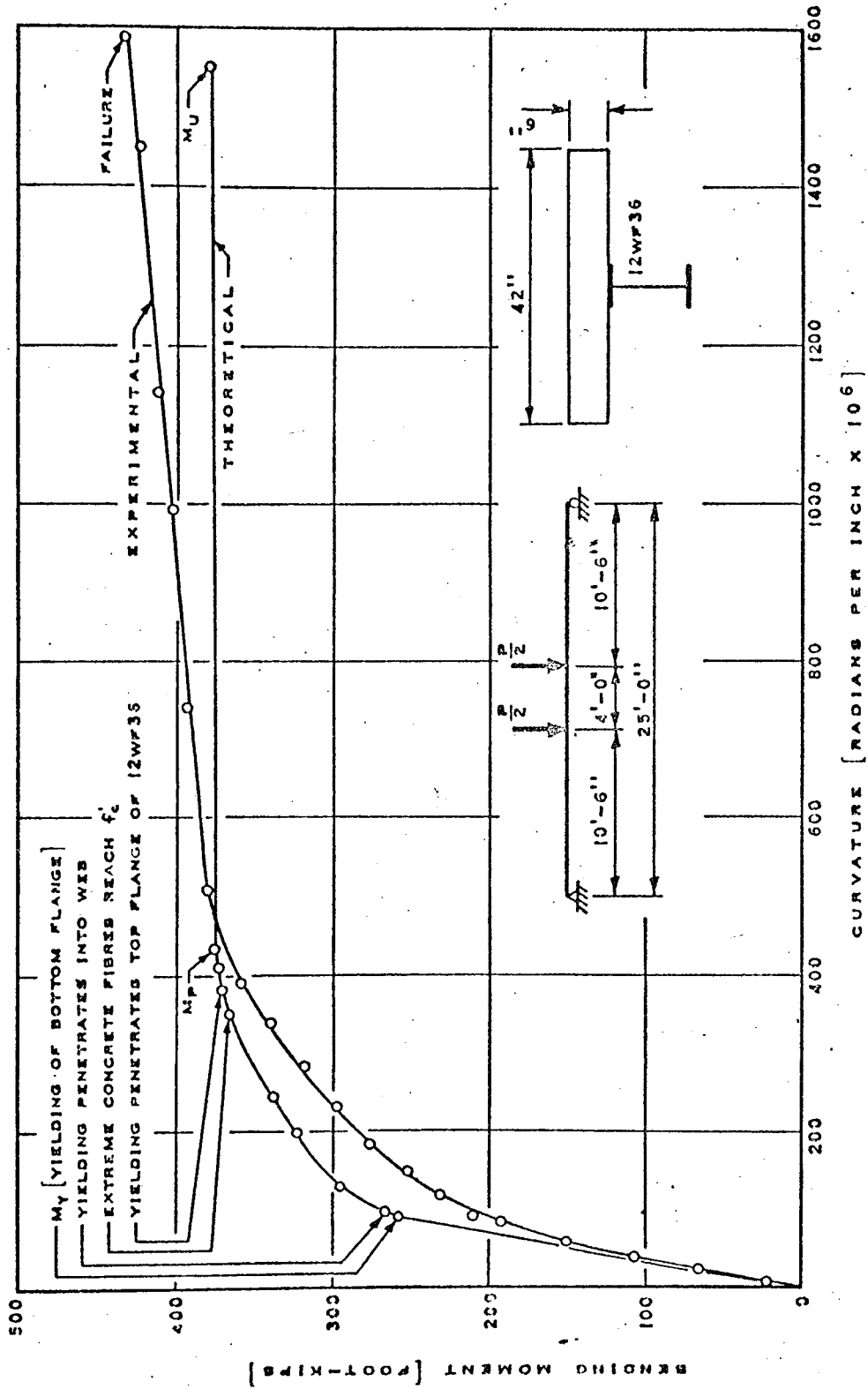
d) Shear Connector Details

Shear connectors are required to be embedded in concrete for their full length and must have at least 1 inch of concrete cover. The diameter of welded studs must not exceed 2.5 times the thickness of the part to which it is welded. Maximum spacing of shear connectors parallel to the span must not exceed 24 inches unless greater spacing can be justified by analysis and verified on the basis of a suitable test program.

e) Slabs on Cellular Floor Units

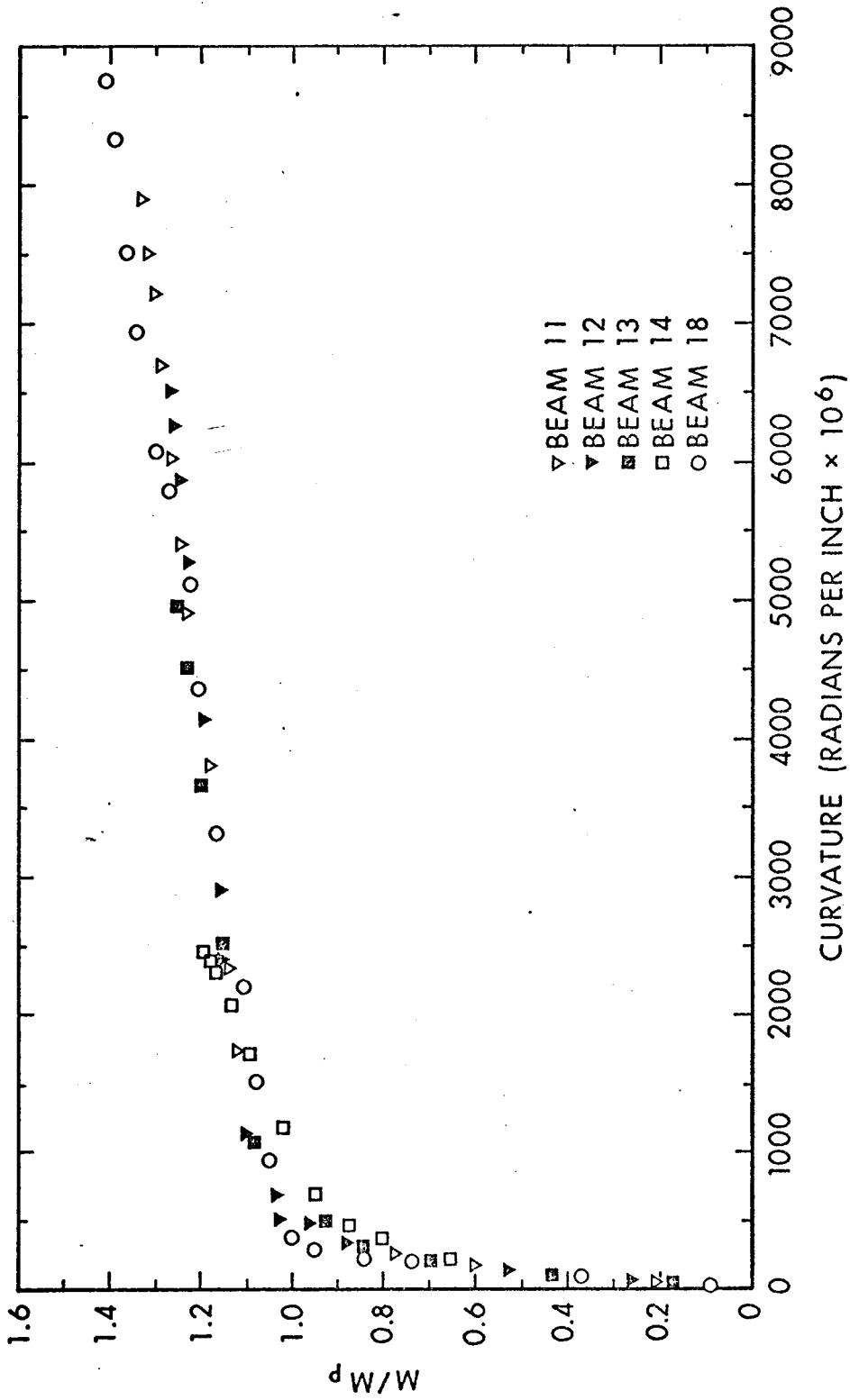
For certain rib dimensions it is permissible to ignore the effects of the ribs and consider the full thickness of the concrete as effective. If the rib dimensions are such as to result in reduced efficiency of the shear connectors, the effective slab thickness must be reduced to the clear thickness above the ribs. In all cases limitations are placed on maximum rib height, minimum width of concrete rib and maximum spacing of connectors. Requirements are summarized in Figure 7.

The 3/4 inch welded stud is the only connector which has been extensively investigated in tests of composite beams with cellular steel deck. Therefore the code only includes shear values for this unit. A 3/4 inch welded stud, 3 inches long is assigned an ultimate shear capacity of 19 kips.



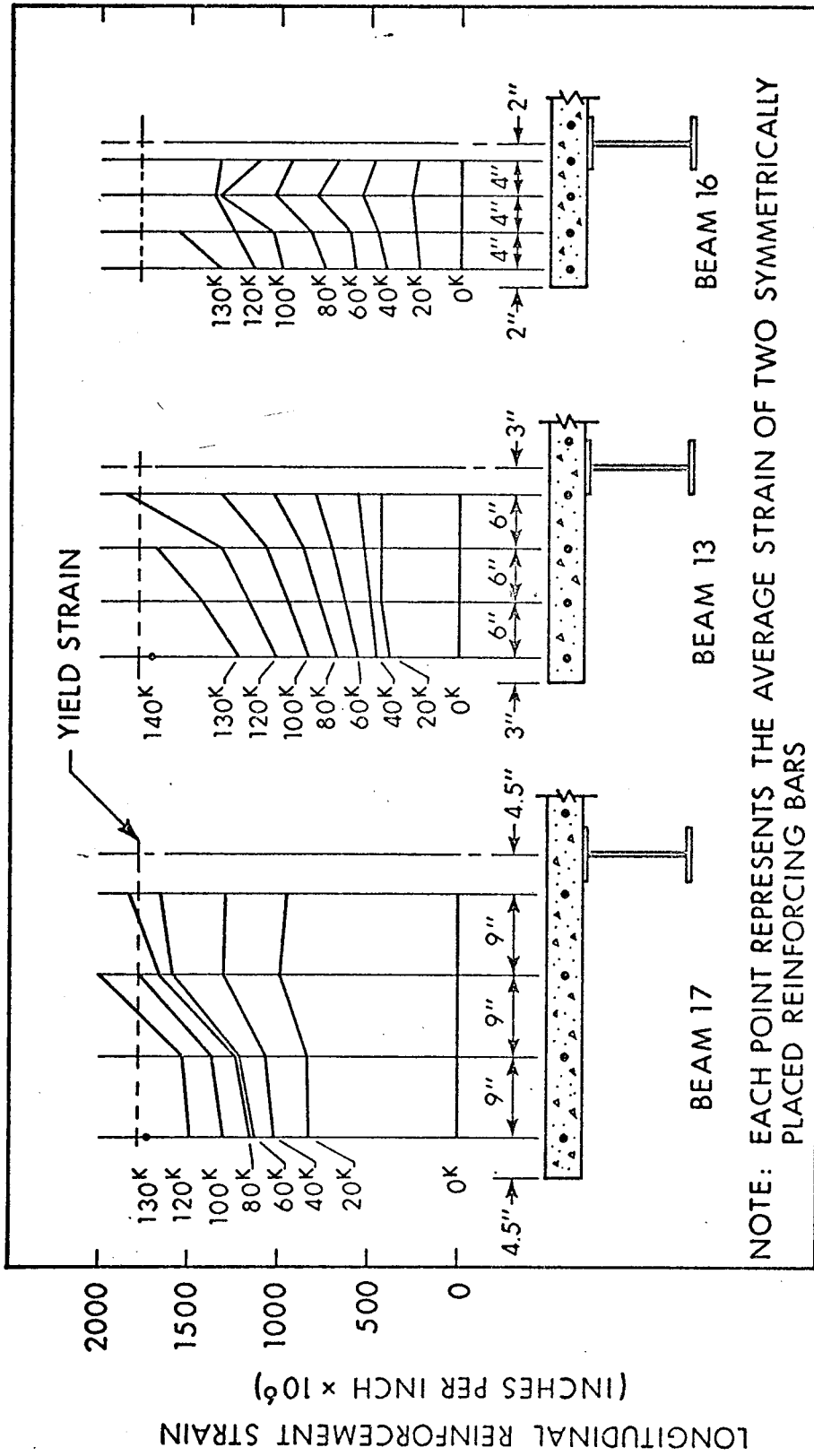
THEORETICAL VS. EXPERIMENTAL MOMENT CURVATURE RELATIONSHIP - BEAM BFI

FIGURE 1



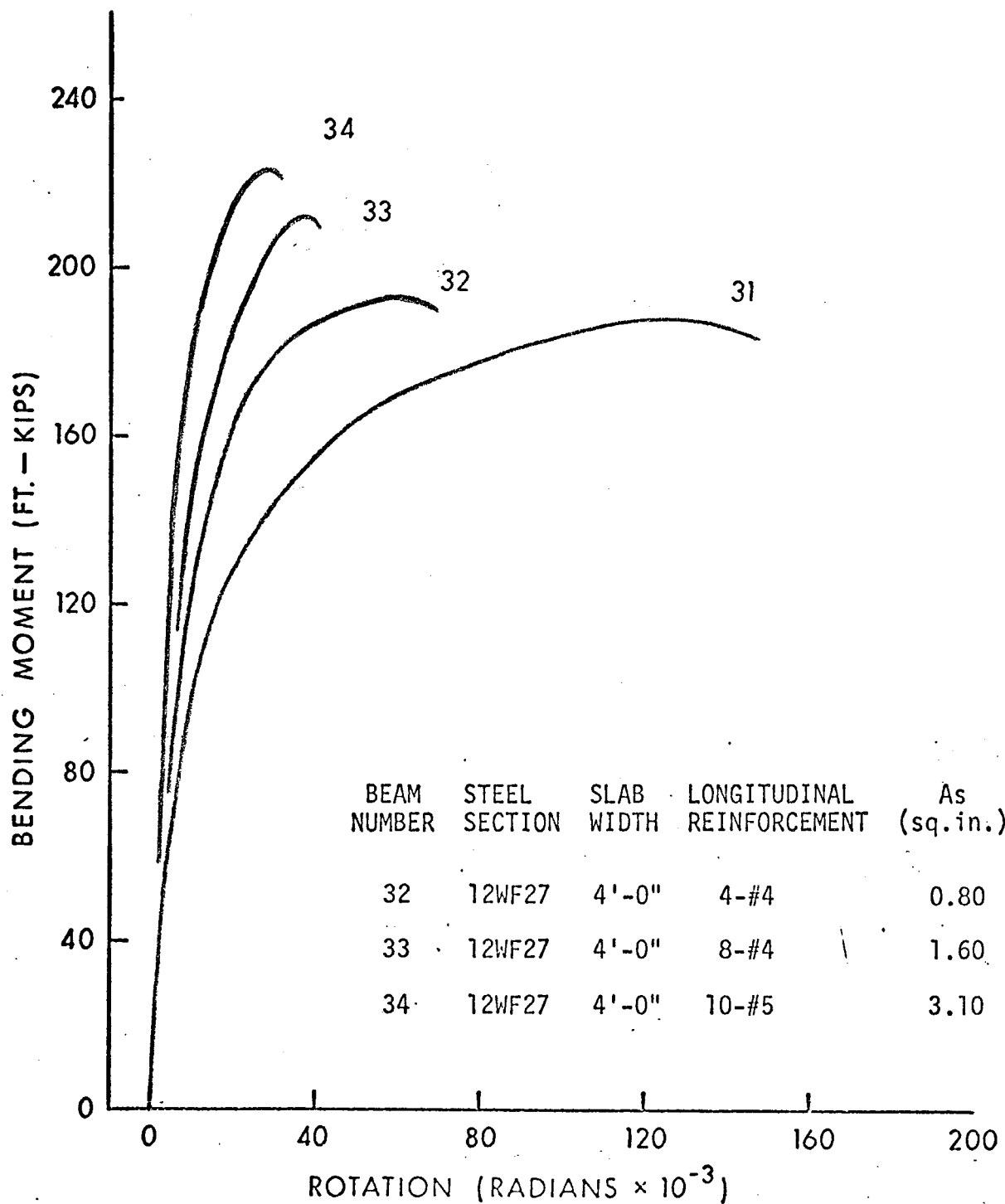
MOMENT CURVATURE RELATIONSHIPS

FIGURE 2



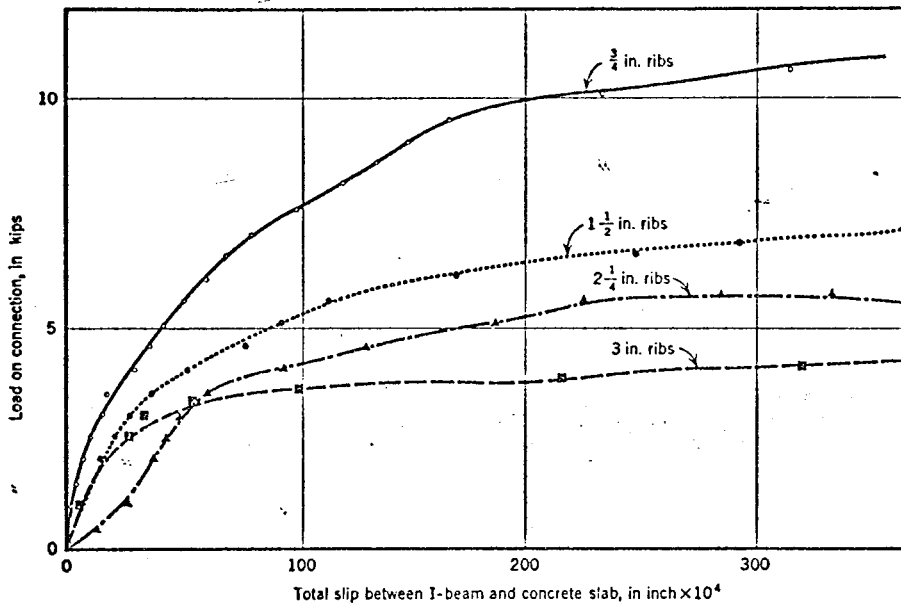
LONGITUDINAL REINFORCEMENT STRAINS AT MIDSPAN

FIGURE 3



MOMENT - TOTAL ROTATION
RELATIONSHIPS

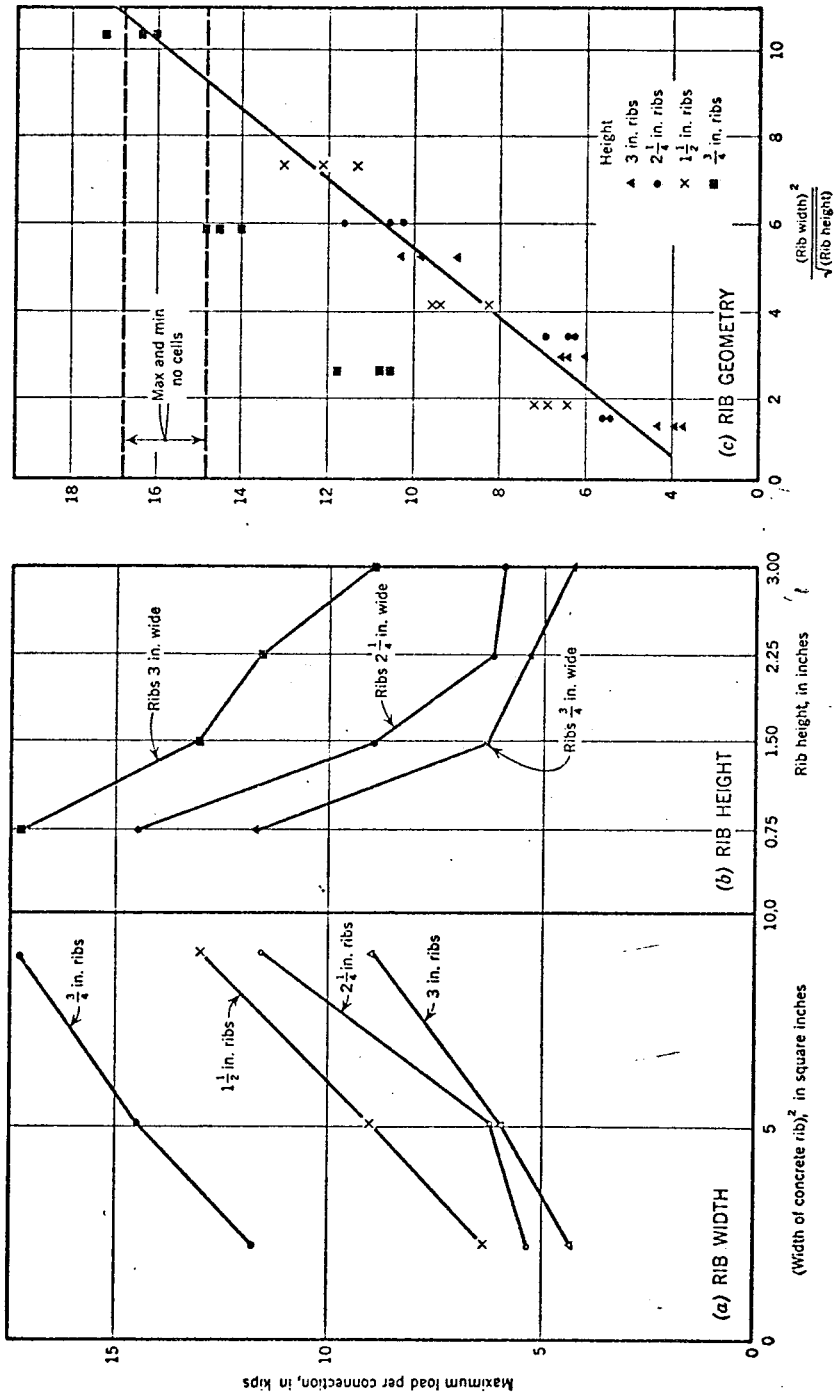
FIGURE 4



TYPICAL LOAD-SLIP CURVES FOR PUSH-OUT SPECIMENS

Rib width = 1 1/2"
 Varying rib height

FIGURE 5



INFLUENCE OF RIB GEOMETRY ON STRENGTH OF PUSH-OUT SPECIMENS

FIGURE 6

CSA S16-1969

COMPOSITE BEAMS WITH CELLULAR DECK

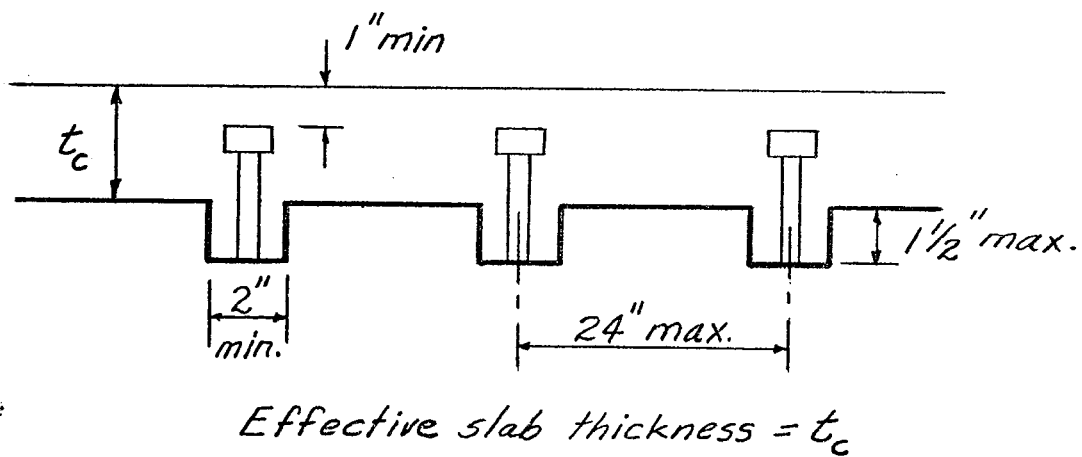
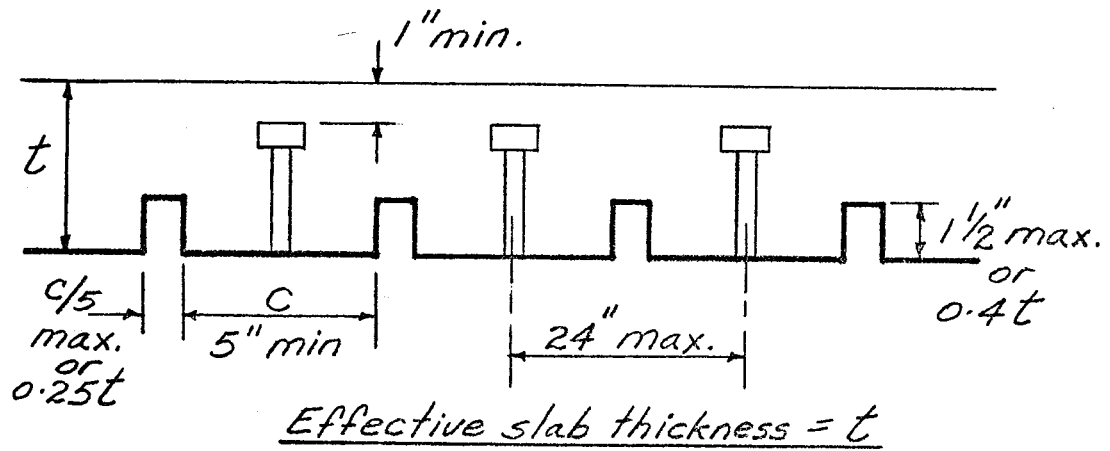


FIGURE 7

Steel Structures for Buildings

LECTURE V

Connection Behavior

G.L. Kulak

Connection Behavior

In Lecture II of this series, the basic behavior of two common fastening elements was presented. This included a discussion of the factor of safety against failure of individual elements, either high-strength bolts or fillet welds. Although S16 does not specifically include the design of various types of connections, I believe that it is now important that we go on and look at a number of common connection types in order to see what the factor of safety is when the fasteners are arranged in practical configurations.

1. Axially Loaded Connections: Long Joints

In tension or compression splices that are loaded axially, the main concern in the past has been with regard to long joints. Using an elastic theory, early researchers showed that, in a bolted or riveted joint for example, the end fasteners would be loaded higher than the interior ones. It was realized that a good deal of inelastic behavior has occurred by the time of failure, however, and the rationale was that this inelastic behavior would tend to equalize the fastener loads. About ten years of research into this problem has been conducted, mostly at Lehigh University, and it has shown that just the opposite is true. As the material in the joint becomes inelastic, the high loading of end fasteners becomes accentuated and the stress in these fasteners can be substantially above the average stress of all fasteners in the joint. Since we have been designing this type of connection on the assumption that all fasteners

do share the load equally, this means that our largest and most important joints have been designed with the lowest factor of safety. As an illustration, Fig. 1 shows the factor of safety of A325 bolts in A36, A440, and A514 steels with the bolts proportioned for the current allowable shear stress of 22 ksi. There are a number of inconsistencies which result from present design practice, notably that shorter joints have a greater factor of safety than longer ones, and that the factor of safety depends upon what type of steel is being fastened. There is no simple way to eliminate these inconsistencies but increasing the allowable bolt stress does reduce the variations involved. An increase in the allowable shear stress to 30 ksi for A325 bolts and to 40 ksi for A490 bolts would still provide an adequate factor of safety for long joints at the same time as minimizing the unrealistic variation of factor of safety with length and with material grade. Direction for higher allowable bolt shear stresses will probably have to come from the Research Council on Riveted and Bolted Structural Joints. Most of the information on high-strength bolts in S16 comes from this source. I expect that the Council will be looking at this question in the next year or so.

Studies into the strength of long joints which use fillet welds have indicated that the strength of the weld is not as seriously affected by joint length as are the bolts in similar joints. In a 50 in. long joint using intermittent fillet welds, the factor of safety is about 3.3. This indicates that the increased allowable weld stresses permitted by S16 still incorporate an adequate factor of safety.

2. Eccentrically Loaded Connections

Connections in which the line of action of the load does not pass through the center of gravity of the fastener group occur frequently in practice. Some examples, as seen Fig. 2, are bracket connections, girder web splices, and beam to column connections using web framing angles.

Whether bolts or welds are used as the fastening element, the approach that is used currently assumes that the fastener response is elastic. This is covered in most textbooks on steel structures and is the basis of design tables such as those in the CISC Handbook.

An extensive program of both analytical studies and experimental work has been carried out in Canada on this type of connection. Both welded and bolted connections were considered and in each case the actual load-deformation response of the fastener was used, rather than some idealized one.

The factor of safety resulting from the use of CISC tabular values for A325 bolted connections of this type is shown in Fig. 3. These were the specific connections tested in the program mentioned. The factor of safety, although higher than necessary and somewhat inconsistent, is perhaps not excessive. However, use of the analytical expressions that have been developed and a higher allowable bolt shear stress would allow both a constant factor of safety and one of reasonable level to be obtained.

Similar information has been obtained for eccentrically loaded connections using welds. Both vertical line welds and C-shaped configurations were tested in the program. As Fig. 4 shows, the factor of safety is clearly excessive, even at the recently increased allowable shear stress levels for fillet welds. The minimum factor of safety for the case of vertical line welds for the full range of values tabulated in the CISC Handbook is about 5.0. Fig. 5 shows similar information for the C-shaped welds tested. Again, the minimum factor of safety is about 5.0. Although the factor of safety for welds probably should be in excess of that for high-strength bolts, it is apparent that more economical welded connections of this type are possible.

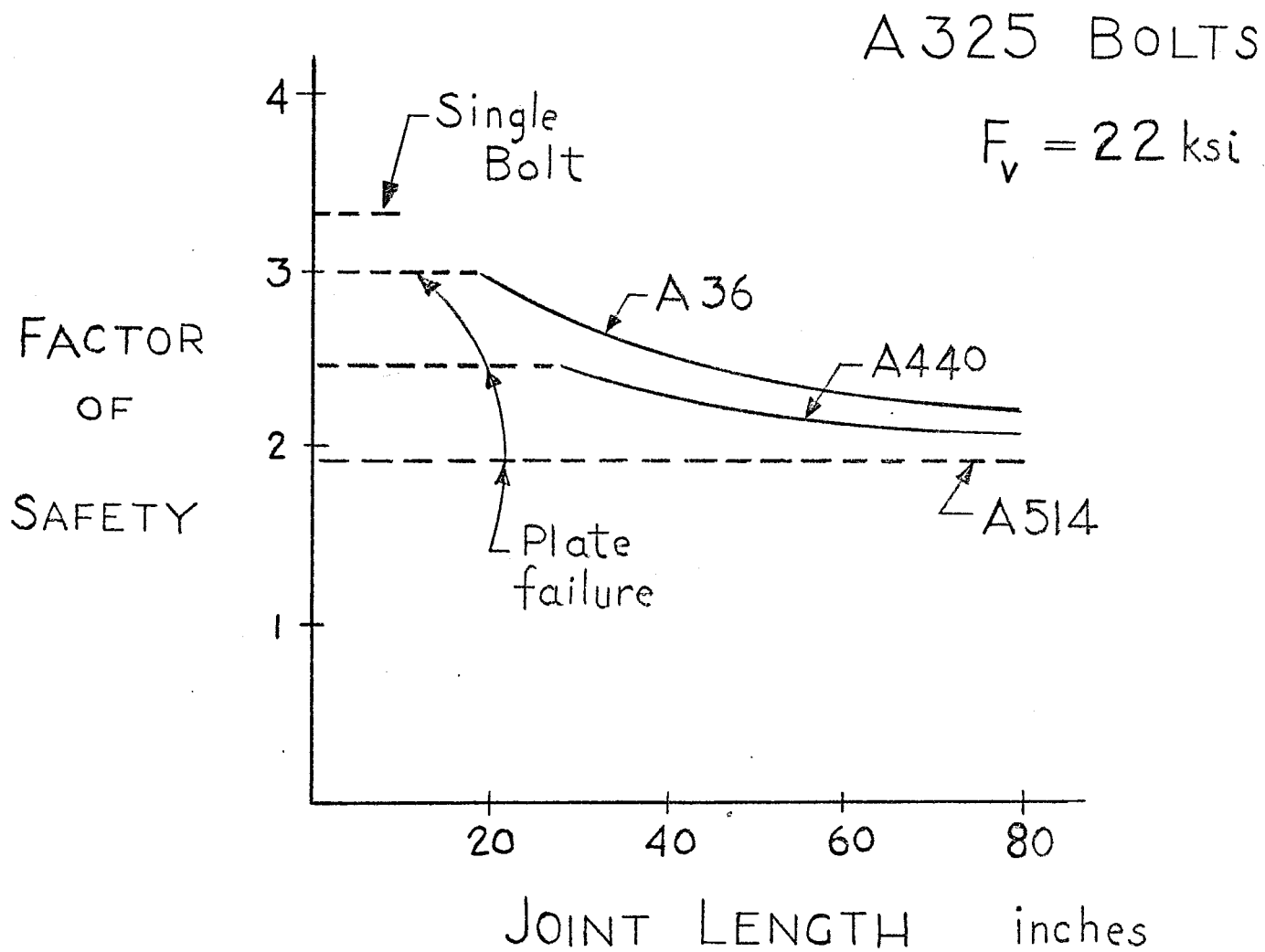


Fig. 1

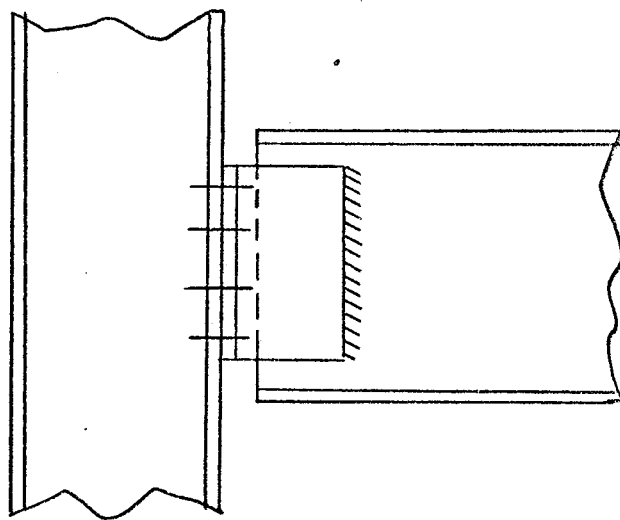
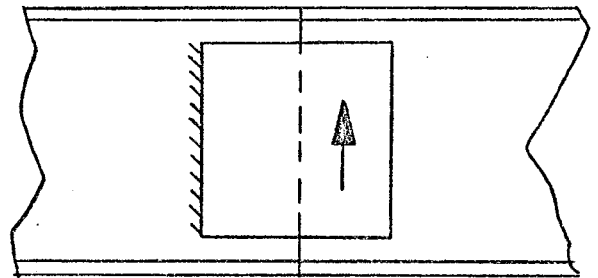
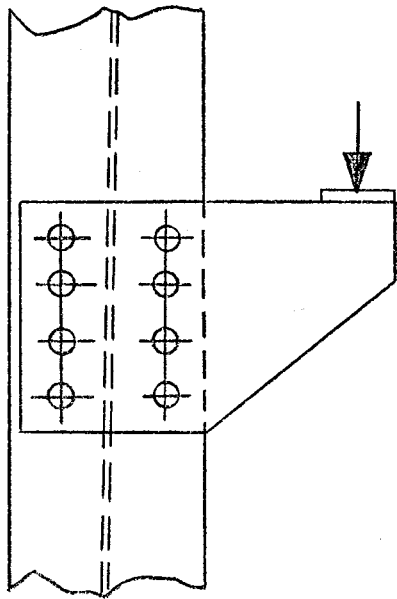
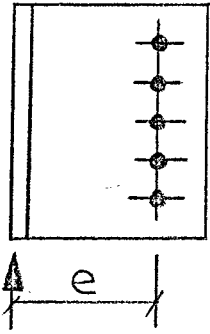
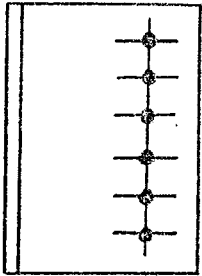
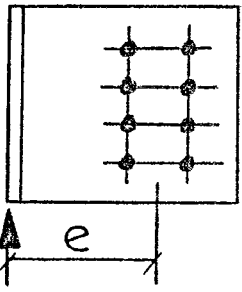
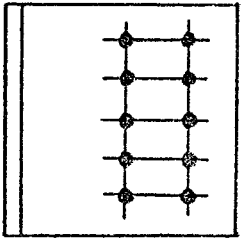
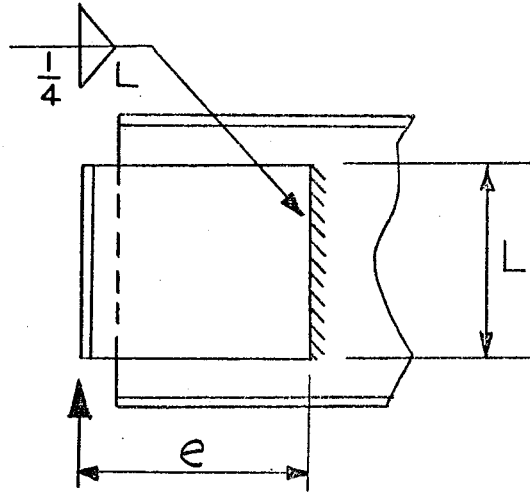


Fig. 2

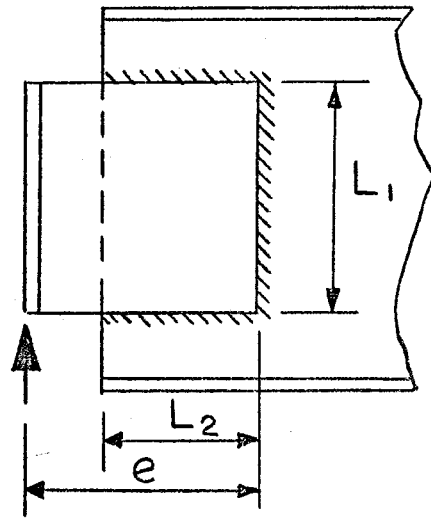
Fig. 3

Specimen	e in.	Factor of Safety
	<p>8</p> <p>10</p> <p>12</p>	<p>2.68</p> <p>3.09</p> <p>3.17</p>
	<p>13</p> <p>15</p>	<p>3.18</p> <p>3.28</p>
	<p>12</p> <p>15</p>	<p>3.10</p> <p>3.36</p>
	<p>15</p>	<p>3.42</p>



	L	e	F.S.
1	8 in.	8 in.	7.5
2	10	6	6.6
3	10	15	5.8
4	12	6	6.4
5	12	8	6.2
6	12	12	6.4
7	16	10	6.1
8	16	16	7.1

Fig. 4



	L_1	L_2	e	F.S.
1	6	3	5	5.8
2	6	6	12	5.3
3	8	4	8	5.4
4	8	6	12	5.3
5	12	4	14	5.0

Fig. 5

Steel Structures for Buildings

LECTURE VI

OVERALL STABILITY PROVISIONS IN CSA-S16-1969

STEEL STRUCTURES FOR BUILDINGS

P.F. Adams

Introduction

In the design of a building structure, the normal procedure is to first establish preliminary member sizes on the basis of an approximate analysis, then to check the adequacy of the design by re-analyzing the complete structure. According to present specifications, the structure must resist the applied lateral and gravity loads (design values times 0.75) as well as gravity loads only. The required resistance may be provided by the frame action of the members themselves (beams and column) or by an additional bracing system (for example K bracing or diagonal bracing) or by shear walls. In many cases a combination of the above is most suitable. The purpose of this paper is to describe the development of the overall stability provisions of CSA-S16-1969, Steel Structures for Buildings, and to show how these provisions affect the design of the bracing system and the columns in the structure.

Load-Deflection Relationships

The behavior of the structure may be described with reference to the load-deflection relationship plotted in Fig. 1. In this figure the load, P , represents the total vertical load on a particular beam and the deflection index, Δ/h , is the relative lateral deflection of a story divided by the story height. It is assumed that the lateral load is proportional to the vertical loads and that all loads are increased to trace the complete history of the structure.

Assuming that the floor diaphragms are rigid and that the structure is symmetrical in plan, any structure can be visualized as a series of

linked planar bents, similar to that shown in the inset of Fig. 1. Thus the curves plotted in Fig. 1 are typical of the response of the complete structure.

The dashed line shown in Fig. 1 represents the results of an elastic first order analysis. This analysis assumes that the member end moment vs rotation ($M-\theta$) relationship is depicted by the dashed line of Fig. 2. The rotations and deflections at the member ends are assumed to be compatible (no discontinuities) and equilibrium requirements are satisfied at each joint in the structure as shown in Fig. 3, where the sum of the end moments meeting at a joint must be zero. For each story of the structure, the sum of the lateral column reactions, H , must be equal to the applied story shear, as shown in Fig. 4. Computing the reaction for an individual column, H , is taken as:

$$H = \frac{M_T + M_B}{h}$$

Where M_T and M_B represent the end moments at the top and bottom of the member, respectively, and h is the story height.

The above assumptions result in a predicted $P-\Delta/h$ relationship which is linear but which gives no indication of the maximum strength of the structure. At some stage of loading, however, shown as P_1 in Fig. 1, the moment at one critical location in the structure will reach its maximum capacity; M_p for a compact section, M_y if the section is non-compact.

The light solid curve shown in Fig. 1 represents the results of

a second-order elastic analysis. In this analysis the member response is again assumed to be that given by the dashed line in Fig. 2 and the compatibility and equilibrium conditions shown in Figs. 3 and 4 are also satisfied. However, in assessing the reactions developed by an individual column, the secondary moments caused by the axial load, P , acting through the story sway displacement, Δ , are accounted for as shown in Fig. 5, and the column reaction is:

$$H = \frac{M_T + M_B}{h} + \frac{P\Delta}{h}$$

Thus at a given level of applied load the column forces, and the corresponding bending moments and shears throughout the structure, have been increased as well as the deflections and joint rotations. Due to the non-linear nature of the $P\Delta$ effect, the curve bends away from the first order elastic response as shown.

Again, the second order elastic analysis provides no indication of collapse, however, at a load, P_2 , the moment at one critical location in the structure reaches the maximum capacity of the member. Since, for a given level of applied load, the moments and forces predicted by the second order analysis are greater than those corresponding to a first order analysis, P_2 will always be less than P_1 .

A second factor (usually minor in practical steel members) sometimes accounted for in a second order analysis is the secondary moment on an individual member due to its deflection from the chord. For example, the member shown in Fig. 5 would be subjected to secondary moments caused

by the component of P parallel to the chord, acting on the displacements of the member from the chord line. The shape of the resulting bending moment distribution would correspond to the shaded area of Fig. 5.

The simple plastic theory neglects these secondary effects but assumes the moment at each hinge location in the potential failure mechanism to be equal to M_p . The maximum load carrying capacity predicted is shown as P_p in Fig. 1.

If the complete $M-\theta$ relationship for each member were used and the equilibrium and compatibility relationships shown in Figs. 3 and 4 satisfied, with shear equilibrium formulated on the deformed structure (second order) the resulting load-deflection relationship would be that shown as the "true" curve in Fig. 1. This curve would account for the gradual penetration of yielding at points of plastic hinge formation, the redistribution of moment after hinging has occurred and the secondary moments on the structure and on the individual members. This response agrees closely with the result of tests on large scale frames. The maximum load-carrying capacity of the structure predicted by this procedure is denoted as P_M . Since the secondary moments reduce the capacity of the structure to resist the applied loads, P_M will always be less than P_p .

Significance of Frame Reference Loads

In the normal design procedure for a steel structure, two loading cases are considered: gravity (dead and live) loads only, and gravity

loads acting in combination with lateral loads due to wind or earthquake. In this latter case, since the probability of the maximum values of lateral and gravity loads occurring simultaneously is reduced, the design is based on 75% of the design load values. In the remainder of this paper it will be assumed that the structure is subjected to the combined loading case; the same techniques would also be used to treat the gravity load case.

In the allowable stress technique, the internal forces and bending moments due to the design loads are determined from first order elastic analysis of the structure (member sizes obtained from a preliminary design). The stresses corresponding to the internal moments and forces are computed and matched against the allowable stresses at each critical section. If the actual stresses exceed the allowable values, the member sizes are increased. The structure may then be reanalyzed and the process repeated.

As discussed in Lecture 3, the allowable stresses have been selected to provide an adequate factor of safety against the attainment of the maximum moment capacity in the member; M_p for the compact shapes, M_y for non-compact.

Since the member sizes have been selected so that a factor of safety, of approximately 1.70, exists against the attainment of the maximum moment capacity of each member; the design actually ensures that a factor of safety of approximately 1.70 will be supplied against the attainment of P_1 , shown in Fig. 1. This allowable stress design

technique neglects the fact that, after the first hinge has formed, moment redistribution will enable an indeterminate structure to resist a load, shown as P_M , which may be 2 or 3 times P_1 (the plastic strength technique does take advantage of this phase of the behavior).

However, as also shown in Fig. 1, the load P_1 is an unconservative estimate of the stage at which the first plastic hinge will form. Due to the influence of the secondary moments, the first hinge will form at a load P_2 and for slender structures or structures resisting large gravity loads, P_2 may be dangerously below P_1 . In addition, since non-compact sections are used in structures designed by the allowable stress technique, the designer has no guarantee (unless the plate slenderness ratios and bracing spacing meet the plastic design requirements) that sufficient moment redistribution will occur in the structure to compensate for this overestimate of P_2 .

Development of Interaction Equations

Each column in the structure is checked using the interaction equations. The equation relating to the overall stability of the member is repeated below:

$$\frac{f_a}{F_a} + \frac{C_m f_b^\alpha}{F_b} \leq 1.0$$

The forces and moments used in the computation of f_a and f_b are based on an elastic first order analysis of the structure at the design load level.

The terms F_a and α are both functions of the effective slenderness ratio; α is of particular interest as:

$$\alpha = \frac{1}{(1 - f_a / F_e')}$$

where $F_e' = 149000 / (KL/r_x)^2$

and $\frac{KL}{r_x}$ is assumed to be the effective slenderness ratio in the plane of bending.

Multiplying both f_a and F_e' by a factor of safety and the cross-sectional area results in an expression for α as:

$$\alpha = \frac{1}{(1 - F/P_e)}$$

where $P_e = \frac{\pi^2 EI}{(KL)^2}$

This is commonly termed the amplification factor and has the effect (since $F/P_e \leq 1.0$) of magnifying the bending stress, f_b , to account for the secondary moments produced by the axial force, F , acting on the deformed shape of the member.

The buckling load, P_e , represents an artificial loading condition for the member. The two possible situations are shown in Fig. 6. If translation is assumed to be prevented, the buckled shape is shown on the left side of the figure. The end moments shown are restraining moments caused by the rotation of the girders framing into the column

ends. The horizontal reactions, H , are equal to the algebraic sum of these end moments, divided by the story height, h . The secondary moments on the member are a result of the axial force, F , acting through the displacement, δ , shown by the shaded area on the diagram.

If the member is assumed to be free to translate during the buckling motion, through a distance, Δ , the situation is shown on the right in Fig. 6. In this case the end reactions, H , are increased by an amount $F\Delta/h$ and the secondary moments are increased due to the sway of the column. The deflections from the chord line are shown as the shaded region in this figure.

The column, permitted to sway, is shown again in Fig. 7 with the forces, F , resolved into components parallel to the chord and perpendicular to this line. Since the angle Δ/h is assumed to be small, the component of force parallel to the chord is equal to F and that perpendicular to the chord is equal to $F\Delta/h$.

In Fig. 7 the influence of sway on the moments in the column can be more clearly seen. First the component, F , parallel to the chord will produce a secondary moment, $F\delta$, having a distribution similar to the shaded areas in Fig. 6. These secondary moments may be approximated (conservatively) by multiplying the primary bending (moments) stresses, f_b , by the factor α where the value of F_e' is determined by assuming the member ends are prevented from translation. Thus the bending moment distribution on the member due to the first sway effect is the same as that on an equivalent member prevented from sway.

The second influence which must be evaluated for the sway column is the additional horizontal reaction, $F\Delta/h$ necessary to resist the axial force in the deformed position. This effect is equivalent to the addition of a lateral force acting at the ends of each column and having a value $F\Delta/h$.

Returning to the column of Fig. 5, the secondary moments in the column could be estimated by:

- (a) Computing the effective length factor assuming the column free to sway or
- (b) Computing the effective length factor assuming the column prevented from sway but subjecting the column to additional forces at its ends, equal to $F\Delta/h$.

Another way of looking at the problem is that the use of the effective length (in the amplification factor) actually serves to account for two factors normally included in a second order analysis.

- (1) The additional horizontal forces due to the sway of the structure.
- (2) The additional moments in the columns due to the axial loads.

The interaction equations are formulated so that an increase in member size is required to compensate for the neglect of the above secondary factors in the original first order analysis. Thus the use of moments and forces from an elastic first order analysis, coupled with the use of the interaction equations, actually insures that the

designer has provided a factor of safety against the attainment of the load P_2 , see Fig. 1.

Design Implications

It follows that if the structure is to be designed using moments and forces from a first order analysis in combination with the interaction equations and allowable stresses from CSA-S16-1969, then the effective length must be computed by assuming the frame free to translate, since the sway forces have not been accounted for.

On the other hand, if the structure is analyzed under the action of the sway forces and the applied loads, the sway forces have been included in the basic analysis and need not be considered a second time. Under these conditions, the interaction equations are used to compensate for the neglect of the secondary moments in the columns ($F\delta$) and the effective lengths are computed assuming that translation is prevented.

Thus the choice of the nomograph to use in computing the effective length factor does not depend on whether the structure does or does not contain a bracing system or shear wall, but rather whether the sway forces are to be accounted for in the basic analysis procedure or within the interaction equations.

If it is desired to resist all the lateral forces in a particular portion of the structure, such as a shear wall or vertical truss, this portion must be designed for the sway forces as well as the applied

lateral loads. The effective length factors for the columns may then be computed assuming translation is prevented.

If the bracing is designed to resist lateral loads only, without consideration of the sway forces, no guarantee exists that the system is capable of resisting the sway forces and therefore, in computing the effective length factor for the columns in the structure, the conservative assumption would be that the columns were permitted to sway.

Computation of Sway Forces

The computation of sway forces for the combined loading case is relatively simple. The lateral and vertical loads are applied to the structure as shown in Fig. 8, (using a probability factor of 0.75) and the relative lateral displacement at each floor level computed. These displacements are denoted as Δ_i^1 in Fig. 9, where i denotes the floor level and the subscript 1 denotes the first trial. The additional story shears due to the vertical loads are computed as $\sum F_i \frac{\Delta_i}{h_i}$ where F_i represents the axial force in a column of the i th story and the summation is performed for all columns in the story. At a given floor level, the sway force will be the algebraic sum of the story shears from the columns above and below the floor, as shown in Fig. 9.

If the sway forces are small relative to the applied lateral loads than the deflections, Δ_i^1 , will be approximately correct and the sway forces have been correctly determined. These are added to the applied

lateral loads and the total forces and moments in the structure are computed.

If the sway forces are large these must be added to the original lateral loads and new deflections Δ_i^2 computed. New sway forces are computed and the process repeated.

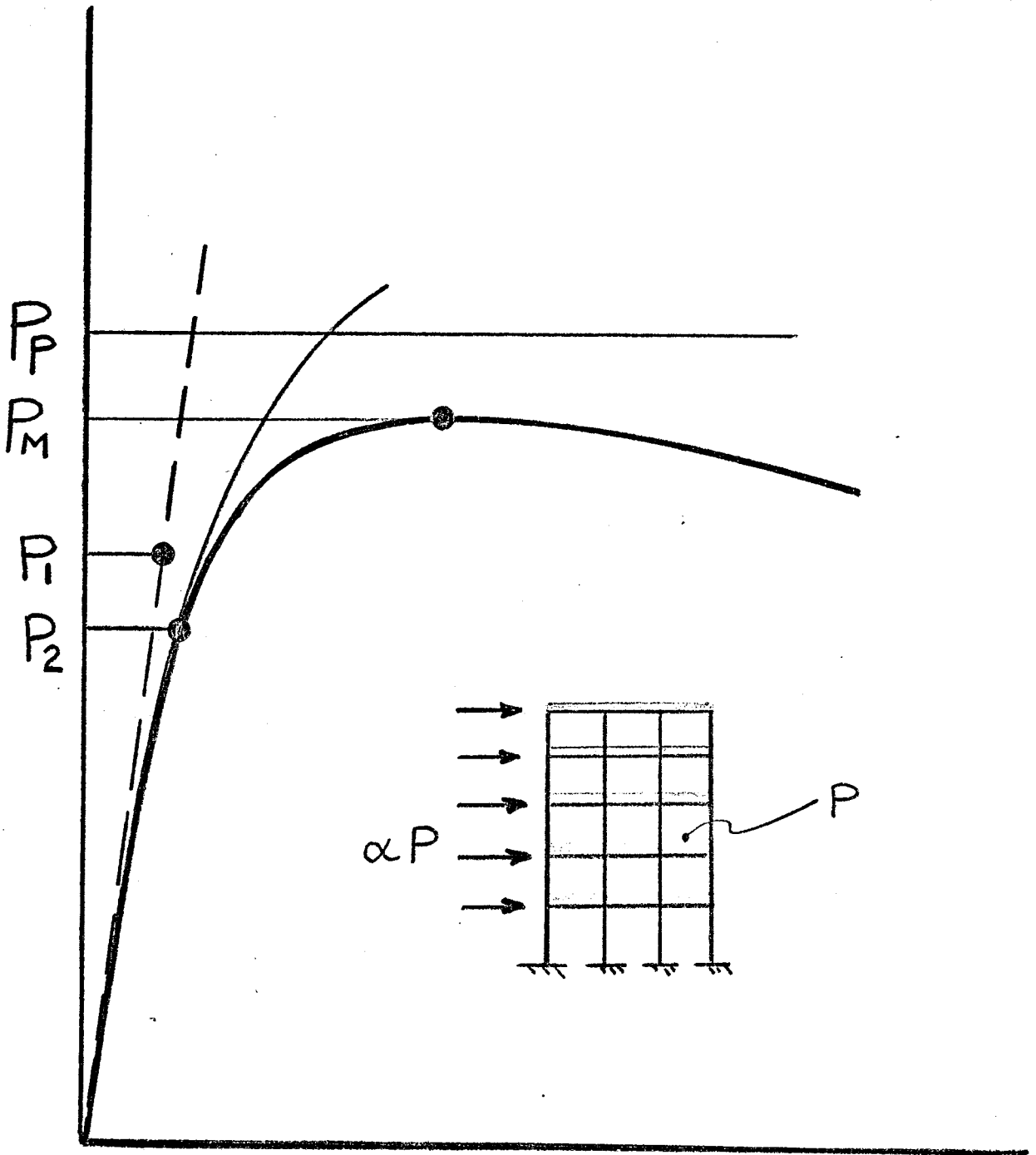
If the structure is perfectly symmetrical then, when it is subjected to (symmetrical) gravity loads only, artificial lateral loads must be applied initially (perhaps 1% of the wind loads) in order to produce an initial sway displacement. Once the sway loads have been computed, however, those artificial loads need not be added to the sway loads.

Summary

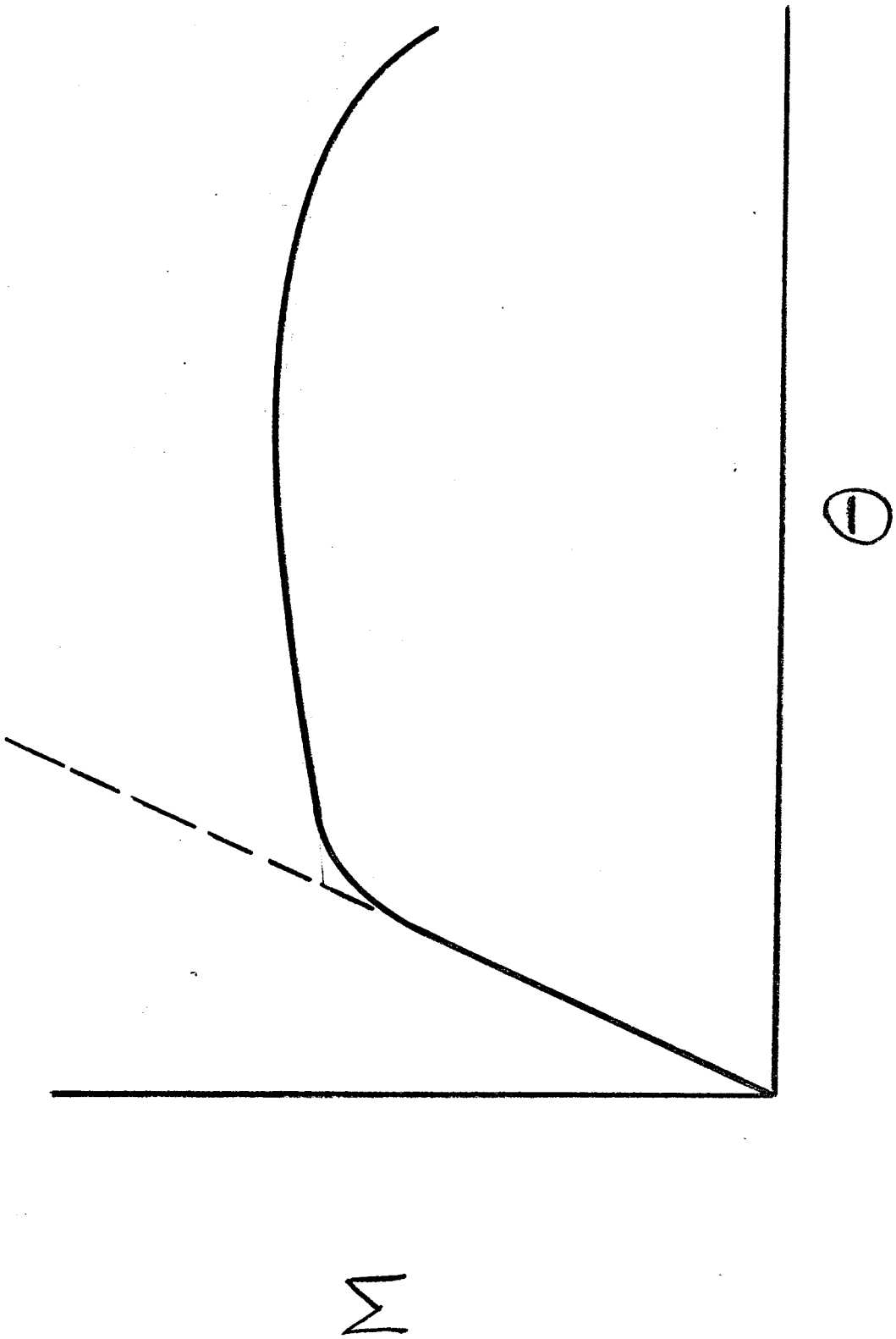
By assuming a column is free to translate during the buckling motion, the sway forces, produced by the axial loads acting on the deformed structure, are taken into account. If the effective length computed on this basis is used together with the interaction equations, then a suitable factor of safety against the load producing the first plastic hinge is guaranteed.

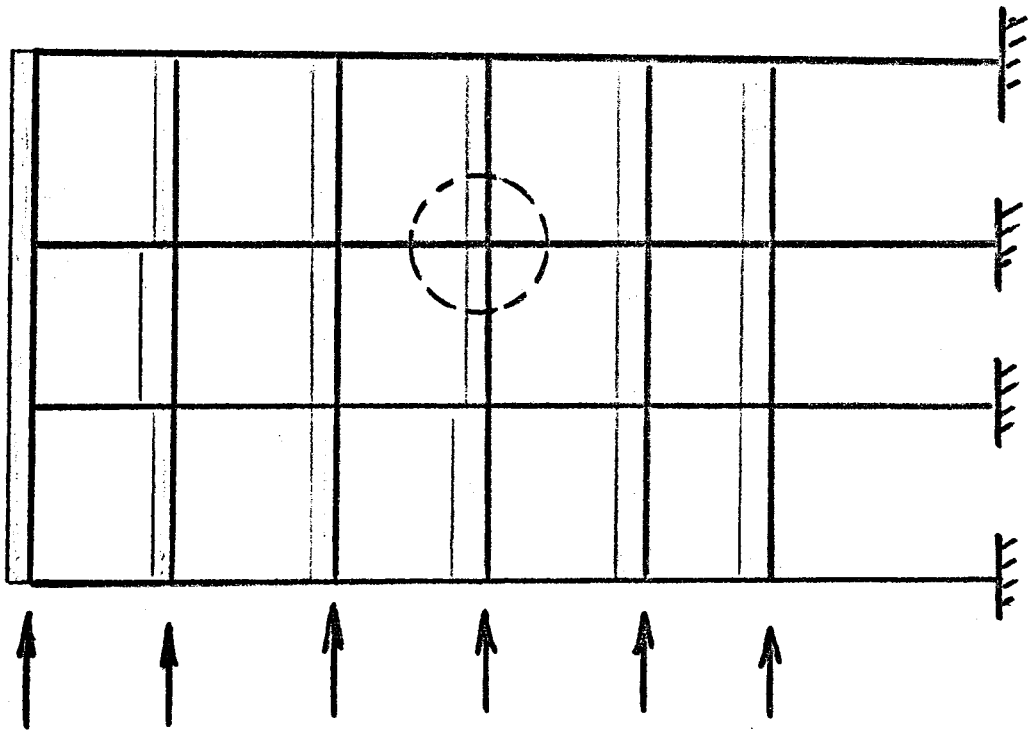
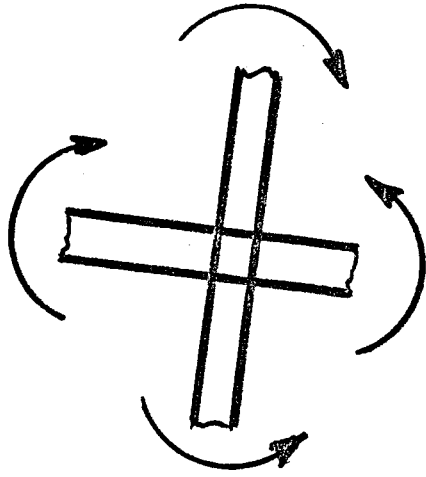
If the sway forces are computed as part of the basic analysis procedure, however, then the column should be assumed prevented from sway during the determination of the effective length factor. This procedure may result in substantial economy in the design of steel columns.

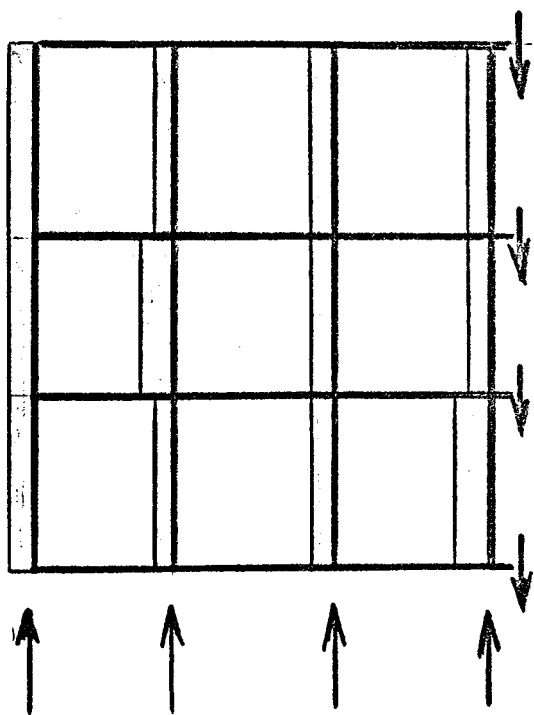
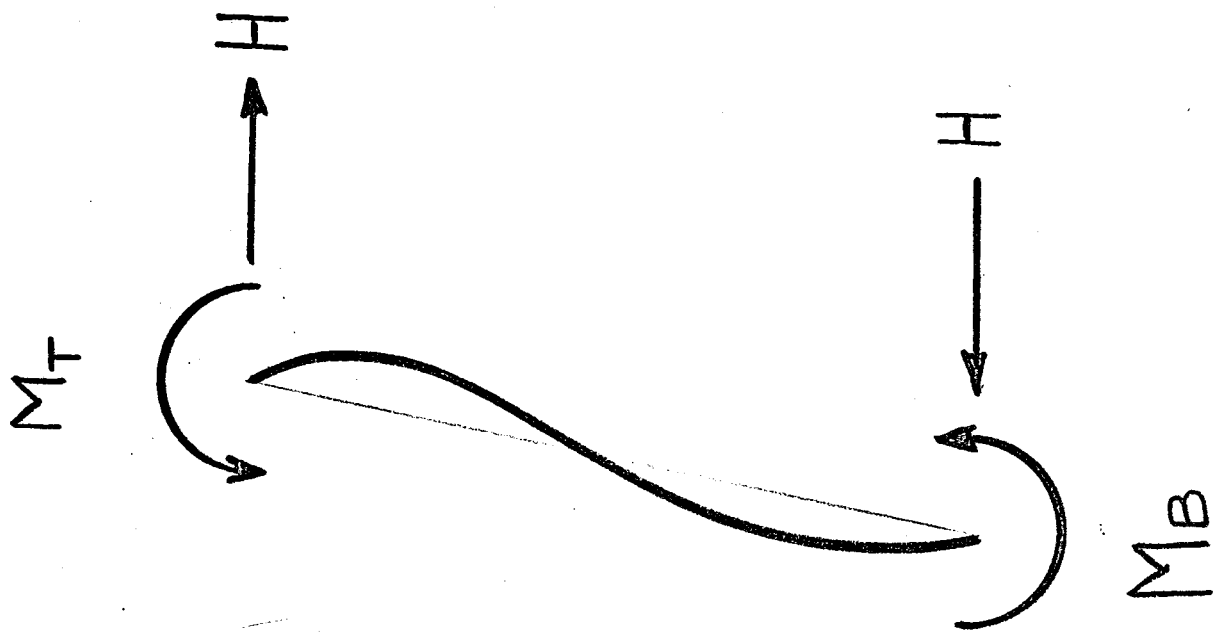
D

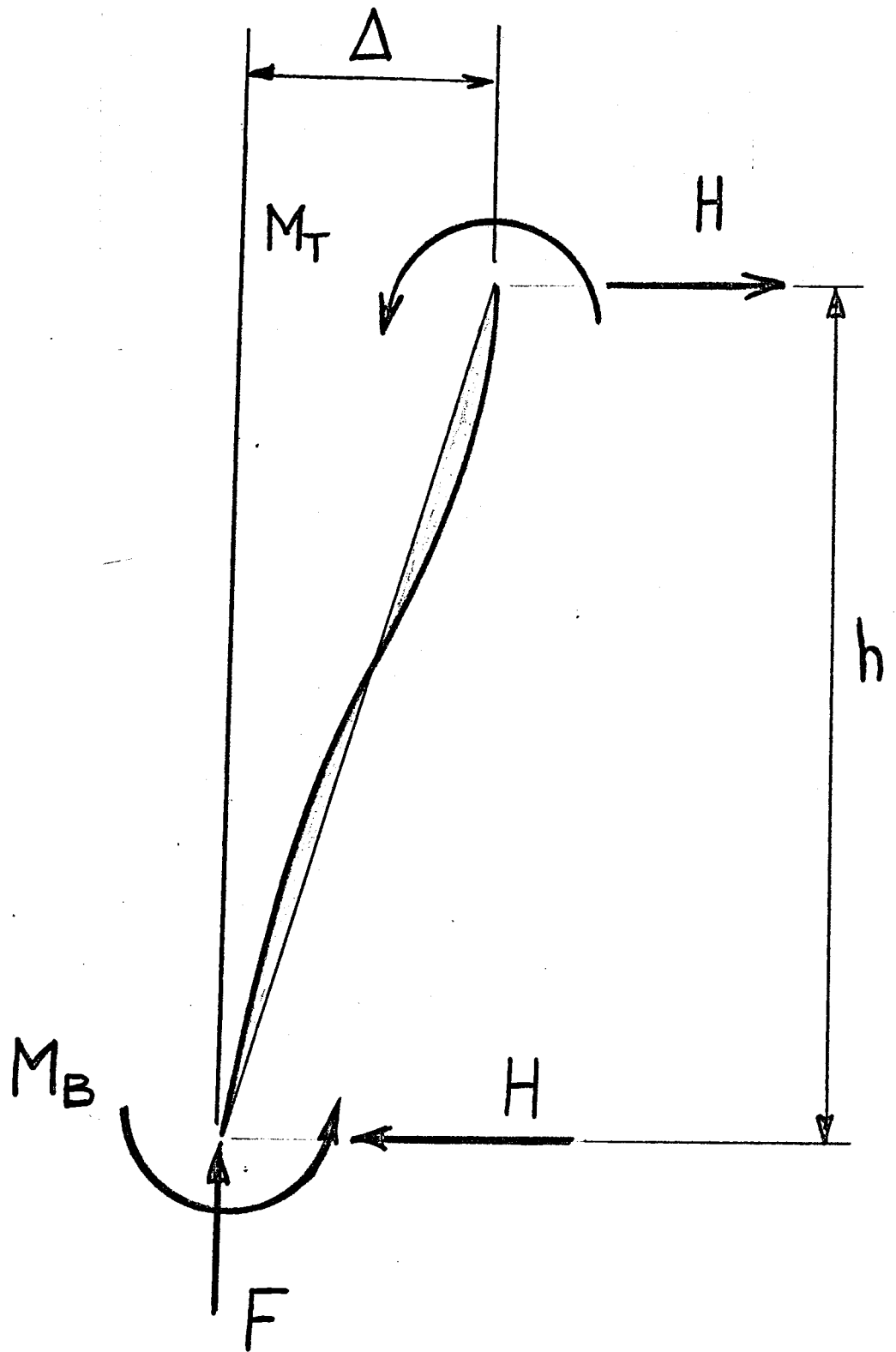


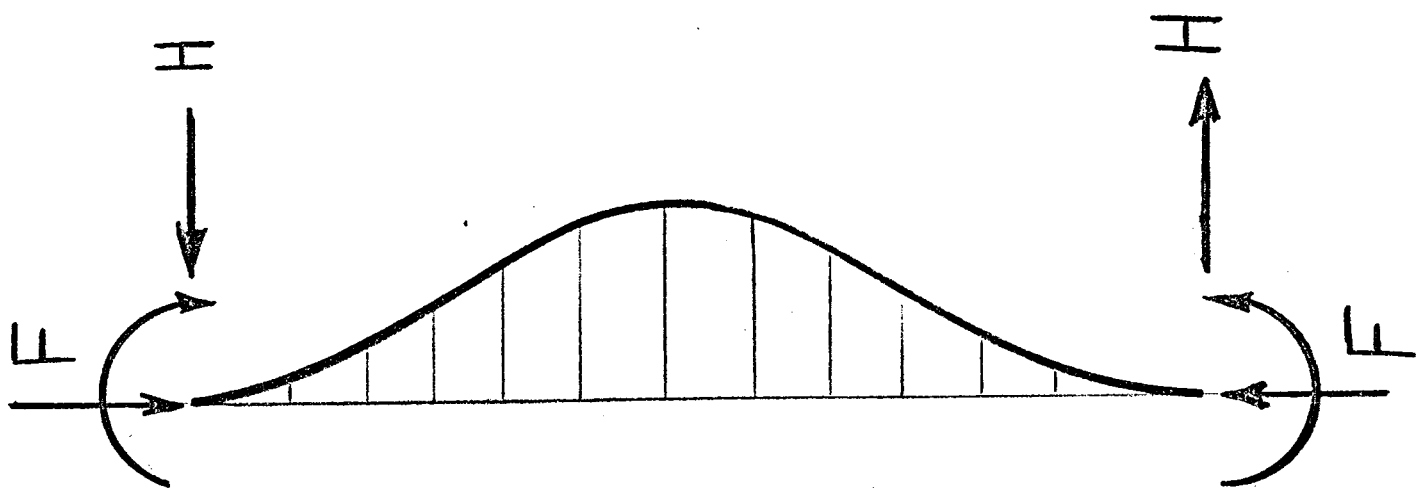
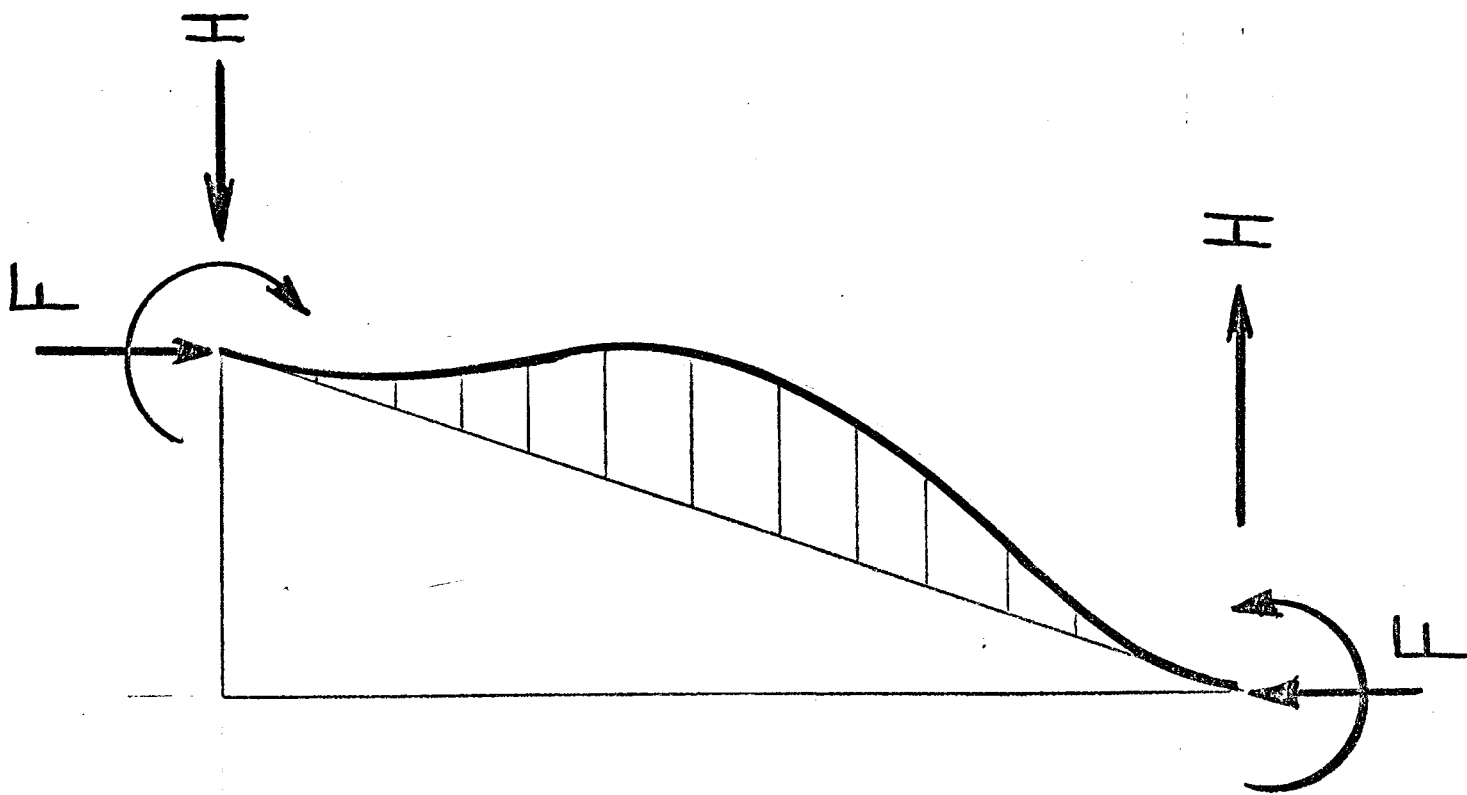
Δ/h

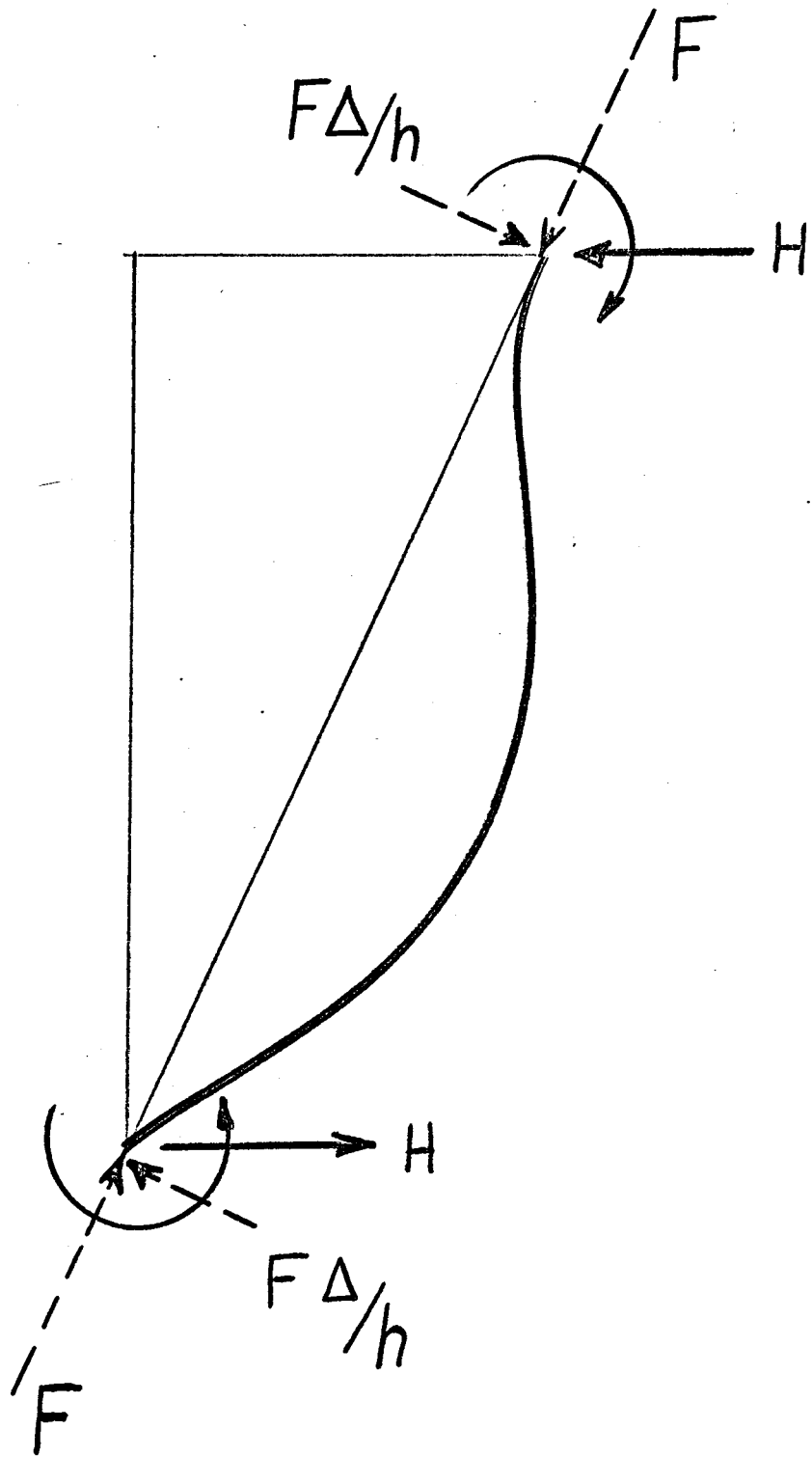


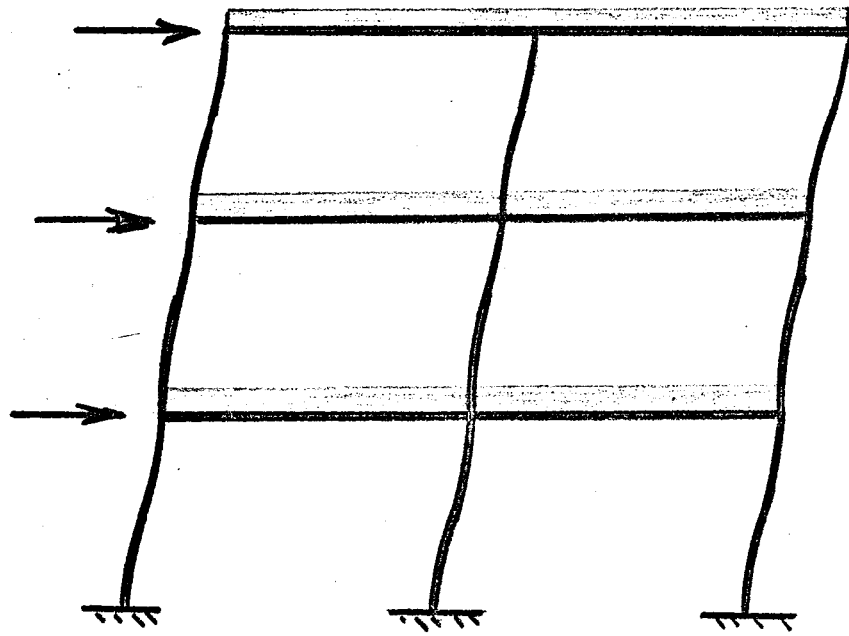


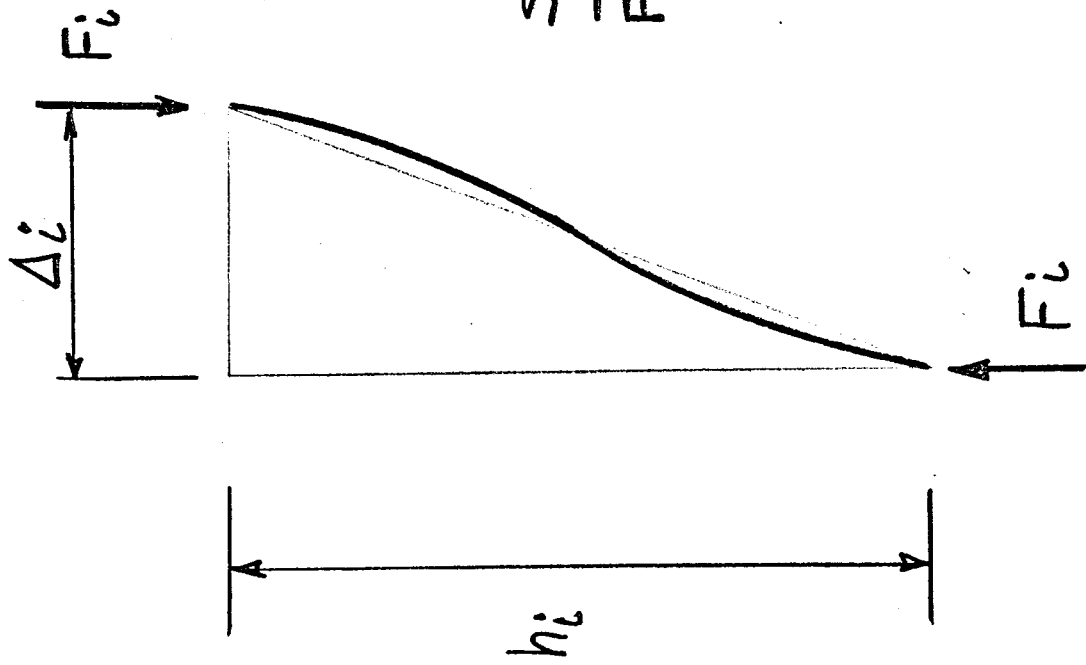












$$\sum \frac{F_{i+1} \Delta i_{i+1}}{h_{i+1}}$$



$$\sum \frac{F_i \Delta i}{h_i}$$

STRUCTURAL ENGINEERING REPORTS

1. THE BEHAVIOR OF SHEAR PLATES IN SLOPING GRAIN SURFACES - No. 1, by J. Longworth, September, 1963.
2. TESTS OF ECCENTRICALLY LOADED CONCRETE COLUMNS BENT IN DOUBLE CURVATURE, by S.L. Barter, May, 1964.
3. THE BEHAVIOR OF SHEAR PLATES IN SLOPING GRAIN SURFACES - No. 2, by J. Longworth, June, 1964.
4. METHOD OF ANALYSIS OF SHALLOW TRANSLATIONAL SHELLS, by I. Rajendram and S.H. Simmonds, February, 1965.
5. TORSIONAL STRENGTH AND BEHAVIOR OF CONCRETE BEAMS IN COMBINED LOADING, by G.S. Pandit and J. Warwaruk, July, 1965.
6. ULTIMATE STRENGTH AND BEHAVIOR OF PLATES, by A. Gyi and S.H. Simmonds, November, 1965.
7. THE BEHAVIOR OF RESTRAINED REINFORCED CONCRETE COLUMNS UNDER SUSTAINED LOAD, by R.F. Manuel and J.G. MacGregor, January, 1966.
8. PRETENSIONED BEAMS WITH CONFINED COMPRESSED CONCRETE, by R.L. Ward and J. Warwaruk, April, 1966.
9. AN ANALYTICAL STUDY OF INCLINED CRACKING IN REINFORCED CONCRETE BEAMS, by J.R.V. Walters and J.G. MacGregor, July, 1966.
10. ROTATION CAPACITY OF WIDE-FLANGE BEAMS UNDER MOMENT GRADIENT, by A.F. Lukey and P.F. Adams, May, 1967.
11. TORSIONAL STRENGTH OF RECTANGULAR REINFORCED CONCRETE BEAMS SUBJECTED TO COMBINED LOADING, A.E. McMullen and J. Warwaruk, July, 1967.
12. THE INFLUENCE OF COLUMN SHAPE ON THE BEHAVIOR OF FLAT PLATE SLABS, by R.J. Kavanagh and S.H. Simmonds, November, 1967.
13. EXPERIMENTS ON WIDE-FLANGE BEAMS UNDER MOMENT GRADIENT, by R.J. Smith and P.F. Adams, May, 1968.
14. APPROXIMATE ANALYSIS OF FRAME-SHEAR WALL STRUCTURES, by S.N. Guhamajumdar, R.P. Nikhed, J.G. MacGregor, and P.F. Adams, May, 1968.
15. ELASTIC TORSIONAL ANALYSIS OF MULTI-STORY STRUCTURES, by J.H. Wynthoven and P.F. Adams, October, 1968.
16. ANALYSIS OF REINFORCED CONCRETE SHEAR WALL-FRAME STRUCTURES, by W.J. Clark and J.G. MacGregor, November, 1968.
17. MOMENT CURVATURE RELATIONSHIPS OF PRESTRESSED CONCRETE BEAMS WITH CONFINED COMPRESSED CONCRETE, by M.K. Wilkinson and J. Warwaruk, January, 1969.
18. FATIGUE STRENGTH OF DEFORMED REINFORCING BARS, by I.C. Jhamb and J.G. MacGregor, May, 1969.

19. SHALLOW SHELLS SUPPORTED BY ELASTIC EDGE BEAMS, by D.H. Quapp and S.H. Simmonds, May, 1969.
20. COMPOSITE BEAMS IN NEGATIVE BENDING, by J.H. Davison and J. Longworth, May, 1969.
21. TEST OF FLAT PLATE SUPPORTED ON COLUMNS ELONGATED IN PLAN, by A.E. Smith and S.H. Simmonds, May, 1969.
22. CONTINUOUS PRESTRESSED CONCRETE BEAMS WITH CONFINEMENT, by I.H.G. Duncan and J. Warwaruk, September, 1969.
23. REINFORCED CONCRETE CELLULAR ORTHOTROPIC SLABS, by R.G. Quinton and S.H. Simmonds, October, 1969.
24. PRESTRESSED CONCRETE BEAMS WITH WEB REINFORCEMENT UNDER COMBINED LOADING, by P. Mukherjee and J. Warwaruk, May, 1970.
25. STUDIES OF REINFORCED CONCRETE SHEAR WALL-FRAME STRUCTURES, by R.P. Nikhed, J.G. MacGregor and P.F. Adams, June, 1970.
26. BUCKLING STRENGTHS OF HOT ROLLED HAT SHAPED SECTIONS, by D.A. Heaton and P.F. Adams, July, 1970.
27. EXPERIMENTAL AND ANALYTICAL INVESTIGATION OF THE BEHAVIOR OF COUPLED SHEAR WALL-FRAME STRUCTURES, S.N.G. Majumdar and P.F. Adams, August, 1970.
28. COMPARATIVE STUDY OF SLAB-BEAM SYSTEMS, by J. Misic and S.H. Simmonds, September, 1970.
29. ELASTIC-PLASTIC ANALYSIS OF THREE DIMENSIONAL STRUCTURES, by J.H. Wynhoven and P.F. Adams, September, 1970.
30. FLEXURAL AND LATERAL-TORSIONAL BUCKLING STRENGTHS AND DOUBLE ANGLE STRUTS, by N.J. Nuttall and P.F. Adams, September, 1970.
31. STIFFNESS INFLUENCE COEFFICIENTS FOR NON-AXISYMMETRICAL LOADING ON CLOSED CYLINDRICAL SHELLS, by S.H. Iyer and S.H. Simmonds, October, 1970.
32. CSA-S16-1969 STEEL STRUCTURES FOR BUILDINGS - Seminar Notes, by P.F. Adams, G.L. Kulak and J. Longworth, November, 1970.